1962

Flame spectroscopy of the rare earth elements

Ronald Howard Curry
Iowa State University

FLAME SPECTROSCOPY OF THE RARE EARTH ELEMENTS

by

Ronald Howard Curry

A Dissertation Submitted to the
Graduate Faculty in Partial Fulfillment of
The Requirements for the Degree of
DOCTOR OF PHILOSOPHY

Major Subject: Analytical Chemistry

Approved:

Signature was redacted for privacy.

In Charge of Major Work

Signature was redacted for privacy.

Head of Major Department

Signature was redacted for privacy.

Dean of Graduate College

Iowa State University
Of Science and Technology
Ames, Iowa

1962

TABLE OF CONTENTS

		Page
I.	INTRODUCTION	1
II.	PREVIOUS STUDIES OF RARE EARTH FLAME SPECTRA	4
III.	APPARATUS	11
	A. Burner	11
	B. Gas Flow Metering Equipment	14
	C. Beckman DK-2 Spectrophotometer	18
	D. Spectrographic Equipment	19
	E. Grating Flame Photometer	23
IV.	RECORDING OF SPECTRA	32
	A. Preparation of Solutions	32
	B. Selection of Optimum Excitation Conditions	33
	C. Spectrophotometric Recording of Rare Earth Flame Spectra	41
	D. Photographic Recording of Rare Earth Flame Spectra	50
V.	EXCITATION MECHANISM	89
	A. Flame Excitation Theories	89
	B. The Measurement of Flame Temperature	98
	C. Conclusions	114
VI.	ANALYTICAL APPLICATIONS	120
	A. Recording of Line Spectra	121
	B. Interference Assessment and Detection Limits	130
	C. Calibration Experiments	136
VII.	SUGGESTIONS FOR FUTURE WORK	149
VIII.	SUMMARY	151
IX.	LITERATURE CITED	152
X.	ACKNOWLEDGMENTS	157

I. INTRODUCTION

Although excitation of spectra in flames is one of the oldest techniques in spectroscopy, it is one of the most neglected and least understood. Only in the past few years have any significant contributions been made to the understanding of the flame excitation process. Likewise, until very recently, the tendency in analytical flame spectroscopy has been to report the spectrum of an element but to pay very little attention to the type of excitation process involved. Because of this pragmatic approach to flame spectroscopy, the full potential of the method has never been exploited.

The complex chemical equilibria which obtain in and beyond the reaction zone of hydrocarbon flames present to the spectroscopist a wealth of potential control over the spectra which he may excite; removing him from the role he has so often played in the past, that of passive observer. Nowhere is this better illustrated than in the case of the flame spectra of the rare earth elements. As shall be seen in a subsequent section of this thesis, the problems involved in the development of analytical methods for the determination of these elements in the presence of one another make the use of physical analytical methods mandatory in most cases. Over 30 years ago it was recognized that excitation of these elements in a flame might provide one solution to these

problems. Unfortunately it was found that the spectra of these elements, except in isolated cases, consisted of molecular band spectra arising from diatomic molecules of the type MO. Only europium and ytterbium exhibited intense line radiation. These monoxide bands suffer from a high degree of spectral interference and have proven to be of little value in determining the individual rare earth elements in mixtures except in the case of one element, lanthanum. In the 30 years that the rare earth flame spectra have been under investigation, the essential character of the monoxide band systems have been described several times. The lack of characteristic atomic line spectra has been attributed to the inability of the flame to dissociate molecules of such high thermal stability as the rare earth monoxides (dissociation energies of these molecules are in the five to eight ev range) and to excite the resultant atoms. This explanation is borne out by the fact that the two elements which exhibit strong lines in ordinary flames, europium and ytterbium, do not show intense molecular band emission. The plausibility and seeming irrefutability of this explanation has led one author to state, in the case of lanthanum: "The high energy of dissociation of the LaO molecules eliminates any possibility of atomic spectra being observed in a flame". (1, p. 37)

In spite of this wealth of negative evidence, it has been found that by a careful selection of excitation condi-

tions, all of the rare earth elements, except cerium, can be made to exhibit moderate to strong atomic line spectra using conventional burners, fuels, and instrumentation. The work reported in this thesis is an attempt to characterize these line spectra. The effect of several variables upon the intensity of the lines has been studied and the analytical utility of many of the stronger lines has been assessed. Since this effect has not previously been observed in the flame, an attempt has been made to gain some insight into the type of excitation process responsible for these spectra. It is hoped that the techniques used in this investigation will be useful not only for the rare earth elements but also for many of the other elements to which the flame has not proven analytically applicable in the past.

II. PREVIOUS STUDIES OF RARE EARTH FLAME SPECTRA

It was in 1860 that Bunsen and Kirchoff (2) reported the discovery of cesium and rubidium through the characteristic lines which these elements emit in a flame. Even though this qualifies the flame as the oldest of all excitation techniques in spectroscopy, it was not until the publication of the work of Lundegårdh (3) in 1929 that any extensive use was made of the flame as an analytical tool. Spectra of the rare earth elements were included among Lundegårdh's data although, unfortunately, the work is scanty and rather too full of errors in identification to be of great practical utility.

Giorgio Piccardi (4-17), in a series of papers published during the period 1929-1941, described the principal features of the oxygen-hydrogen flame spectra of most of the elements. Piccardi, as well as Lundegårdh, noted that most of the spectra were remarkably devoid of atomic lines. The most prominent feature in most of the spectra was the MO band systems. Piccardi observed three strong atomic lines of europium and attributed their appearance to the instability of the EuO molecule at the prevailing flame temperature.

Pinta (18), using an air-acetylene flame, systematically studied the rare earth band spectra from 4000 to 9000 Å, and made a thorough study of their analytical utility. In order to determine the rare earths in complex mixtures, he found it

necessary to apply corrections for the many spectral interferences which occurred. It is also interesting to note that Pinta observed line spectra for certain rare earths in the air-acetylene flame; two strong lines of ytterbium at 3988 and 5556 Å, two weak samarium lines at 4842 and 4884 Å, and four somewhat stronger thulium lines at 4094, 4106, 4187 and 4203 Å. With the exception of the ytterbium lines, none of these were intense enough to be of any practical application. The band spectrum of neodymium contained some structures which Pinta thought might be atomic lines. Careful study of his published spectrograms neither confirms nor denies this possibility, but as shall be seen later, the strong flame lines of neodymium lie in the region in which Pinta thought he observed lines. The three strong europium lines noted by Piccardi were also observed by Pinta.

Tremmel (19) recorded the oxygen-hydrogen flame spectra photoelectrically with a Beckman DK-2 spectrophotometer. These tracings, which are reproduced in Figure 1, represent the first complete set of rare earth flame spectra ever recorded on a modern photoelectric instrument. The problems involved in using the band spectra for the analysis of rare earth mixtures are graphically illustrated in this figure. It is seen that the majority of the spectra lie in the region from 500 to 700 mμ and the inherent width of the molecular band systems cause the incidence of spectral interference to

Figure 1. O_2-H_2 flame spectra of the rare earths as recorded by Tremmel (19)

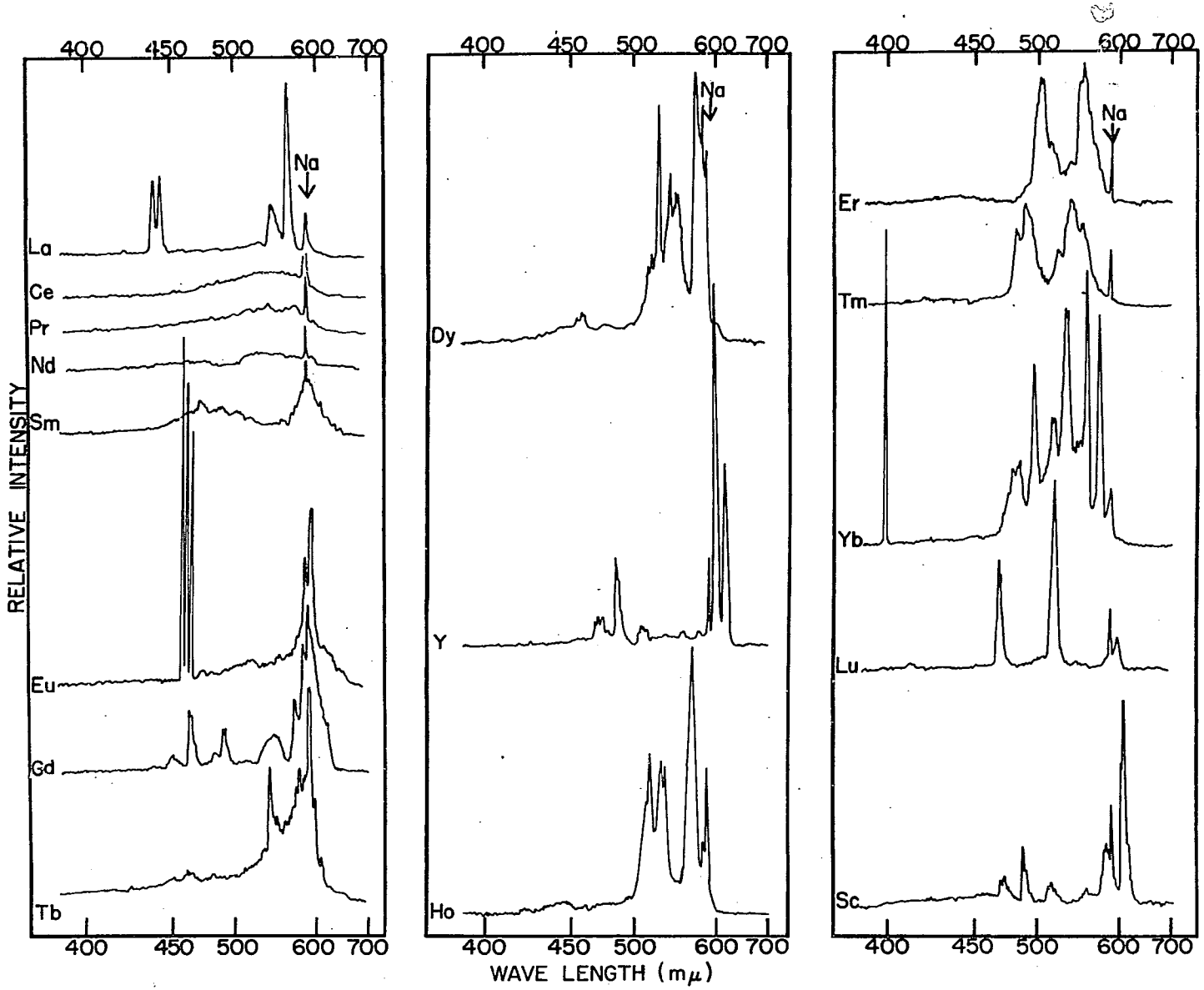
400 450 500 600 700
Na
La
Ce
Pr
Nd
Sm
Eu
Gd
Tb
Dy
Y
Ho
Er
Tm
Yb
Lu
Sc
RELATIVE INTENSITY
WAVE LENGTH (mμ)

be exceedingly great. To compound an already difficult situation, the wavelengths of the band heads tend to decrease periodically with increasing atomic number. This makes the determination of the rare earths difficult when neighboring elements are present, which is likely to be the case for many types of rare earth mixtures. From these considerations, it must be concluded that only ytterbium, through the resonance line at 3988 Å; europium, through the resonance line at 4594 Å; and lanthanum, through the intense LaO bands at 7900 Å (not shown in Figure 1) can be determined in rare earth mixtures without fear of spectral interference from other rare earths. Figure 1 also shows that under his experimental conditions, Tremmel observed no lines other than those originating from ytterbium and europium already mentioned.

More recently the oxygen-hydrogen flame spectra of the rare earths have been studied by Rains et al. (20). They recorded the spectra photoelectrically and measured the wavelength of the prominent bands and lines photographically. These investigators reported line spectra for samarium, terbium, dysprosium, holmium, and thulium in addition to the strong europium and ytterbium lines. These lines were observed photographically, for the most part, only after long (four to ten minute) exposures of concentrated rare earth solutions. In no case was new line emission of analytical

value found. Several emissions in the thulium spectrum were identified as atomic lines. Data which will be presented later in this thesis cast some doubt on the accuracy of these assignments. Rains et al. suggested the use of the NdO bands at 7000 and 7120 Å for the determination of this element in rare earth mixtures but otherwise found no new lines or bands of any analytical utility.

Specific analytical applications of the band spectra have been concentrated on lanthanum. Piccardi (16) and de Albiniti (21) have described techniques for its determination after removal from the rest of the sample. Ishida (22) gave a method for the determination of lanthanum in rare earth mixtures and in rare earth-containing glasses. His method is relatively insensitive and subject to some interference from other rare earths. Menis et al. (23) studied the effect of interferences on all of the prominent LaO bands. They also made a rather complete study of the ability of 4-methyl-2-pentanone to extract lanthanum from most interfering elements. Using this extraction technique, they were able to develop analytical methods for lanthanum in a wide variety of samples. Tremmel (19) has developed a method for the determination of lanthanum as a major constituent (2.5 to 100%) in rare earth mixtures. Under his experimental conditions, no interferences from other rare earths were encountered. Poluektov and Nikonova (24), using the standard addition technique, were

able to determine lanthanum in mixtures containing up to 30% lanthanum.

Analytical methods for the other members of the rare earth group are somewhat less available. Pinta (18), using his correction method, developed methods for all the rare earths. The technique which he used is limited to simple binary and ternary mixtures and is not conducive to the attainment of high accuracy. Poluektov and Nikonova (24), in addition to the method for lanthanum noted above, employed the yttrium monoxide bands at 5970 Å and 6130-6160 Å and the atomic lines of europium and ytterbium for the determination of these elements.

Because of the high degree of interference, it seems obvious that the utility of these spectra will not be extended significantly beyond the applications noted above. Most of the previous investigators have observed some weak atomic line spectra in their flames, but none of these workers have concentrated on the intensification of the lines. It is also worthy of note that no one has investigated the rare earth spectra in oxygen-acetylene flames. The technique described in this work takes advantage of the ability of the oxygen-acetylene flame to intensify the atomic line spectra of the rare earth elements already weakly observed by many investigators, as well as many lines not previously observed in other types of flames.

III. APPARATUS

A. Burner

Of the burners used in analytical flame spectroscopy, the Beckman integral-aspirator type is by far the most popular. This burner was used throughout the studies reported here. The schematic diagram shown in Figure 2 illustrates its important features. As can be seen, this burner consists of three concentric tubes. The sample solution is drawn up the inner tube by the passage of oxygen through the narrow orifice of the central annulus. The outer tube or jacket feeds the combustible gas to the flame. Fuel jackets of different dimensions are required for acetylene or hydrogen. This burner is supplied by Beckman Instruments Co. in two models, either for oxygen-hydrogen (#4020) or for oxygen-acetylene (#4030). However, the outer jackets are interchangeable. The material used in construction is brass except for the capillary inlet which is palladium.

Although the Beckman burner has some favorable features; viz., ease of use, small size, low sample consumption (maximum is about 2 ml/min), and excellent reproducibility; it suffers some shortcomings which limit its applicability as a research instrument. Chief among these is that sample aspiration is dependent entirely upon the oxygen flow rate.

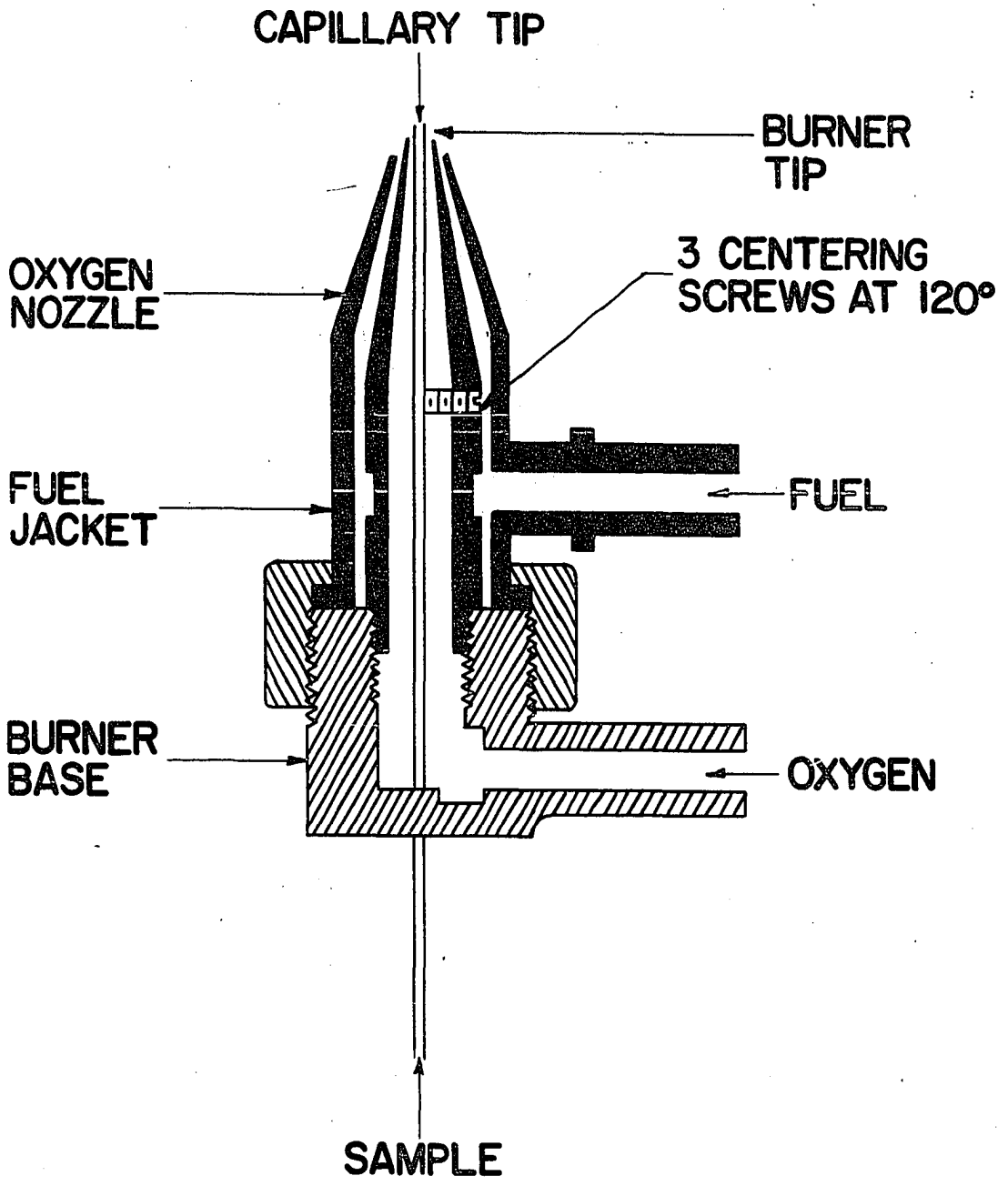

Figure 2. Beckman integral-aspirator burner

This inability to vary the sample aspiration and oxygen flow rates independently is a sizable disadvantage. Another undesirable feature is that the type of flame formed by the Beckman burner does not conveniently fall into either of the classifications into which flames are normally placed, i.e. diffusion or premixed. Diffusion flames, as the name implies, depend almost entirely on diffusion of the reacting species to control the burning process. An ordinary candle flame is a good example of this type. The diffusion flame does not lend itself well to theoretical treatment and has not been studied extensively. Premixed flames, in which the fuel and oxidant are completely interspersed before they issue from the burner mouth and ignite, possess well defined flame fronts, reaction zones, and interconal regions. Gaydon and Wolfhard (25) have described the characteristics of both types of flames, as well as a great many other subjects of value to the spectroscopist interested in flame structure. The characteristics of the Beckman flame make it necessary to classify it as a type of diffusion flame. However, the high velocities of the fuel and oxygen probably cause an appreciable amount of premixing before the gases are burned. Moreover, the flow characteristics appear to be turbulent rather than laminar which adds to the mixing process. At any rate, no well defined flame regions are observable and the flame has never been studied systematically.

B. Gas Flow Metering Equipment

One of the major sources of error in flame photometry is inaccurate metering of the fuel and oxidant being delivered to the burner. Many bands and lines show intensity maxima over very narrow ranges of fuel and/or oxygen flows. The normal method of metering the gases, which consists only of a Bourdon type pressure gauge in conjunction with a diaphragm type regulator, does not permit an accurate, dynamic measurement of the gas flow.

The system shown in Figure 3 was designed to minimize errors due to inaccuracy and variability of oxygen and fuel flow rates. As can be seen from the diagram, the standard Bourdon gauge-diaphragm valve combination (H, J) (Beckman Instruments #9220) permitted constant pressure to be maintained in the system. High accuracy rotameters, E (Schutte and Koerting, Fig. 18210), 600 mm in length, and having an accuracy of ± 1 percent were used as flow measuring devices. Variable orifices consisting of low taper needle valves, A, (Hoke #280-25) making exact reproducibility of the valve setting possible. Separate flow systems were necessary for the oxygen and fuel gases. The oxygen system consisted of a single rotameter designed to operate in the range from one to ten liters/min oxygen. For maximum flexibility, the fuel system consisted of two rotameters, one designed specifically

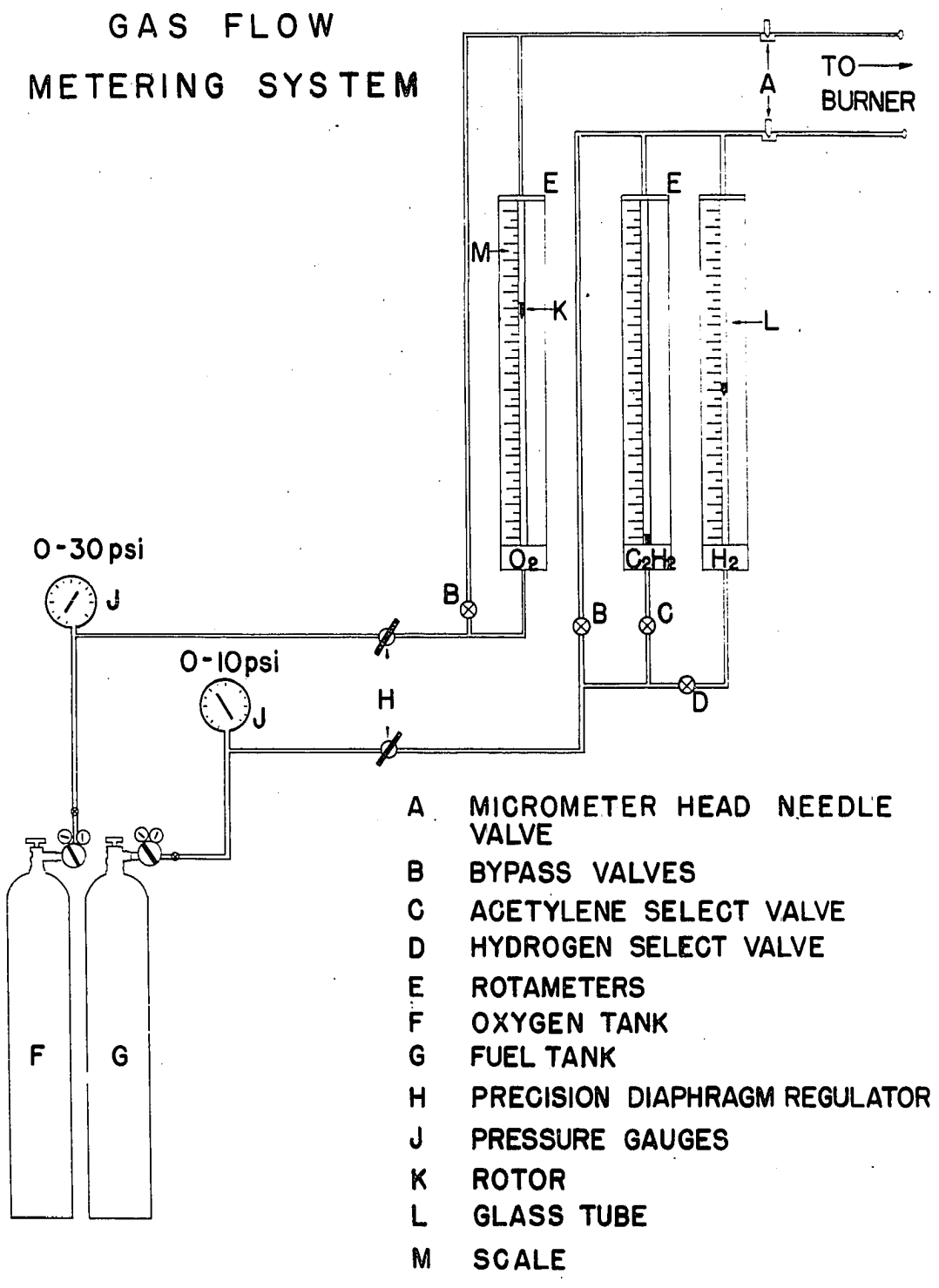

Figure 3. Equipment used to measure oxygen and fuel flows

for the measurement of acetylene flow rate in the range from one to ten liters/min, and the other designed to measure hydrogen in the range from one to fifteen liters/min. As Figure 3 shows, these two meters were connected so that one or the other could be placed in the system by the proper operation of valves C and D. This provided a large amount of selectivity in choice of fuel gas since not only acetylene and hydrogen could be metered with this system, but also many other fuel gases having flow characteristics intermediate between these two. The rotameters were provided with by-passes, B, to remove them from the system should this ever become desirable. Except for the regulating valves, toggle valves (Hoke, Series 450) were used throughout the system. Copper tubing having an inner diameter of one eighth inch or greater was used throughout, and all connections were either silver soldered or made with brass compression fittings. The entire system was mounted in a portable sixty inch relay rack. The inlet and outlet connections were Swagelok bulkhead quick-connects (Swagelok #400-QC-61). With these provisions it was possible to transport the equipment from one flame facility to another with a minimum of time and effort.

As a flow monitoring device, the rotameter is unsurpassed for accuracy, simplicity, ruggedness, and ease of operation. It consists of a tapered tube (L) in which a small weight called a rotor (K) is free to ride. As gas enters the

smaller diameter (at the bottom) of the tapered tube, the flow is restricted until the gas exerts sufficient force to overcome the weight of the rotor. As the rate of flow is increased, the rotor establishes a higher position in the tube. The taper of the tube is designed so that the rotor position is a linear function of the gas flow. The rotameter must be operated at constant pressure in order to maintain the calibration. Although rotameters may be supplied with scales reading directly in gas flow, those used in this study were calibrated after being placed in the system. A wet-test meter (Precision Scientific) connected directly to the burner outlet was used for calibration. A constant pressure of 15 psig was used in the oxygen system, while a constant pressure of 2 psig was used for all fuel gases. Recalibration of the oxygen rotameter was necessary each time the burner was changed because the orifice combination formed by the needle valve and the burner orifice varied when burners of different orifice sizes were used. This resulted in a change of pressure between the two orifices, thereby altering the rotameter calibration. Since the fuel jackets of the burners were comparatively large, the needle valve represented the only controlling orifice. Hence, only a single calibration was necessary for each fuel gas, regardless of the burner used.

C. Beckman DK-2 Spectrophotometer

Some of the early exploratory work was done on a Beckman DK-2 spectrophotometer. This instrument consists of a monochromator, identical to that used in the Beckman DU spectrophotometer, together with an electronic readout system allowing either ratio or direct energy recording. A flat bed recorder is an integral part of the instrument. The monochromator is of the Littrow type and uses a silver-backed quartz prism as the dispersing element. The instrument is provided with bilateral entrance and exit slits which are operated by the same slit mechanism. Two radiation detectors are used in the DK-2. For the region between 600 mμ and 3 μ, a lead sulfide cell is available. An RCA 1P28 photomultiplier tube is used for the region between 2000 and 7000 Å. An attenuator in the photomultiplier circuit allows the operator to decrease the output of the photomultiplier by a factor of 20. No provision is made for adjustment of the dynode voltage. Although the DK-2 is basically a double beam spectrophotometer, provision is made for the substitution of a fixed reference signal in place of the variable reference beam used in ratio recording. This is known as the energy mode and is used when the DK-2 is employed as a flame photometer. The following controls are available for the adjustment of experimental conditions: sensitivity (gain),

time constant, zero and 100 percent setting, and slit width. A detailed explanation of the mode of operation of these controls has been given elsewhere (19) and will not be repeated here.

For recording of flame spectra the DK-2 was equipped with a Beckman flame attachment (Beckman Instruments #92490). This attachment consists of a block for holding the burner in a fixed position and a concave mirror which focuses the radiation from a selected portion of the flame onto the entrance slit of the monochromator. Three adjustment screws mounted in a triangular array on the back of the mirror mount provide the only means of selecting the portion of the flame to be studied.

D. Spectrographic Equipment

1. Spectrograph

Photographic recording of many of the flame spectra were made with a 21-foot Jarrell-Ash Wadsworth stigmatic, concave grating spectrograph. The particular instrument used here was equipped with a 15000 ruling/inch grating having a strong blaze at 3000 Å, and provided a reciprocal linear dispersion in the first order of approximately 5.2 Å/mm.

2. External optics

The choice of external optics was largely dictated by the requirement that the spectrograph be maintained in normal operating capability, i.e. conventional DC arc excitation. In normal operation, the external optical system consists of a three lens system similar to that described by Feldman and Ellenburg (26). The radiation from the sample gap is focused on a diaphragm by a single spherical condensing lens. The diaphragmed radiation then passes through two cylindrical lenses which have their axes perpendicular to one another. The function of the lenses is twofold: to illuminate the slit uniformly and to fill completely the aperture of the spectrograph. Both of these characteristics are highly desirable since the former is necessary if accurate emulsion calibration curves are to be drawn, and the latter ensures maximum speed with a minimum of scattered light. In order to maintain these desirable characteristics without affecting the normal operation of the spectrographic system, the burner was placed on the optical bench at the position normally occupied by the electrode diaphragm. With the burner placed in this position, all of the light from the flame passes through the crossed cylindrical lenses and all of the desirable optical features of this lens system remain fulfilled for the flame. Interchanging the burner and diaphragm is relatively simple since both are mounted on standard optical

bench riders. The only apparent disadvantage of this arrangement is that the vertical dimension of the solid angle subtended at the burner is relatively large (7 mm), limiting the utility of the spectrograph in studying flame parameters as a function of distance from the burner tip.

In order to provide a means of reproducibly varying the portion of the flame sampled, the device shown in Figure 4 was fabricated. The burner mounting slide (A) rides snugly in the keyways of the assembly plate (B). The position of the burner is determined by the fine screw (40 threads/inch) (C) which in turn threads into the assembly plate and is affixed to the bottom of the burner block (D). This entire assembly is mounted on a standard rider rod and base. Since no provision is made for horizontal adjustment of the burner position, it is necessary to center the burner by "reverse optics" at the time of original installation. This device was used for all studies in which any variable was studied as a function of the vertical dimension of the flame.

3. Intensity and wavelength measurements

A rotating eight step sector having a step factor of 1.585 was used in all of the spectrographic experiments. For those studies in which highly accurate relative intensities or intensity ratios were required, a Jarrell-Ash Model 2100 Console Microphotometer was used to measure line densities.

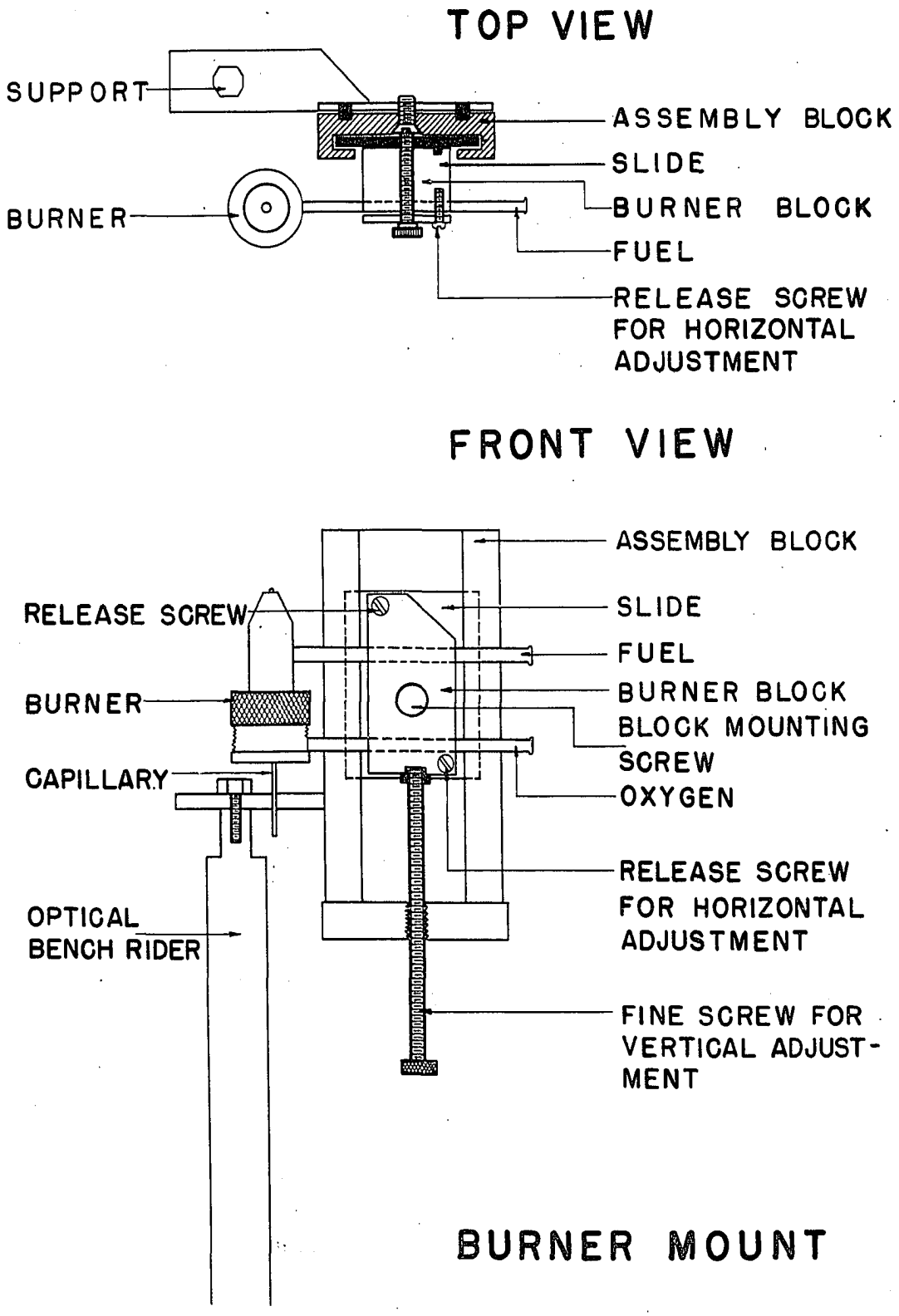

Figure 4. Adjustable burner mount

In those cases where maximum accuracy in the intensity measurements was neither required nor warranted, intensities were estimated by the expedient of counting the difference in step heights between the line in question and the chosen standard. The intensity ratios or relative intensities were then determined by the formula: Rel. Int. = $1.585^{\Delta n}$; where Δn is the difference in the number of steps between the two lines.

The microphotometer was fitted with a vernier attachment (Jarrell-Ash #22310). This attachment made it possible to use the microphotometer as a spectral comparator capable of measuring wavelengths with an accuracy of better than $\pm$ 0.1 Å. All of the wavelengths reported in this thesis were measured using this instrument.

All plate development, photographic photometry, plate calibration, and intensity calculation followed standard practices (27).

E. Grating Flame Photometer

The Beckman DK-2 spectrophotometer suffers from several faults which make it inadequate as a flame photometer for use in the type of study undertaken in this work. The resolution of this instrument, while adequate for the very simple spectra usually encountered in flame photometry, cannot successfully

cope with the more complex spectra which the rare earth elements exhibit. It has been stated (1, p. 80) that this monochromator will resolve 2.5 Å at 2000 Å with the slit widths normally used in flame photometry. Since this is a prism monochromator, the resolution becomes poorer at higher wavelengths until at 6000 Å, the instrument is capable of resolving only about 15 Å.

Another disadvantage of the DK-2 is the low electronic sensitivity. The instrument is designed for work with absorption spectra and is only incidentally convertible to use as a flame photometer. Consequently, the low intensity of flame spectra requires the use of maximum available sensitivity and high solution concentration. The sensitivity is limited by the electronic characteristics of the instrument rather than by the flame noise.

Inadequate zero suppression and poor wavelength reproducibility increase the difficulties encountered with this instrument.

To overcome the inadequacies enumerated above, a more elegant, grating flame photometer providing good resolution, precision, and stability was assembled. The building-block design of this instrument allows the selection of components for their ability to perform specific tasks. Ready interchange of components is possible, making the instrument versatile as well as specific.

The diagram shown in Figure 5 illustrates the mode of connection of the various components. The characteristics of each of these components are enumerated below.

1. Monochromator and optical components

The Jarrell-Ash #82000 Scanning Ebert Monochromator was used as the dispersing device. The characteristics of this instrument are given in Table 1.

The monochromator was bolted onto a metal stand, 17.5 cm high, to which a standard Jarrell-Ash optical bench was attached. The burner was mounted in a fashion identical to that described previously for the Wadsworth spectrograph. The radiation from the flame was focused on the entrance slit of the monochromator by means of a single spherical quartz condensing lens of 18 cm focal length. The lens was placed 27.5 cm from the entrance slit, while the burner was placed 44.0 cm from the same point. This system sampled a 4 mm high portion of the flame.

2. Detector

An EMI 6255B photomultiplier tube was used for detection of the spectral radiation. This tube is a two inch diameter end-on type having a 44 mm cathode. The photocathode surface is of the CsSbO (S-11) type. A quartz window gives the tube an overall S-13 response making it especially useful in the

Figure 5. Arrangement of electronic and optical components of the grating flame photometer

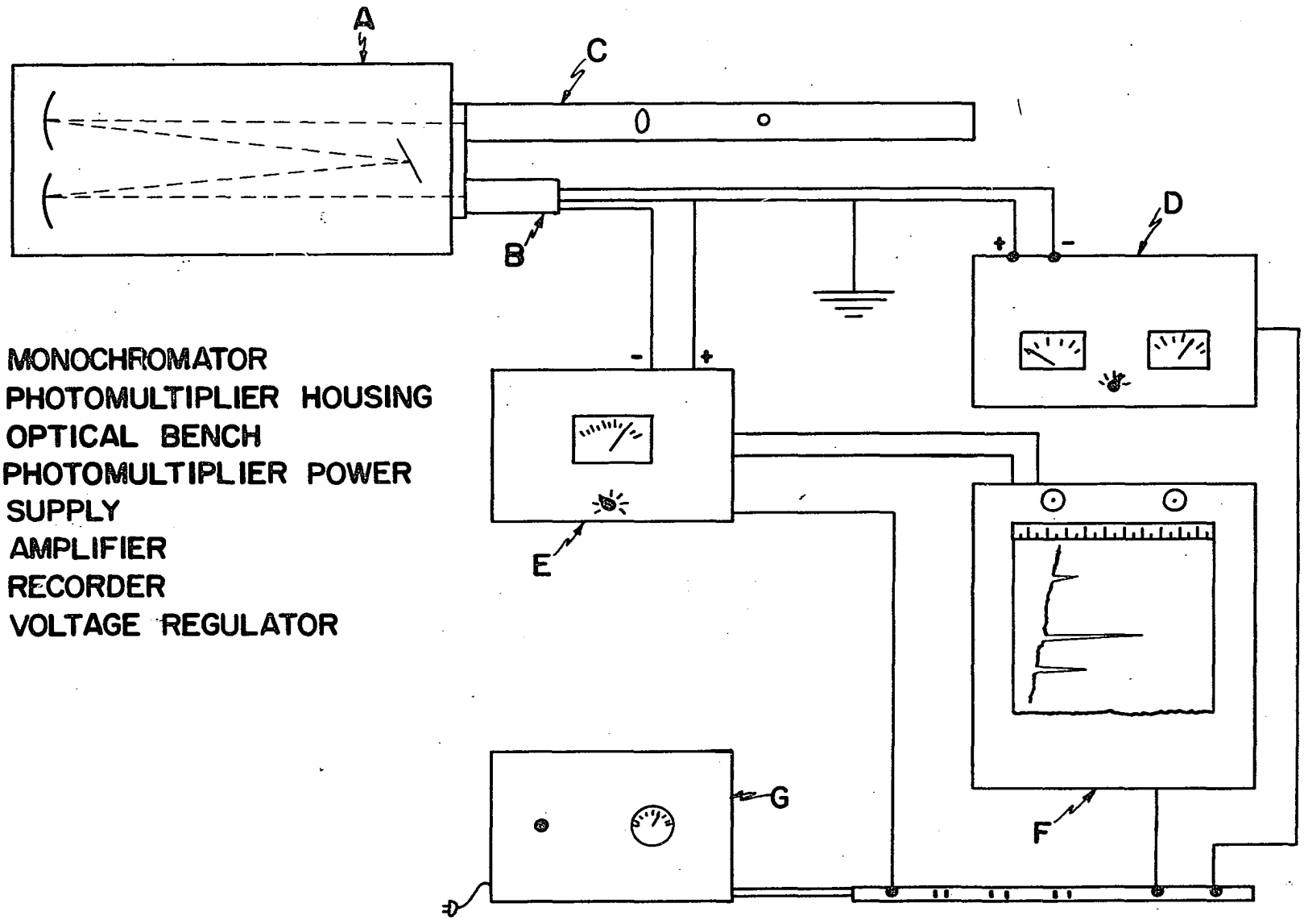

A. MONOCHROMATOR
B. PHOTOMULTIPLIER HOUSING
C. OPTICAL BENCH
D. PHOTOMULTIPLIER POWER SUPPLY
E. AMPLIFIER
F. RECORDER
G. VOLTAGE REGULATOR

Table 1. Characteristics of Jarrell-Ash #82000 Ebert scanning monochromator

Characteristic	Specifications
Optical arrangement	0.5 meter Ebert grating mount arranged as described by Fastie (28). Aperture f:9.
Grating	Plane, replica grating having a ruled area of 27 cm^2; 1200 lines/mm blazed for 5000 Å.
Slits	Fixed, bayonetting entrance and exit slits. Matched pairs having widths of 0.025 mm were used.
Dispersion and resolution	Reciprocal linear dispersion at exit slit is 16 Å/mm, first order. Resolution is at least 0.2 Å, first order using 0.010 mm slits.
Scanning action	Eight automatic scanning speeds are available. These are 500, 250, 125, 50, 20, 10, 5, and 2 Å/min. Manual scanning is possible. Accuracy of wavelength counter is ± 2 Å with reproducibility of ± 0.5 Å.

ultraviolet region of the spectrum. Its maximum response is at 4400 Å, while its useful sensitivity lies in the range from 1650 to 6500 Å.

Thirteen stages of amplification provide the 6255B with an overall sensitivity of 2000 amp/lumen when operated at 1400 volts. At this voltage the dark current is specified to be 2×10^{-7} amperes. In actual operation at 1500 volts, however, the dark current was found to be only 5×10^{-9} amperes. The high sensitivity of this tube is the major reason for the greatly improved overall sensitivity of this instrument over the DK-2. (The 1P28 photomultiplier used in the DK-2 has an S-5 response and a luminous sensitivity of 50 amp/lumen.)

The photomultiplier was mounted directly in front of the exit slit in a Jarrell-Ash #82060 photomultiplier housing.

3. Photomultiplier power supply

An NJE model S-325-RM power supply was used to provide the dynode voltage for the photomultiplier tube. This power supply was capable of supplying any voltage from 500 to 2500 volts at currents from 0 to 10 ma. The stability of the power supply was such that no discernible drift in the voltage output, and consequently in the photomultiplier output, was noticed for periods up to 40 hours.

4. Recorder preamplifier

A Leeds and Northrup 9836-B micro-microammeter was used to amplify the photomultiplier output up to the range of a standard potentiometer recorder. The 9836-B achieves an accuracy of ± 0.5 percent by using a combination of AC amplification and overall DC feedback. The incoming DC signal is converted to AC (60 cps) by use of a chopper. After four stages of AC amplification, the signal is reconverted to DC and fed back into the input circuit. The gain of the amplifier is sufficiently high that the output signal can drive a ten millivolt potentiometer recorder. Eleven equally spaced ranges from 2×10^{-6} to 10^{-9} amperes are available. The zero drift is negligible and the response time is less than 1.5 seconds.

5. Recorder

The output of the amplifier was fed into a Leeds and Northrup Speedomax G, Model S millivolt recorder. The recorder was modified to provide a continuously adjustable zero from -50 to +50 mv, and a continuously adjustable range from 1 to 50 mv full scale. The response time of the recorder was one second. A chart speed of one inch per minute was used in all cases.

All of the electronic components which required external line voltage were powered through a 2 KVA Sorensen

voltage regulator.

This instrument was used for all of the analytical studies which will be reported in this thesis.

IV. RECORDING OF SPECTRA

A. Preparation of Solutions

All solutions were prepared from pure rare earth oxides. The desired amount of oxide, after drying, was weighed and dissolved in a 1:1 mixture of water and acid. Both hydrochloric and perchloric acids were used in this investigation. After evaporating the solution to a thick slurry which solidified on cooling, the slurry was redissolved in the proper solvent (water, absolute ethanol, n-propanol, or acetone) and diluted to the desired volume. This procedure was applicable to all rare earth oxides except cerium dioxide. In the case of CeO_2 it was necessary to add periodically 30 percent hydrogen peroxide to the water-acid suspension of the oxide. Continuous stirring for one to three days, without heating, was necessary to effect dissolution of the cerium dioxide. After dissolution, the solution could be handled in the normal manner.

As will be seen, the anion-solvent combination which was found to be most useful was perchlorate-absolute ethanol. Certain precautions had to be observed in preparing these solutions because of the explosive nature of the compound which can form between perchloric acid and ethanol when these two are heated together (29). Special care was taken to

remove the excess perchloric acid upon evaporation, and to cool the solution before the addition of the absolute ethanol. No difficulty was experienced when these simple precautions were observed, nor was any to be expected (29). The perchlorate anion was found useful, not because of the effect it had upon the spectra, but because of the great ease with which redissolution of the evaporated slurry could be effected, both in aqueous and non-aqueous solvents.

B. Selection of Optimum Excitation Conditions

Figure 6 graphically illustrates the striking intensification of the rare earth line spectra observed when these elements are excited under proper experimental conditions. The four spectra of thulium shown in this figure were all run under experimental conditions which were as nearly identical as possible.

When an aqueous solution of thulium (as the perchlorate) was aspirated into the oxygen-hydrogen flame under the very low instrumental sensitivity employed here, only very weak radiation due to the TmO band was observed. Some intensification of the band was obtained when ethanol was substituted for water as the solvent. A few very weak thulium lines may also be observed in this spectrum. The most striking change in the character of the thulium flame

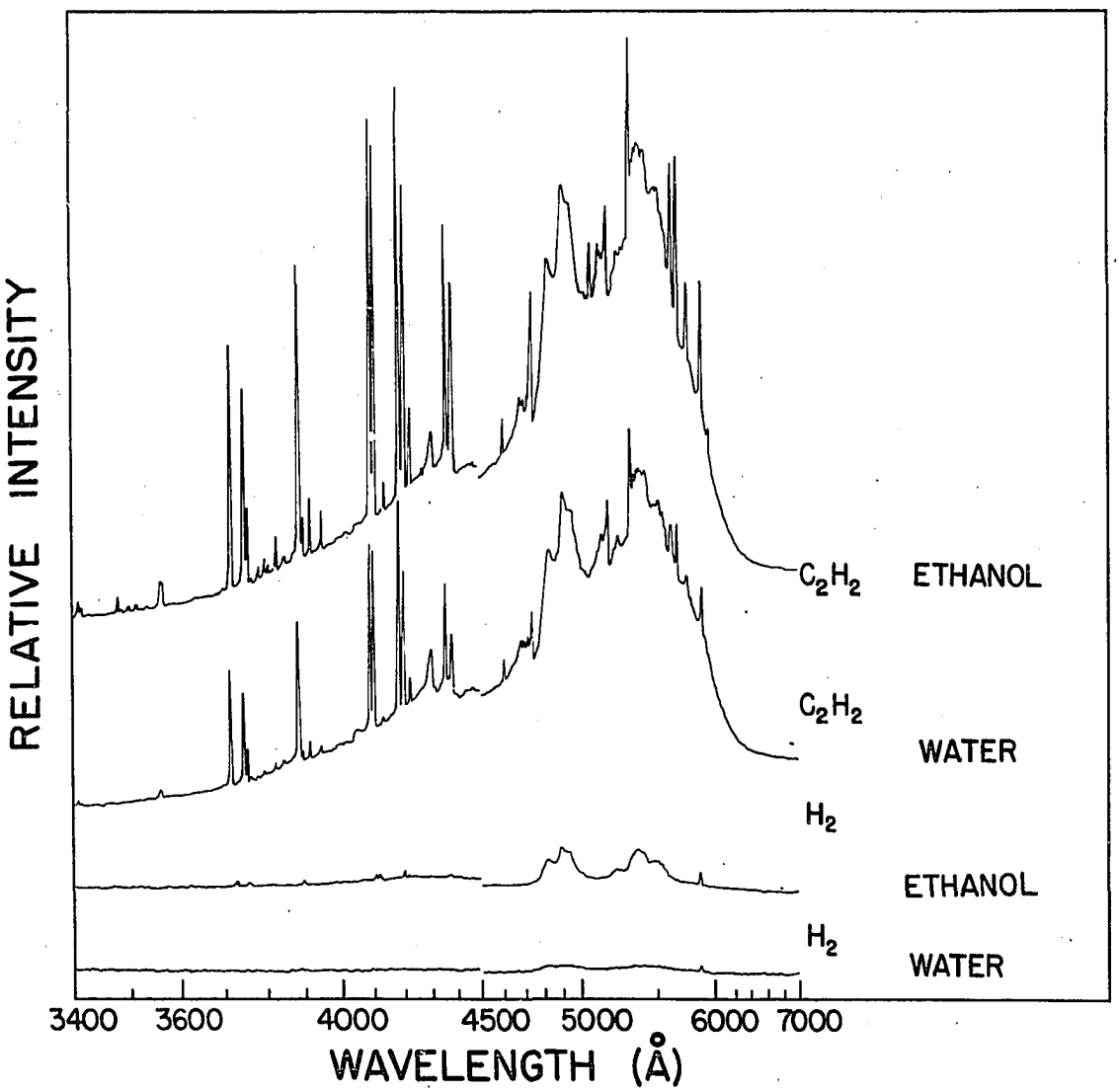

Figure 6. Effect of fuel and solvent on flame spectrum of thulium

spectrum occurred when acetylene was substituted for hydrogen as the combustible gas. Many rather strong thulium lines can be readily observed when an aqueous solution of this element is aspirated into the oxygen-acetylene flame. Of the four cases depicted in Figure 6, line spectra of maximum intensity are obtained when ethanol solutions are used with the oxygen-acetylene flame. It is interesting to note that while both the line and monoxide band spectra of thulium are enhanced by the oxygen-acetylene flame, the line spectra are enhanced to a much greater extent. The high background of oxygen-acetylene in the region of the TmO radiation makes this spectrum seem much stronger than it actually is. The effect which is illustrated here for thulium is typical of all the rare earths, the only difference being the degree of enhancement.

In order to obtain quantitative data on the experimental conditions which yielded maximum rare earth line intensity, systematic investigations were carried out to determine the effect of various organic solvents and mixture strength of the flame on line intensity. The large number of elements under investigation and the large number of lines which these elements exhibit made it impractical to study the individual behavior of each element or line. Rather, the study was conducted in such a fashion that the specific behavior of only a few elements (or lines) was determined. Spot checks were then made to determine if this behavior represented a trend.

Fortunately, it was found that the rare earths react in a remarkably similar manner to changes in the experimental variables studied.

1. Effect of organic solvents

Intensification of spectra through the use of organic solvents has become an accepted and widely applied technique in analytical flame photometry (1, pp. 51-64). The exact nature of the enhancements provided by organic solvents is a matter which is much debated and little understood. To date, no successful correlation of all the possible contributing factors, the sum of which might account for the overall enhancement, has been made.

The organic solvents which were investigated for possible use with the rare earth elements were acetone, n-propanol, and absolute ethanol. Of these three, absolute ethanol was found to have the most desirable characteristics. Acetone produced the greatest line intensification of the three, but salts of the rare earths proved to be sparingly soluble in it. Moreover, at the low oxygen flow rates which were found to produce maximum intensity, the acetone solution aspirated so slowly that reproducible atomization could not be maintained. n-propanol, even though it provided about the same enhancement as absolute ethanol, was not used because the dissolution of the rare earths in this solvent was

somewhat more difficult than in absolute ethanol.

The effect of the common anions; chloride, nitrate, sulfate, and perchlorate, on the spectra of the rare earths was assessed concurrently with the organic solvent studied. Chloride, nitrate, and sulfate had no discernible effect on the spectra. Perchlorate, however, did show some ability to modify the intensity of the rare earth lines. The magnitude of the effect depended on the element being studied; small enhancements being observed for some elements and small depressions for others when ethanol solutions were used. In aqueous solutions a small enhancement resulting from the substitution of perchlorate for chloride was always observed. Because of the great solubility of metal perchlorates, the ease of preparation of solutions was greatly enhanced. For this reason, the anion-solvent combination of perchlorate-absolute ethanol was chosen for use throughout this study.

Table 2 shows the magnitude of the enhancement due to ethanol and perchlorate for some lines and bands of dysprosium, holmium, and thulium. The relative intensities reported in the table were measured photographically. The index for all of the intensity measurements was the exposure of the aqueous solution of the element when chloride was used as the anion. This exposure was chosen because it was always the weakest and yielded numbers larger than unity for the other anion-solvent combinations.

Table 2. Effect of absolute ethanol and perchlorate on some rare earth flame spectra

Origin	Wavelength (Å)	Anion-solvent combination[a]		
		ClO_4^--C_2H_5OH	Cl^--C_2H_5OH	ClO_4^--H_2O
Dy	5974.50	4.60	4.65	1.07
Dy	5988.58	4.80	4.93	1.07
DyO	5855.6	1.78	1.73	1.19
DyO	5868.2	1.78	1.71	1.17
Ho	5860.28	4.01	4.22	1.23
Ho	5921.70	3.38	3.54	1.14
HoO	5728	1.24	1.40	1.35
Tm	3896.62	2.69	2.32	1.24
Tm	3916.47	3.05	2.60	1.18

[a]All intensities measured relative to Cl^--H_2O.

Enhancements of the same order of magnitude were observed for the other rare earth elements. It is pertinent to note that the use of an organic solvent has a much greater enhancement effect on the lines than it does on the monoxide bands. The significance of this observation will be discussed in a later section.

These experiments were conducted with the tip of the burner 22 mm below the portion of the flame being sampled. When a portion of the flame 37 mm above the tip of the burner was sampled and the experiments repeated, it was found that the line intensity from the spectra of aqueous

solutions was greatly reduced or completely quenched. On the other hand, the ethanol solutions gave line spectra which were only reduced in intensity by a factor of about two. The band spectra, while slightly less intense than at the lower flame position, were not affected to as great an extent as the lines. These observations are of some importance in terms of the excitation mechanism involved in production of the rare earth lines and consequently will be discussed in the section dealing with this subject. The most important conclusion which can be drawn is that the absolute intensities of the lines (and bands) were found to be at a maximum at the 22 mm position. Consequently, this burner position was used for all subsequent experiments when maximum line intensity was desired.

2. Selection of optimum mixture strength

Optimum line/background ratios were found to occur at oxygen and acetylene flow rates which produced a significantly fuel rich flame. Moreover, the optimum oxygen flow rate was found to be lower than would normally be encountered with the Beckman burner (1, p. 74). The low oxygen flow rate led to a sample aspiration rate of only about 0.7 ml/min. Because of the interdependence of sample aspiration rate and the oxygen and acetylene flow rates, it was not possible to find an oxygen-acetylene mixture which was best for all burners.

However, only slight variations from burner to burner were noted. Oxygen flow rates of 2.7 l/min and acetylene flow rates of 3.2 l/min were typical values. The optimum sample aspiration rate was largely dependent on the identity of the solvent being aspirated and was in the range from 0.7-0.9 ml/min for ethanol. Aqueous solutions aspirated almost twice as fast at the same oxygen flow rate. The aspiration rate was determined directly by aspirating the solution from a 5 ml graduate cylinder for a given period of time (usually two minutes) and noting the decrease in volume. The gas flows were measured directly with the equipment designed for this purpose.

Since both the oxygen and acetylene are expanded to atmospheric pressure before they are burned, the volume flow rates may be considered to be proportional to the molar flow rates. For a typical burner the oxygen/acetylene mole ratio is 2.7/3.2 = 0.84. For a stoichoimetric flame, assuming complete combustion to carbon monoxide and water

$$C_2H_2 + 1.5O_2 \rightarrow 2CO + H_2O$$

the oxygen/acetylene ratio would be 1.5. The above equation is only approximately true since other products such as CO_2, H_2, H, and OH are also formed (25, pp. 283-301). It does, however, represent the best single statement of the overall stoichiometry involved.

Physically, the flame produced by this very rich mixture is large, brilliantly white, and uniform, having no discernible flame zones. The background is characterized by high continuous radiation presumably from incandescent carbon particles, high CH and C_2 emission, and low OH omission.

C. Spectrophotometric Recording of Rare Earth Flame Spectra

Complete recordings of all of the rare earth spectra from 2800 to 9000 Å which are excited in the fuel-rich oxygen-acetylene flame are given in Figures 7-12. Instrumental conditions employed for these recordings are summarized in Table 3.

Comparison of these spectra with those shown in Figure 1 (obtained on the same instrument) reveal many interesting and surprising differences between the spectra excited in oxygen-hydrogen and those excited in fuel-rich oxygen-acetylene. Many of the rare earths exhibit strong atomic line spectra in oxygen-acetylene which were not observed in oxygen-hydrogen. This effect is not limited to elements such as samarium and thulium, for which weak line spectra have been observed in oxygen-hydrogen, but extends to many others. Europium and ytterbium, which exhibit strong line spectra in oxygen-hydrogen, are found to exhibit even more lines in the oxygen-acetylene flame. In fact all of the rare earths except lanthanum, cerium, praseodymium, gadolinium, and terbium show line spectra which appear to have analytical potentialities.

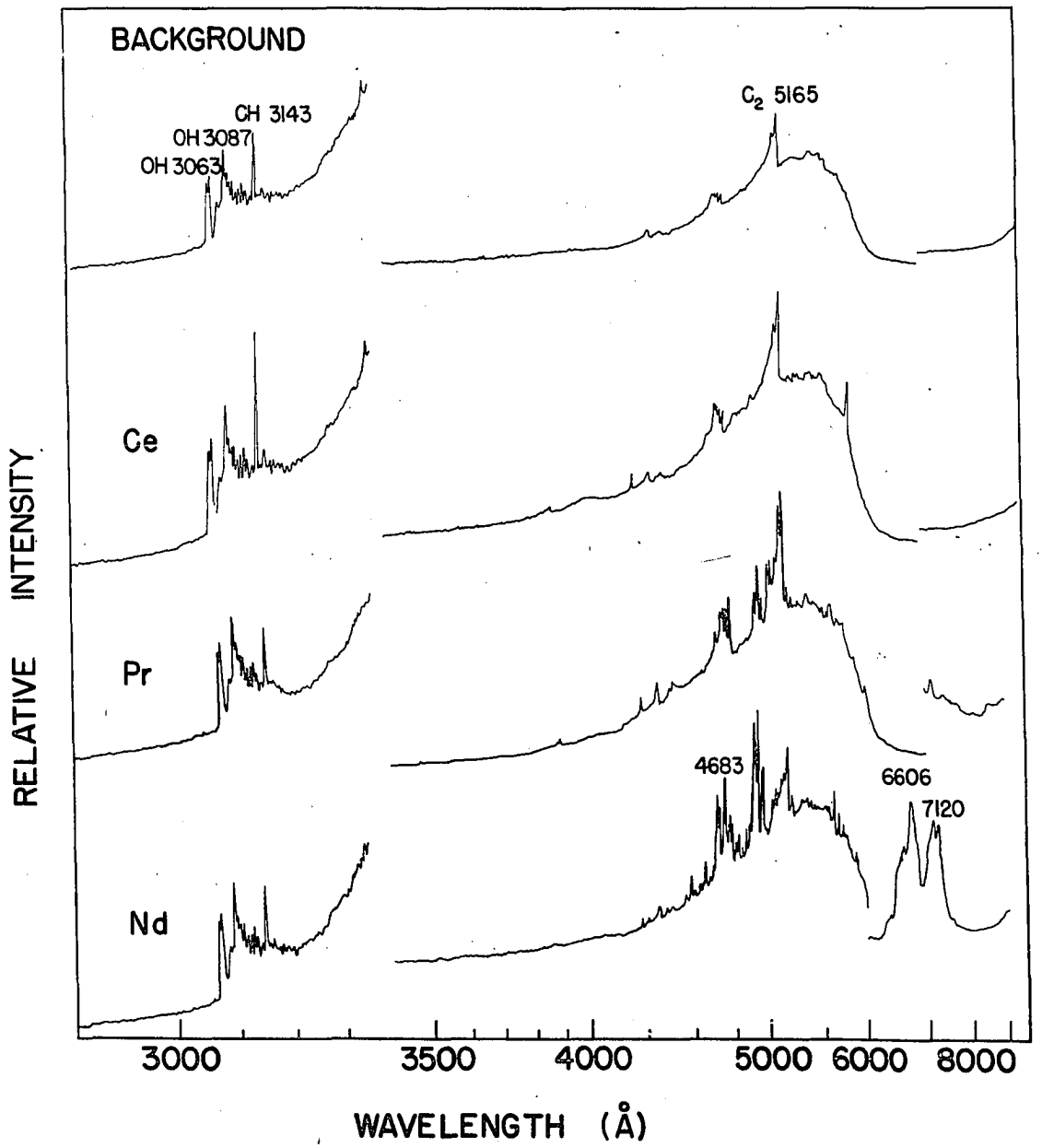

Figure 7. Fuel-rich oxygen-acetylene flame spectra of the flame background, cerium, praseodymium, and neodymium

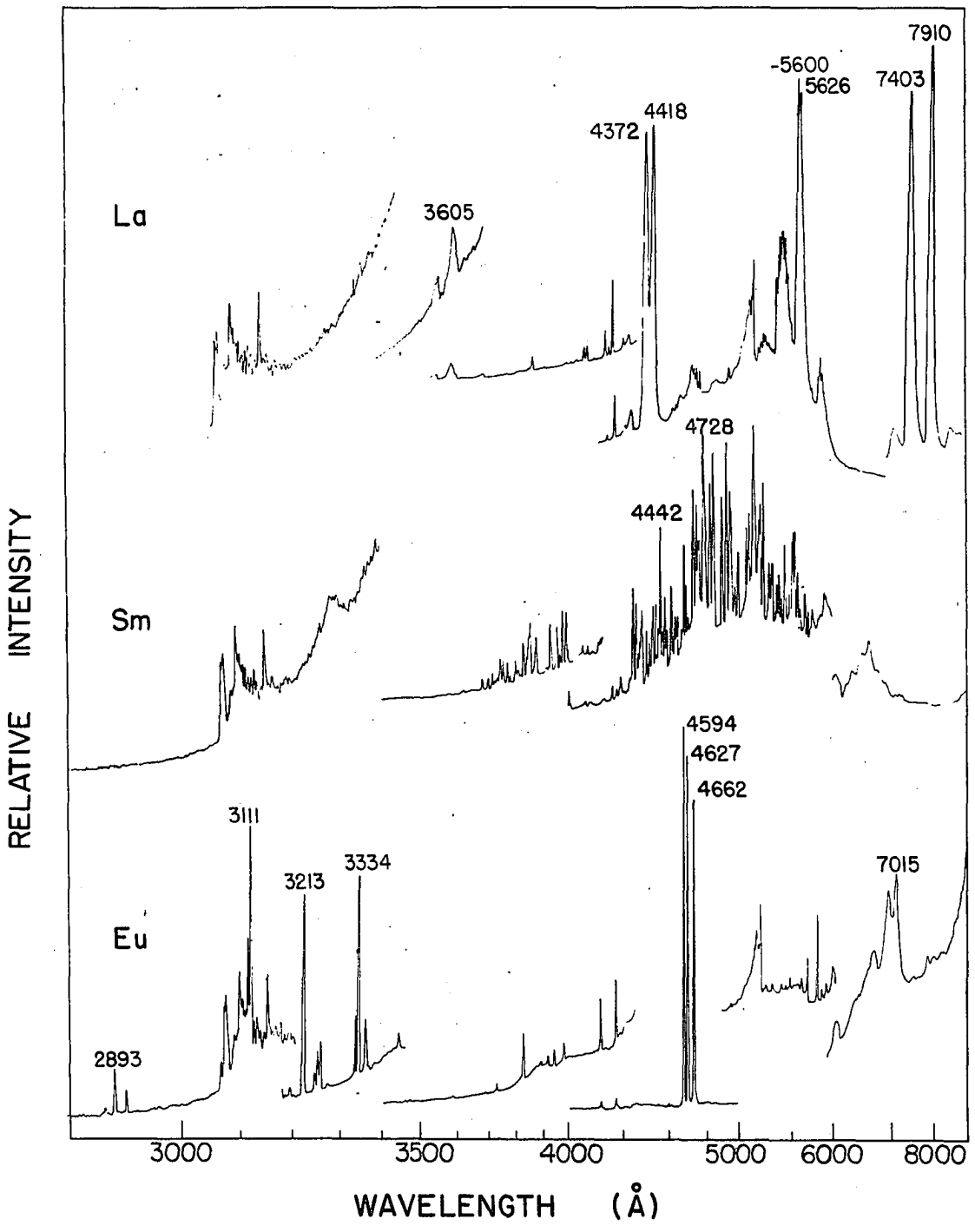

Figure 8. Fuel-rich oxygen-acetylene flame spectra of lanthanum, samarium, and europium

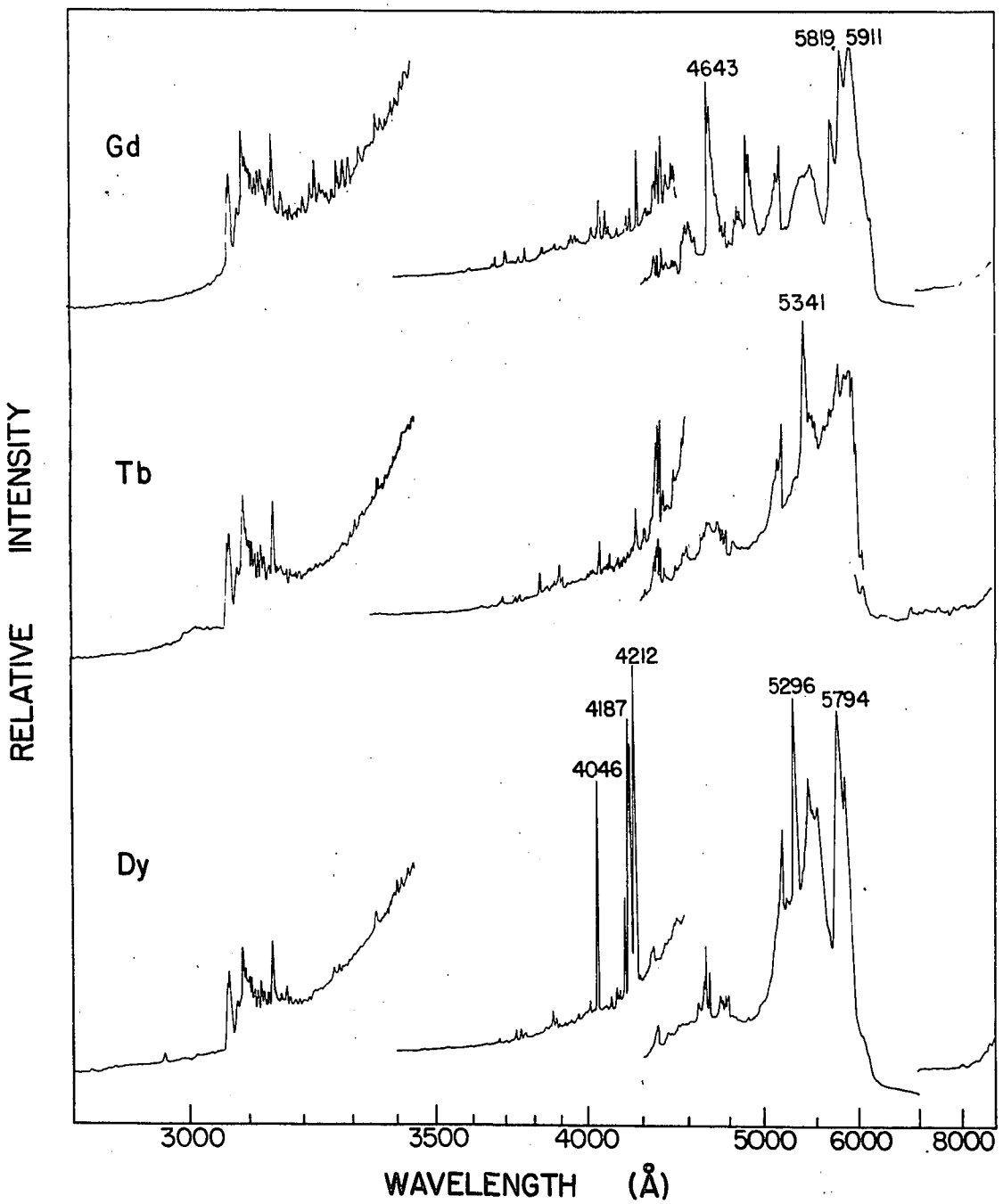

Figure 9. Fuel-rich oxygen-acetylene flame spectra of gadolinium, terbium, and dysprosium

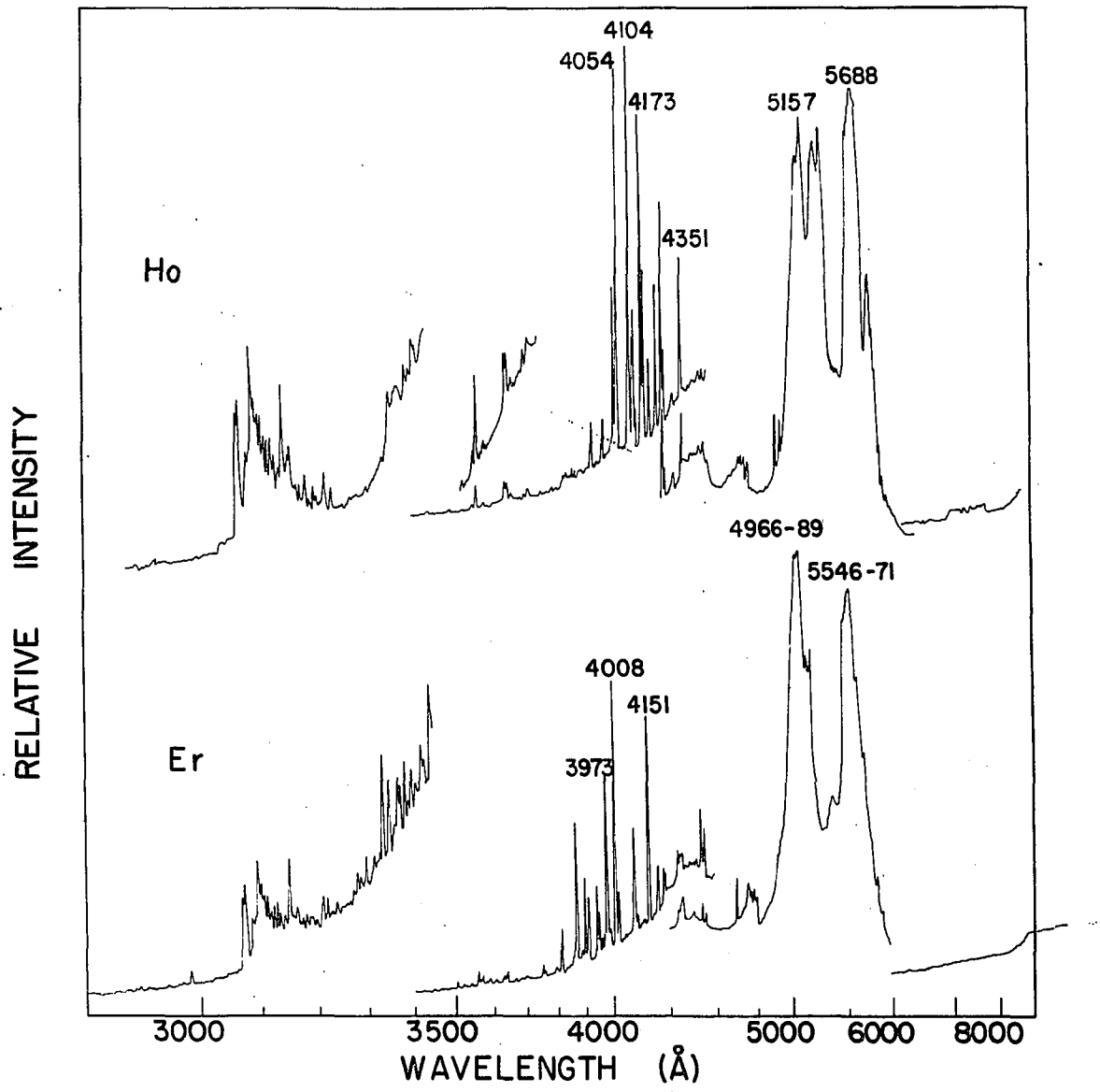

Figure 10. Fuel-rich oxygen-acetylene flame spectra of holmium and erbium

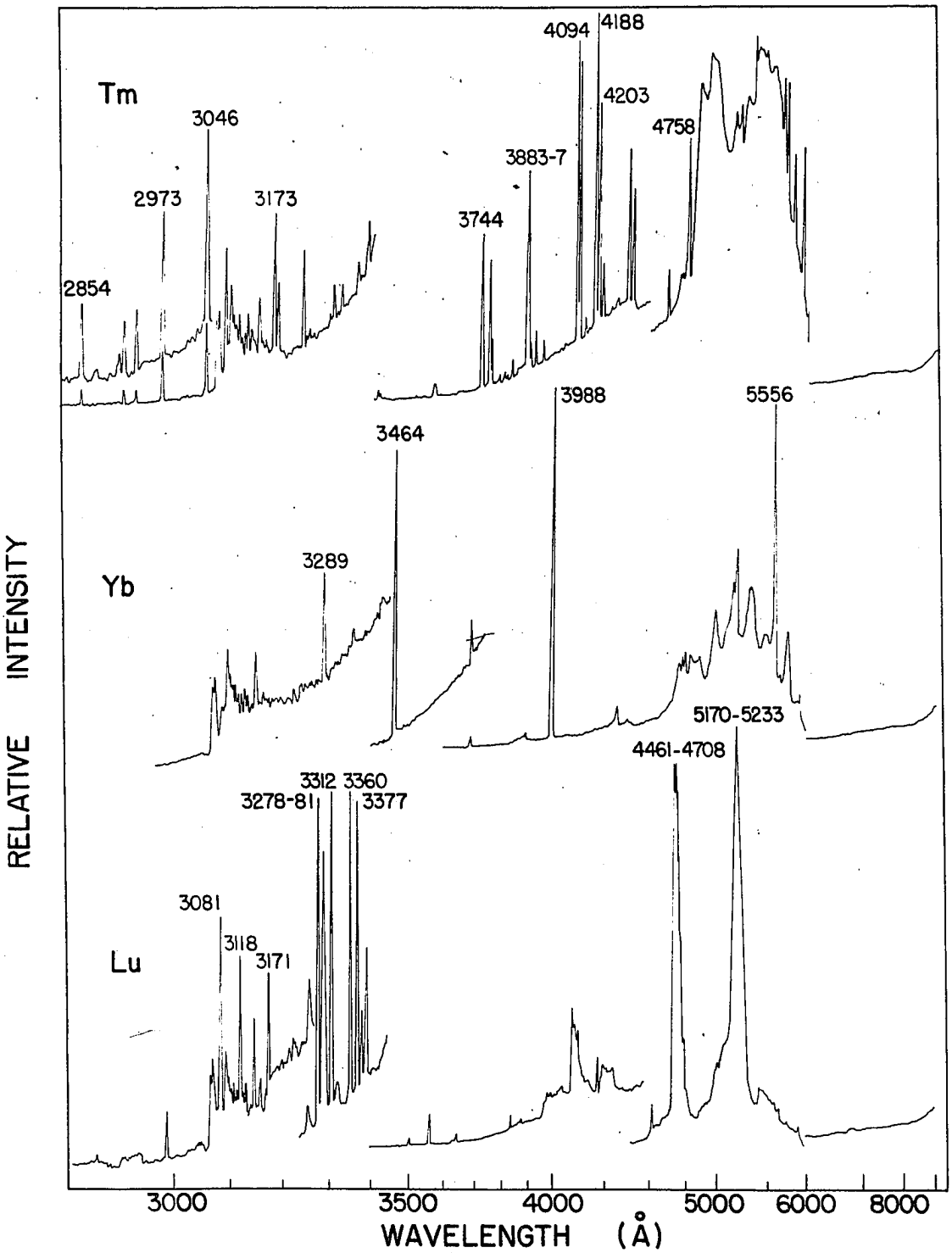

Figure 11. Fuel-rich oxygen-acetylene flame spectra of thulium, ytterbium, and lutetium

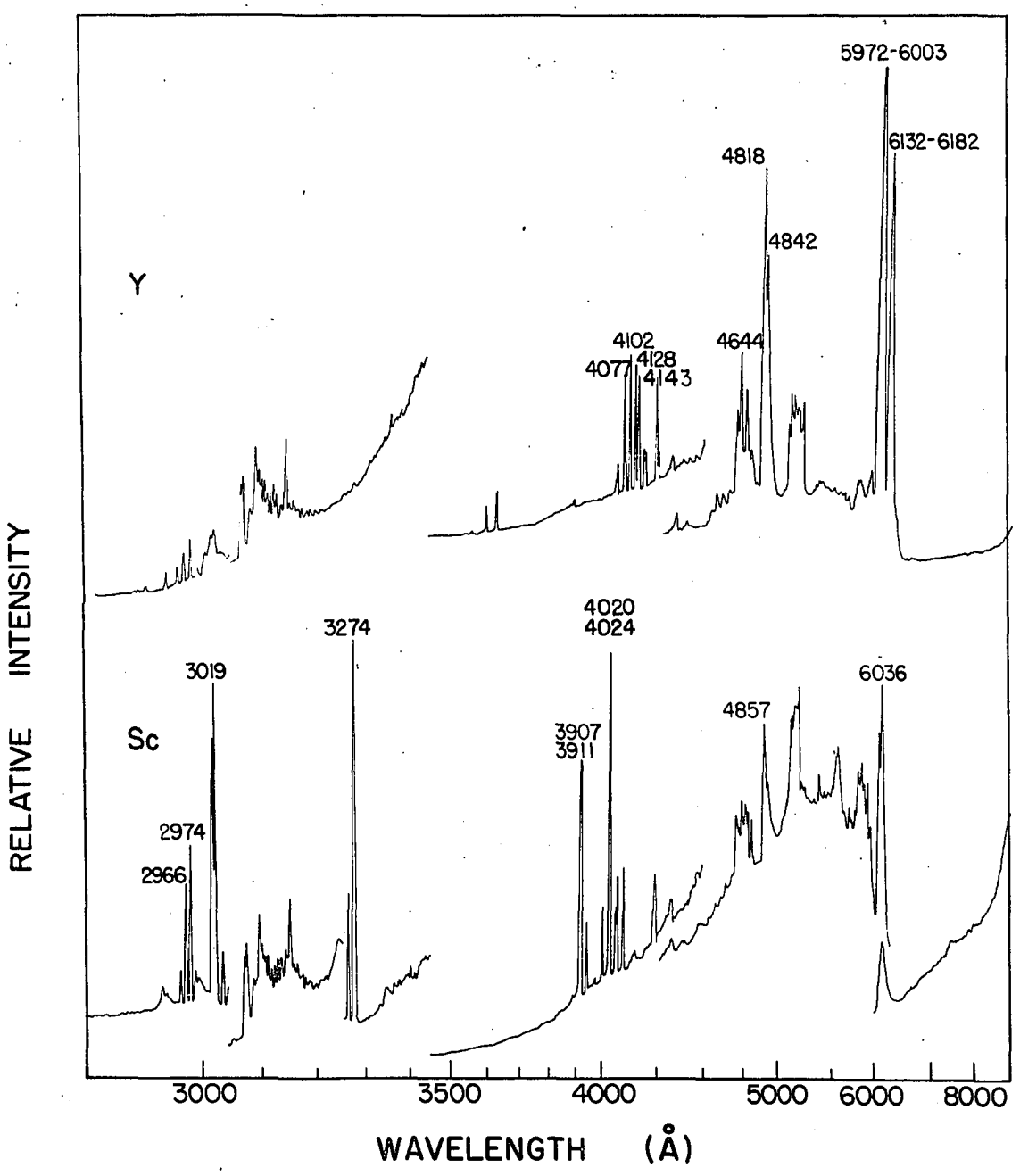

Figure 12. Fuel-rich oxygen-acetylene flame spectra of yttrium and scandium

Table 3. Experimental conditions for recording of rare earth flame spectra with Beckman DK-2 spectrophotometer

Gas flow rates	oxygen: 2.68 l/min acetylene: 3.16 l/min
Sample aspiration rate	0.68 ml/min
Concentration and constitution of solutions	2.00 percent rare earth oxide by weight as the perchlorate dissolved in absolute ethanol
Detectors	2800-6000 Å: RCA 1P28 photomultiplier tube. Sensitivity selector in 20x position. 6000-9000 Å: lead sulfide photoconductive cell (Beckman #92163)
Slit widths[a]	2800-3500 Å: 0.025mm 3450-6000 Å: 0.010 mm 6000-9000 Å: 0.050 mm
Sensitivity	3.10 (maximum)
Time constant	0.6 sec
Scan speed	50 min/revolution of the wavelength scroll

[a]These slit widths were used for the basic scan throughout the wavelength region. In some cases, however, a more sensitive scan was included along with the basic scan. The greater sensitivity was obtained through use of wider slits.

The appearance of most of the rare earth monoxide band spectra is considerably modified by the presence of high continuous background and the C_2 band with its head at 5165 Å. For the most part, however, the intense line spectra occur at lower wavelengths (3000-4500 Å) where this background does not interfere to any great extent.

The nature of the line spectra is a matter of considerable interest from the standpoint of the mechanism involved in their excitation. Unfortunately, however, little can be done toward identification of these spectra from the tracings shown here beyond the few tenuous identifications marked directly on the tracings. The rare earths show thousands of lines when excited in arcs and sparks which would make identification of the flame lines difficult even if the relative intensities were the same for the arc (or spark) as the flame. This proved not to be the case, however. Attempts to identify many of the strongest arc lines in the flame were unsuccessful. In a like manner, many of the strong flame lines could not be identified unambiguously in the atlases of arc and spark spectra. The inaccuracy of the wavelength scale and the low resolution of the DK-2 were responsible for much of the uncertainty but it was obvious that the intensity distribution of the lines observed here was vastly different from that found in the other emission sources. For these reasons, the further investigation of

these spectra was conducted on an instrument of much higher dispersion and capable of much greater accuracy in measuring wavelengths--the Wadsworth grating spectrograph.

D. Photographic Recording of Rare Earth Flame Spectra

Using the experimental arrangement described previously for the Wadsworth spectrograph, the spectra of the rare earths excited in oxygen-acetylene were photographed over the wavelength range from 2500 to 6900 Å. The experimental conditions used to make the exposures are given in Table 4.

Table 4. Experimental conditions for photographic recording of rare earth flame spectra with Jarrell-Ash Wadsworth grating spectrograph

Condition	Wavelength region	
	2500-4900 Å	4500-6900 Å
Photographic emulsion	Eastman III-O	Eastman II-F(3)
Exposure time	3 min	3 min
Order	first	first
Filter	none	Corning #7380
Slit width	0.040 mm	0.040 mm

Since it was necessary to photograph two wavelength regions in order to cover the desired range, the experimental conditions were chosen so that the intensity of the two exposures would be as nearly identical as possible. The solutions used and the flame conditions were identical to those listed in Table 3.

In order to obtain accurate wavelength measurements and intensity estimations from the same spectra, a special two position slit diaphragm was used. This diaphragm made it possible to photograph a reference iron arc spectrum in juxtaposition with an eight step flame spectrum. A rotating step sector having a step factor of 1.585 was used to attenuate the intensity of the flame spectra.

A reference plate containing an exposure of the flame background in juxtaposition with a 3 ampere iron arc was exposed. Iron lines were identified every 30 to 50 Å on the reference plate from the atlas of Gatterer (30). This plate was placed in the reference position in the Jarrell-Ash microphotometer and aligned with the plate containing the rare earth flame spectrum and iron arc. The vernier attachment was then employed to measure accurately the distance between an identified iron line and the rare earth line of unknown wavelength. The reciprocal linear dispersion of the spectrograph was determined by measuring the distance between two identified iron lines. From these data, the wavelength

of the rare earth line could be easily determined. The relative intensity of each rare earth line was estimated at the same time its wavelength was measured. Visual examination of the flame spectra indicated that the europium line at 4594 Å was the strongest rare earth line emitted in the flame. Consequently, this line was chosen as the intensity standard and assigned a relative intensity of 100. The relative intensities of the other lines were estimated by counting the difference in steps between the eighth (least intense) step of the europium line, which had a transmission of about 50 percent, and the step of the line in question having the same transmission. The relative intensity was then calculated by the formula:

$$\text{Rel. Int.} = \frac{100}{1.585^{\Delta n}}$$

where Δn is the difference in the number of steps. Since no corrections were made for variations in the sensitivity of the spectrograph-plate combination over the broad wavelength region employed here, the measured intensities were not necessarily consistent over the entire range. They are least accurate in regions where a high continuous background was present on the plate.

The measured wavelengths were corrected to the values given in the M.I.T. Wavelength Tables (31). If no corresponding line could be found in these tables, the atlas of rare earth lines of Gatterer and Junkes (32) was consulted. Wavelengths were corrected to these values only when the wavelength was not available in the M.I.T. Tables. In some instances no lines corresponding to the wavelengths measured in the flame could be found in either of these works.

The wavelengths and intensities of the rare earth flame lines are given in Table 5. All available energy level data for these lines are also listed in this table. No rare earth monoxide band spectra are included since the wavelengths of these bands have been reported elsewhere (20, 33).

All of the rare earths except cerium exhibited line spectra strong enough to be included in Table 5. The approximately 1200 lines listed in this table represent about half of the total rare earth lines actually observed on the photographic plates. The lines not included were so weak, however, that they would represent a very small fraction of the total intensity. Even cerium was found to emit 72 very weak lines under these conditions.

Table 5. Wavelengths of rare earth lines excited in a fuel-rich oxygen-acetylene flame

Wavelength[a] (Å)	Intensity	Origin[b]	Energy levels	
			Lower	Upper
		Lanthanum[c]		
3574.43	2	I	0.00	3.47
3927.56	2		0.00	3.15
4007.66	2	II	unclassified[d]	
4015.39	3	I	0.13	3.22
4037.21	3		0.00	3.12
4060.32	2		0.51	3.56
4064.78	2		0.43	3.48
4079.18	2		0.00	3.04
4089.61	1		0.37	3.40
4104.88	2		0.33	3.35
4137.02	1		0.13	3.12
4160.26	1		0.13	3.11
4187.32	4		0.00	2.95
4280.26	5		0.13	3.01
4549.50	1		0.37	3.08
4567.91	1		0.43	3.13
4570.03	1		0.51	3.21
4766.89	2		0.00	2.60
4850.82	1		0.13	2.68

[a]Measured wavelengths are corrected to values given in M.I.T. Wavelength Tables (31) except those marked by * which denotes wavelength corrected to value given by Gatterer and Junkes (32) or by ** which denotes a line for which no corresponding wavelength was found in either of the above works. In this case the wavelength is given to the nearest 0.1 Å as measured by the author.

[b]I indicates neutral atom line; II indicates ion line; N indicates no data available; no entry in this column means that origin is the same as the last entry above.

[c]Energy level data taken from Russell and Meggers (34).

[d]A line which the classifying authors observed but could not classify is denoted throughout the table by the word "unclassified".

Table 5. (Continued)

Wavelength[a] (Å)	Intensity	Origin[b]	Energy levels	
			Lower	Upper
		Lanthanum[c] (Continued)		
4949.77	3	I	0.00	2.49
5145.42	3		0.37	2.77
5158.69	3		0.13	2.40
5177.31	3		0.43	2.82
5211.87	2		0.51	2.88
5234.27	2		0.51	2.87
5253.46	2		0.13	2.49
5271.20	3		0.13	2.47
5455.15	6		0.13	2.39
5501.34	8		0.00	2.24
5740.66	2		0.33	2.48
5761.84	1		0.33	2.48
5769.35	2		0.37	2.51
5789.25	4		0.43	2.56
5791.34	4		0.51	2.64
5930.63	7		0.13	2.21
5930.67			0.00	2.08
6249.93	6		0.51	2.48
6325.92	3		0.13	2.08
6394.23	8		0.43	2.36
6410.99	5		0.37	2.30
6454.53	3		0.33	2.25
6455.99	8		0.13	2.04
6543.15	5		0.33	2.22
6578.51	10		0.00	1.88
6616.58	1		0.43	2.30
6644.41	1		0.13	1.99
6650.80	4		0.00	1.86
6661.40	1		0.51	2.37
		Praseodymium[e]		
4163.01	2	N		
4408.84	1	II	0.00	2.80
4519.63	1	N		

[e]Energy level data taken from Moore (35).

Table 5. (Continued)

Wavelength[a] (Å)	Intensity	Origin[b]	Energy levels	
			Lower	Upper
	Praseodymium[e] (Continued)			
4532.34	1	N		
4541.27	1			
4552.26	2			
4632.28	2			
4635.69	3			
4639.55	3			
4639.88	2			
4646.99	1			
4660.91	1			
4674.80	2			
4687.81	3			
4695.77	3			
4713.10	2			
4730.69	3			
4744.16	2			
4808.19	1			
4896.13	1			
4906.98	1			
4914.03	4			
4924.59	5			
4936.00	1			
4939.73	5			
4940.30	4			
4951.36	15			
4960.26	1			
4974.92	1			
4975.75	1			
4976.40	2			
5018.58	4			
5019.75	4			
5026.97	7			
5033.38	3			
5043.83	4			
5045.53	4			
5053.40	4			
5087.11	3			
5133.42	15			
5139.80	1			
5194.41	2			

Table 5. (Continued)

Wavelength[a] (Å)	Intensity	Origin[b]	Energy levels	
			Lower	Upper
	Praseodymium[e] (Continued)			
5195.31	1	II	0.79	3.17
5228.00	4	N		
5285.63	1			
5460.25	1			
	Neodymium[f]			
4256.48	1	N		
4343.50	1			
4444.98	3			
4456.13	3			
4477.88	4			
4480.97	7			
4481.89	4			
4497.38	1			
4527.24	2			
4529.76	3			
4542.05	4			
4548.24	2			
4559.18	1			
4559.67	5			
4560.42	4			
4561.85	2			
4567.34	1			
4586.61	4			
4594.67	1			
4603.82	1			
4609.87	4			
4621.94	8			
4624.20	2			
4626.50	2			
4627.99	3			
4631.29	1			
4634.23	25			
4637.21	3			
4639.14	4			

[f]No energy level data available.

Table 5. (Continued)

Wavelength[a] (Å)	Intensity	Origin[b]	Energy levels	
			Lower	Upper
	Neodymium[f] (Continued)			
4641.10	4	N		
4644.98	1			
4646.40	6			
4649.67	8			
4651.02	4			
4652.39	5			
4654.73	7			
4671.09	3			
4673.97	1			
4675.52	1			
4683.44	20			
4684.04	4			
4688.56	1			
4690.34	7			
4696.44	4			
4698.30	1			
4706.96	7			
4719.03	15			
4726.56	2			
4731.78	7			
4734.91	2			
4749.75	5			
4755.85	2			
4758.50	2			
4759.34	2			
4760.46	2			
4770.19	4			
4772.26	2			
4778.40	2			
4779.46	6			
4787.43	1			
4806.62	4			
4835.66	2			
4836.62	5			
4853.34	3			
4855.32	3			
4859.59	2			
4866.73	5			
4869.28	1			

Table 5. (Continued)

Wavelength[a] (Å)	Intensity	Origin[b]	Energy levels	
			Lower	Upper
		Neodymium[f] (Continued)		
4879.79	2	N		
4881.71	1			
4883.81	8			
4885.01	2			
4891.06	10			
4893.22	4			
4896.93	20			
4901.54	7			
4901.85	13			
4907.28	1			
4907.79	1			
4910.06	5			
4913.42	10			
4924.53	35			
4944.83	15			
4950.28	1			
4950.72	1			
4952.51	3			
4954.78	15			
4963.33	3			
4969.75	2			
4975.49	3			
4988.65	1			
5014.54	1			
5027.15	1			
5029.45	3			
5040.19	2			
5056.89	5			
5071.87	2			
5074.6 **	2			
5103.11	3			
5105.35	2			
5149.56	2			
5198.07	2			
5199.73	2			
5204.38	3			
5213.23	1			
5284.35	1			
5288.16	1			
5291.66	1			

Table 5. (Continued)

Wavelength[a] (Å)	Intensity	Origin[b]	Energy levels	
			Lower	Upper
		Neodymium[f] (Continued)		
5298.88	1	N		
5334.33	1			
5349.58	1			
5377.79	3			
5523.94	1			
5525.72	1			
5529.07	2			
5561.17	5			
5611.18	15			
5669.77	3			
5675.97	15			
5729.29	8			
5749.19	1			
5749.66	3			
5772.16	2			
5776.12	3			
5784.96	3			
5788.22	2			
5800.09	2			
5826.74	2			
5839.13	1			
5887.91	5			
5921.22	2			
6000.04	1			
6007.67	1			
6310.49	1			
6385.20	3			
6397.3 **	1			
6485.69	3			
		Samarium[g]		
3629.22	2	N		
3657.32	2	I	0.04	3.42
3687.88	2		0.39	3.75
3690.08	4		0.28	3.64

[g]Energy level data taken from Albertson (36, 37).

Table 5. (Continued)

Wavelength[a] (Å)	Intensity	Origin[b]	Energy levels	
			Lower	Upper
	Samarium[g] (Continued)			
3721.02	1	I	0.18	3.51
3722.02	1		0.10	3.43
3728.16	1		0.10	3.42
3730.73	1		0.28	3.60
3737.13	2	N		
3745.46	3	I	0.18	3.49
3748.51	3		0.04	3.34
3756.41	3		0.10	3.40
3760.05	1		0.10	3.39
3773.34	3	N	unclassified	
3782.68	1			
3803.94	5	I	0.00	3.26
3809.95	2		0.50	3.64
3813.82	2		0.50	3.75
3818.35	1		0.18	3.43
3822.96	1		0.10	3.34
3832.80	2		0.28	3.51
3834.47	7		0.50	3.73
3846.76	1		0.04	3.26
3848.81	3	N		
3853.29	5	I	0.39	3.60
3854.56	5		0.18	3.40
3858.74	5		0.28	3.49
3860.14	3	N		
3877.47	4	I	0.50	3.69
3881.79	7	N		
3925.20	10	I	0.10	3.26
3951.88	8	N	unclassified	
3962.14	4			
3974.66	10	I	0.28	3.40
3978.24	1		0.18	3.30
3990.00	10		0.39	3.55
3991.02	3	N	unclassified	
3998.35	5		unclassified	
4054.51	1			
4062.32	2	I	0.39	3.44
4079.83	3		0.28	3.32
4099.95	2	N		
4125.24	2			

Table 5. (Continued)

Wavelength[a] (Å)	Intensity	Origin[b]	Energy levels	
			Lower	Upper
	Samarium[g] (Continued)			
4135.50	3	I	0.18	3.18
4145.24	3	N	unclassified	
4151.21	2	I	0.18	3.17
4183.33	8		0.18	3.15
4205.77	5	N	unclassified	
4218.63	2			
4219.30	3	I	0.04	2.97
4226.17	8		0.10	3.03
4230.77*	2		0.00	2.93
4240.45	3		0.18	3.11
4244.24	2		0.04	2.95
4266.31	4		0.10	3.00
4271.86	5		0.28	3.18
4282.20	15		0.39	3.28
4282.83	15		0.28	3.17
4283.50	15		0.10	2.99
4296.75	20		0.50	3.37
4299.14	5		0.04	2.92
4301.28	2		0.10	2.98
4312.85	5		0.28	3.15
4313.87	2		0.10	2.97
4319.53	15		0.18	3.05
4324.46	8		0.28	3.15
4325.15	2		0.28	3.15
4326.13	2		0.50	3.36
4330.01	20		0.04	2.90
4331.44	20	N	unclassified	
4334.15	7	II	0.28	3.12
4336.13	20	I	0.39	3.24
4339.35	5	N		
4339.93	2	I	0.10	2.95
4350.81	3		0.18	3.03
4355.83	2		0.04	2.88
4357.89	2		0.39	3.23
4362.91	15		0.00	2.84
4365.95	3		0.10	2.94
4380.42	13		0.18	3.01
4386.22	5		0.28	3.11
4393.18	1		0.50	3.32
4397.35	10		0.10	2.92

Table 5. (Continued)

Wavelength[a] (Å)	Intensity	Origin[b]	Energy levels	
			Lower	Upper
	Samarium[g] (Continued)			
4401.17	20	I	0.39	3.20
4403.05	40		0.28	3.09
4411.58	30		0.18	2.99
4419.34	45		0.04	2.84
4420.53	1	II	0.33	3.12
4421.14	1		0.38	3.17
4423.38	7	I	0.04	2.84
4424.34	3	II	0.48	3.27
4429.64	40	I	0.10	2.90
4433.07	40		0.04	2.83
4433.88	3	II	0.43	3.22
4434.32	3		0.38	3.16
4441.80	40	I	0.18	2.97
4443.27	5		0.28	3.07
4445.15	40		0.39	3.17
4450.5 **	20	N		
4456.71	1	I	0.10	2.88
4458.7 **	1	N		
4459.29	25	I	0.10	2.88
4463.89	2		0.28	3.06
4467.34	1	II	0.66	3.42
4470.89	50	I	0.28	3.15
4477.49	5		0.39	3.15
4480.31	30		0.00	2.76
4490.02*	2		0.39	3.15
4499.10	35		0.18	2.94
4503.38	35		0.04	2.79
4511.31	8		0.50	3.24
4522.54	10		0.18	2.92
4523.18	15		0.10	2.84
4527.42	6		0.10	2.84
4532.44	7		0.18	2.92
4533.80	20		0.28	3.01
4537.56	2		0.10	2.83
4550.04	3		0.28	3.00
4556.63	2		0.39	3.11
4566.78	7		0.18	2.90
4569.58	5		0.28	2.99
4581.58	50		0.10	2.80
4596.75	20	N	unclassified	

Table 5. (Continued)

Wavelength[a] (Å)	Intensity	Origin[b]	Energy levels	
			Lower	Upper
	Samarium[g] (Continued)			
4598.36	3	I	0.18	2.88
4611.26	10		0.10	2.79
4629.43	1		0.50	3.17
4645.40	35		0.04	2.70
4648.08	15		0.39	3.05
4649.49	35		0.10	2.76
4663.55	18		0.28	2.94
4670.77	35		0.18	2.84
4681.56	15		0.18	2.83
4688.74	25		0.28	2.92
4716.11	30		0.39	3.01
4717.09	30		0.00	2.63
4718.67	3		0.39	3.01
4728.44	50		0.18	2.80
4750.73	10		0.28	2.88
4760.26	50		0.10	2.78
4770.19	6		0.28	2.88
4783.10	35		0.04	2.63
4785.87	30		0.10	2.69
4789.96	8		0.39	2.97
4841.70	35		0.50	3.06
4848.33	20		0.28	2.84
4883.78	40		0.04	2.57
4904.98	15		0.10	2.63
4910.41	30		0.28	2.80
4918.98	27		0.18	2.70
4924.06	7		0.50	3.01
4946.31	8		0.18	2.69
4975.99	20		0.10	2.57
5044.28	20		0.18	2.64
5049.50	3		0.04	2.49
5060.92	3		0.18	2.63
5071.19	20	N	unclassified	
5088.32	4		unclassified	
5117.16	35		unclassified	
5122.14	25	I	0.39	2.81
5157.22	7		0.04	2.44
5172.74	15		0.28	2.68
5175.42	20	N	unclassified	

Table 5. (Continued)

Wavelength[a] (Å)	Intensity	Origin[b]	Energy levels	
			Lower	Upper
	Samarium[g] (Continued)			
5187.08	3	I	0.18	2.57
5200.59	55		0.18	2.57
5210.75	1		0.28	2.66
5251.89	17		0.28	2.64
5265.65	3		0.00	2.35
5271.40	40		0.10	2.45
5282.91	15		0.18	2.53
5320.60	13		0.28	2.61
5341.29	15		0.04	2.36
5348.09	3		0.04	2.35
5349.14	4		0.10	2.42
5350.62	3	N		
5368.36	15	I	0.50	2.81
5403.69	15		0.18	2.48
5405.24	20		0.04	2.33
5416.35	5	N		
5421.57	5	I	0.28	2.57
5453.02	20		0.39	2.66
5466.73	20		0.18	2.45
5485.42	15		0.00	2.26
5493.72	33		0.10	2.36
5498.21	18		0.04	2.29
5511.10	3		0.28	2.53
5512.10	15		0.10	2.35
5516.14	30		0.04	2.27
			0.28	2.52
5548.95	10	N	unclassified	
5550.40	15	I	0.18	2.42
5561.38	1		0.10	2.33
5573.43	3		0.39	2.61
5574.91	5		0.04	2.26
5588.19	2		0.28	2.50
5621.80	8		0.04	2.24
5626.01	12		0.00	2.20
5659.86	15		0.10	2.29
5725.59	2	N		
5732.95	5	I	0.50	2.66
5773.77	1	N		
5778.33	1			

Table 5. (Continued)

Wavelength[a] (Å)	Intensity	Origin[b]	Energy levels	
			Lower	Upper
	Samarium[g] (Continued)			
5779.25	5	I	0.18	2.33
5788.39	4	N		
5790.92	1	I	0.10	2.24
5800.50	1	N		
5803.11	10	I	0.28	2.42
5840.9 **	1	N		
5867.79	10	I	0.39	2.50
5868.62	5		0.50	2.61
5871.06	5		0.39	2.50
5874.19	7		0.10	2.09
5875.93	3		0.18	2.29
5895.15	1	N		
5898.96	1			
5902.60	5	I	0.28	2.38
5906.07	5		0.18	2.28
5909.04	5		0.28	2.37
5916.37	7		0.04	2.13
5979.39	7		0.18	2.26
5989.69	1		0.00	2.07
5995.10	1		0.28	2.35
6004.20	5		0.10	2.16
6027.16	5		0.39	2.44
6044.99	8		0.28	2.33
6070.07	8		0.18	2.22
6084.13	10	N	unclassified	
6099.92	2	I	0.04	2.07
6117.79	2		0.18	2.21
6159.56	3		0.28	2.29
6174.96	1	N		
6194.41	1	I	0.39	2.39
6347.43	1		0.18	2.13
6425.91	1		0.28	2.21
6528.02	4		0.28	2.18
6551.80	2	N	unclassified	
6563.52	1	I	0.28	2.17
6580.53	2	N	unclassified	
6588.92	7	I	0.39	2.26
6671.48	10		0.50	2.35
6725.90	7		0.00	1.84

Table 5. (Continued)

Wavelength[a] (Å)	Intensity	Origin[b]	Energy levels	
			Lower	Upper
		Samarium[g] (Continued)		
6775.30	1	I	0.10	1.93
6779.16	3		0.04	1.86
6802.96	2		0.10	1.92
6827.81	2		0.18	2.00
6853.92	1		0.28	2.09
6861.06	4	N		
		Europium[e]		
3106.17	2	N		
3111.43	6			
3210.57	4			
3212.81	6			
3213.75	4			
3241.40	1			
3247.53	1			
3322.26	2			
3334.33	10			
3350.43	1			
3467.89	1			
3588.55	2			
3724.99	3	II	0.00	3.31
3819.66	10	N		
3907.11	5	II	0.21	3.36
3930.50	5		0.21	3.35
3971.99	5		0.21	3.31
4129.62	15	N		
4129.74	15	II	0.00	2.99
4205.05	10		0.00	2.93
4435.53	10		0.21	2.99
4522.58	3		0.21	2.93
4594.02	100	I	0.00	2.69
4627.12	90		0.00	2.67
4661.88	85		0.00	2.65
4907.17	1	N		
4911.41	1			
5114.36	2			
5129.08	1			
5133.48	2			

Table 5. (Continued)

Wavelength[a] (Å)	Intensity	Origin[b]	Energy levels	
			Lower	Upper
	Europium[e] (Continued)			
5160.07	1	N		
5166.72	1			
5215.09	2			
5223.48	1			
5266.40	1			
5271.95	2			
5282.82	1			
5357.61	2			
5402.79	3			
5451.53	3			
5452.96	3			
5488.65	1			
5510.55	1			
5547.45	2			
5570.36	2			
5577.13	2			
5580.04	1			
5645.80	25			
5765.20	60			
5783.71	1			
5800.27	1			
5831.05	10			
5963.76	1			
5967.16	10			
5972.78	2			
5992.86	2			
6018.19	1			
6029.01	80			
6044.67	1			
6057.36	1			
6083.87	3			
6099.38	3			
6188.10	4			
6195.06	3			
6262.28	6			
6266.95	10			
6291.34	20			
6299.76	5			
6335.78	2			
6350.04	2			
6355.88	1			

Table 5. (Continued)

Wavelength[a] (Å)	Intensity	Origin[b]	Energy levels	
			Lower	Upper
	Eurpoium[e] (Continued)			
6369.24	2	N		
6382.74	1			
6383.86	2			
6400.93	4			
6406.11	1			
6410.10	4			
6411.34	3			
6457.99	2			
6693.97	1			
6802.79	5			
6816.11	1			
6864.55	70			
	Gadolinium[h]			
3513.66	1	I	0.12	3.65
3605.25	2	N		
3674.06	1	I	0.03	3.40
3684.12	2		0.00	3.36
3757.95	1		0.07	3.36
3783.06	3		0.12	3.40
3843.26	2		0.21	3.44
3866.98	2		0.21	3.42
3934.80	1		0.07	3.21
3945.54	1		0.12	3.26
			0.00	3.14
3969.00	1		0.03	3.15
4023.35	5		0.07	3.15
4045.01	3		0.00	3.06
4053.65	6		0.12	3.18
4054.73	3		0.00	3.06
4058.23	6		0.03	3.08
4078.71	6		0.07	3.10
4090.42	2		0.03	3.05
4092.71	3		0.21	3.24
4100.26	3		0.12	3.15

[h]Energy level data taken from King (38).

Table 5. (Continued)

Wavelength[a] (Å)	Intensity	Origin[b]	Energy levels	
			Lower	Upper
		Gadolinium[h] (Continued)		
4134.17	3	I	0.07	3.06
4150.61	1	N		
4157.79	1	I	0.12	3.10
4167.27	1		0.12	3.10
4175.54	4		0.21	3.18
4190.78	3		0.12	3.08
4191.62	2		0.12	3.08
4225.85	8		0.21	3.14
4260.11	3		0.07	2.97
4266.60	2		0.12	3.03
4267.02	2		0.03	2.93
4274.17	1		0.00	2.90
4306.35	3		0.00	2.88
4313.85	5		0.03	2.90
4321.11	1	II	0.60	3.46
4325.57	5		1.37	4.22
4327.10	4	I	0.00	2.86
4346.63	8		0.03	2.88
4373.84	4		0.07	2.90
4401.85	10		0.21	3.03
4403.14	1		0.98	3.80
4411.16	5		0.07	2.87
4414.73	5		0.12	2.93
4422.41	8		0.03	2.83
4430.63	8		0.00	2.80
4476.14	7		0.00	2.77
4486.91	4		0.21	2.97
4497.33	5	N		
4506.35	6	II	0.50	3.24
4519.66	8	I	0.12	2.77
4537.82	7		0.07	2.80
4542.03	2		0.03	2.75
4581.30	2		0.12	2.83
4821.71	3	N		
5015.06	1	I	1.05	3.52
5103.46	1		0.98	3.41
5617.91	2		0.00	2.20
5643.25	2		0.03	2.22
6730.76	1		0.12	1.96
6828.25	1		0.07	1.88

Table 5. (Continued)

Wavelength[a] (Å)	Intensity	Origin[b]	Energy levels	
			Lower	Upper
		Terbium[f]		
3745.07	1	N		
3759.35	2			
3761.12	1			
3783.54	1			
3789.92	2			
3830.0 **	5			
3833.40	1			
3901.35	3			
3907.91	1			
3915.45	2			
4060.38	1			
4061.57	2			
4105.38	1			
4143.53	2			
4158.28	2			
4203.71	2			
4215.13	1			
4235.34	1			
4266.35	2			
4318.85	10			
4320.28	1			
4322.24	1			
4326.48	13			
4332.13	1			
4336.50	5			
4338.45	8			
4340.63	6			
4342.50	1			
4356.84	5			
4372.04	1			
4388.25	1			
4417.99	1			
4420.20	1			
4430.14	1			
4434.06	1			
4491.02	4			

Table 5. (Continued)

Wavelength[a] (Å)	Intensity	Origin[b]	Energy levels	
			Lower	Upper
		Dysprosium[f]		
2964.62	1	N		
3384.03	1			
3393.58	1			
3407.80	2			
3445.58	1			
3460.97	1			
3471.95	1			
3478.23	1			
3494.50	1			
3511.00	2			
3521.13	1			
3531.71	7			
3538.50	1			
3571.02	1			
3595.05	2			
3645.42	2			
3666.85	3			
3678.52	3			
3685.74	7			
3727.99	1			
3739.36	3			
3740.07	3			
3757.06	7			
3767.64	3			
3773.06	2			
3774.84	1			
3781.48	1			
3786.20	1			
3788.45	2			
3808.1 **	1			
3812.29	3			
3825.65*	2			
3840.91	2			
3844.30	1			
3846.99	2			
3858.40	2			
3868.81	8			
3872.12	2			
3873.99	1			
3891.98	1			

Table 5. (Continued)

Wavelength[a] (Å)	Intensity	Origin[b]	Energy levels	
			Lower	Upper
	Dysprosium[f] (Continued)			
3892.87	2	N		
3917.30	3			
3930.15	2			
3936.71	1			
3937.16	1			
3944.69	3			
3962.60	2			
3967.52	2			
3968.39	3			
3973.88	1			
3993.57	1			
3994.53	1			
3996.70	2			
4000.45	3			
4013.83	7			
4023.72	2			
4024.91	1			
4028.42	2			
4038.83	1			
4045.98	75			
4049.37	2			
4077.97	3			
4085.14	3			
4103.88	6			
4126.14	4			
4129.13	2			
4130.42	10			
4133.86	2			
4134.14	1			
4138.54	2			
4139.56	2			
4141.52	2			
4146.07	8			
4157.86	1			
4159.34	1			
4167.97	40			
4171.99	1			
4183.61	8			
4186.81	60			
4190.90	3			

Table 5. (Continued)

Wavelength[a] (Å)	Intensity	Origin[b]	Energy levels	
			Lower	Upper
		Dysprosium[f] (Continued)		
4191.63	25	N		
4194.83	50			
4197.93	6			
4201.32	4			
4202.25	8			
4205.03	1			
4207.68	1			
4211.72	100			
4213.18	17			
4214.38	2			
4215.17	35			
4218.09	35			
4221.10	35			
4222.22	3			
4225.15	25			
4232.03	5			
4239.87	5			
4245.92	3			
4258.14	1			
4258.56	1			
4268.31	1			
4276.74	3			
4291.93	3			
4347.72	1			
4366.73	3			
4390.9 **	1			
4531.59*	2			
4565.12	6			
4577.80	10			
4589.38	35			
4612.27	30			
4791.30	2			
4880.17	4			
4914.73	1			
5022.12	2			
5042.62	3			
5077.66	4			
5236.25	2			
5301.59	20			
5395.58	5			

Table 5. (Continued)

Wavelength[a] (Å)	Intensity	Origin[b]	Energy levels	
			Lower	Upper
		Dysprosium[f] (Continued)		
5423.32	7	N		
5451.09*	15			
5547.27	7			
5639.50	20			
5652.01	15			
5832.03	10			
5974.50	25			
5988.58	25			
6010.81	3			
6088.26	15			
6168.43	10			
6259.09	50			
6386.81	1			
6421.93	15			
6579.38	50			
6643.41	1			
6835.44	35			
6958.3 **	1			
		Holmium[f]		
3153.82*	1	N		
3154.22	1			
3159.3 **	1			
3186.37*	1			
3200.9 **	1			
3206.1 **	1			
3220.06*	1			
3233.36	1			
3398.98	1			
3449.3 **	1			
3451.2 **	1			
3456.00	3			
3510.75	6			
3515.58	1			
3541.4 **	2			
3570.4 **	4			
3579.12	10			
3581.7 **	3			
3599.49	2			

Table 5. (Continued)

Wavelength[a] (Å)	Intensity	Origin[b]	Energy levels	
			Lower	Upper
		Holmium[f] (Continued)		
3600.73	1	N		
3641.25*	1			
3662.27	8			
3662.98	3			
3666.65	4			
3667.97	5			
3669.05	1			
3669.52	3			
3679.19	3			
3679.70	3			
3682.65	3			
3685.16	1			
3690.65	1			
3691.95*	1			
3700.04*	1			
3731.40	3			
3732.09	1			
3735.0 **	1			
3736.35	3			
3748.17	1			
3769.09*	1			
3774.1 **	1			
3774.7 **	1			
3776.15*	1			
3796.73	3			
3797.1 **	2			
3804.1 **	1			
3810.70	3			
3811.9 **	2			
3821.6 **	1			
3825.6 **	1			
3829.2 **	2			
3850.0 **	2			
3852.5 **	1			
3857.65	4			
3863.3 **	1			
3890.42	3			
3891.02	5			
3904.45	2			
3909.56	2			
3911.80	2			

Table 5. (Continued)

Wavelength[a] (Å)	Intensity	Origin[b]	Energy levels	
			Lower	Upper
		Holmium[f] (Continued)		
3919.45	2	N		
3955.74	20			
3959.68	3			
3975.88	1			
3976.86	1			
3998.28	7			
3998.5 **	3			
4003.36	1			
4027.20	1			
4031.75	4			
4037.60	5			
4040.84	50			
4045.43	2			
4053.92	70			
4068.05	1			
4087.35	1			
4101.09	15			
4103.84	75			
4106.50	1			
4108.63	25			
4111.99	1			
4120.20	35			
4125.65	8			
4127.16	35			
4134.56	3			
4136.24	7			
4163.03	60			
4173.42*	35			
4194.34	10			
4222.26	1			
4252.2 **	35			
4261.7 **	10			
4263.8 **	3			
4350.73	30			
4403.27	2			
4444.63*	1			
4497.73*	2			
4534.58	1			
4562.52	1			
4860.39*	1			

Table 5. (Continued)

Wavelength[a] (Å)	Intensity	Origin[b]	Energy levels	
			Lower	Upper
		Holmium[f] (Continued)		
4934.89*	2	N		
4939.01	15			
4979.97	10			
5301.25*	5			
5330.11*	5			
5359.99*	8			
5385.0 **	1			
5860.28	15			
5882.99	1			
5921.76	15			
5948.03	5			
5972.76*	2			
5973.52	10			
5982.90	35			
6081.79	15			
6305.36	10			
6604.94	60			
6607.47	10			
6628.99	30			
6745.05*	1			
		Erbium[f]		
3331.56	2	N		
3442.65*	1			
3469.48	2			
3489.35	1			
3502.78	3			
3505.69	1			
3520.03	2			
3539.60	2			
3546.0 **	1			
3558.02	4			
3558.74	1			
3563.55	2			
3570.76	3			
3590.72	2			
3607.43	1			
3620.18	2			

Table 5. (Continued)

Wavelength[a] (Å)	Intensity	Origin[b]	Energy levels	
			Lower	Upper
		Erbium[f] (Continued)		
3628.04	2	N		
3638.68	3			
3659.55	1			
3662.87	1			
3664.44	2			
3684.01	2			
3692.65	1			
3697.68*	2			
3746.06	3			
3756.34	2			
3792.91	2			
3798.65	1			
3810.33	15			
3850.1 **	1			
3856.1 **	3			
3863.08	30			
3875.0 **	1			
3892.69	20			
3902.77	3			
3903.99	2			
3905.41	15			
3906.32	1			
3937.02	15			
3944.42	12			
3948.07	2			
3956.43	5			
3964.51	4			
3966.36	1			
3973.04	20			
3977.02	5			
3982.33	5			
3987.66	5			
4007.97	40			
4012.58	4			
4020.52	8			
4021.96	3			
4036.12	1			
4037.68	1			
4046.96	2			
4059.51	1			

Table 5. (Continued)

Wavelength[a] (Å)	Intensity	Origin[b]	Energy levels	
			Lower	Upper
		Erbium[f] (Continued)		
4077.97	3	N		
4087.64	25			
4092.90	1			
4098.10	4			
4123.24	1			
4131.50	3			
4151.11	35			
4185.72	3			
4190.70	8			
4218.43	7			
4286.56	4			
4298.91	3			
4331.35*	2			
4348.34	1			
4382.17	1			
4386.40*	3			
4409.36	35			
4418.70	3			
4424.57	7			
4426.77	20			
4496.38	1			
4518.64	1			
4522.74	1			
4531.11	1			
4606.61	35			
4673.16*	7			
4820.75	1			
4857.43	1			
5007.24	2			
5124.57	2			
5172.76	5			
5206.52	5			
5727.02	1			
5762.79	15			
5826.79	35			
5850.06	2			
5855.29	8			
6221.01	30			
6308.79	15			

Table 5. (Continued)

Wavelength[a] (Å)	Intensity	Origin[b]	Energy levels	
			Lower	Upper
		Erbium[f] (Continued)		
6326.11	1	N		
6583.46	10			
6604.97	1			
		Thulium[e]		
2973.23	2	N		
3046.87	2			
3081.13	2			
3172.82	3	II	0.03	3.92
3233.75	3	N		
3299.0 **	1			
3349.99	1			
3385.05*	1			
3410.05	5			
3412.60	1			
3416.60	4			
3462.20	1			
3467.51	1			
3476.69	1			
3480.97*	1			
3487.38	2			
3499.96	1			
3500.9 **	1			
3514.06*	2			
3517.60	1			
3537.91	2			
3563.88	8			
3567.36	8			
3624.20	1			
3638.42	2			
3646.77*	1			
3717.92	30			
3744.07	40			
3751.82	15			
3761.33	1	I	0.00	3.28
3761.92	1		0.00	3.28
3781.14*	3	N		
3795.76	1	II	0.03	3.28

Table 5. (Continued)

Wavelength[a] (Å)	Intensity	Origin[b]	Energy levels	
			Lower	Upper
		Thulium[e] (Continued)		
3798.55	3	N		
3807.72	3			
3826.39	5			
3840.85*	1			
3848.02	2	II	0.00	3.21
3883.13	50	N		
3887.35	35	I	0.00	3.17
3896.62	7	N		
3916.47	10	I	1.08	4.23
3949.27	5		1.08	4.21
4044.47	2	N		
4094.18	60			
4105.84	65			
4138.36	5			
4187.62	50			
4203.73	40			
4222.67	3			
4271.72	1			
4359.93	25	I	0.00	2.83
4386.42	20		0.00	2.81
4394.42	1	N		
4599.00	8			
4681.92	1			
4724.25	6			
4733.32	25			
5060.89	10			
5113.96	4			
5307.11	50			
5631.41	35			
5675.83	60			
5764.29	20			
5971.27	15			
6460.28	1			

Table 5. (Continued)

Wavelength[a] (Å)	Intensity	Origin[b]	Energy levels	
			Lower	Upper
		Ytterbium[e]		
3289.37	4	II	0.00	3.75
3464.19	35	N		
3987.99	100	I	0.00	3.09
5556.48	80		0.00	2.22
6489.10	1		2.13	4.04
6799.61	4		2.22	4.04
		Lutetium[i]		
2989.27	2	I	0.00	4.14
3081.47	5		0.25	4.27
3118.43	4	N	unclassified	
3171.36	3	I	0.00	3.91
3278.97	10		0.00	3.78
3281.74	30		0.25	4.02
3312.11	30		0.00	3.74
3359.56	30		0.25	3.93
3376.50	20		0.00	3.67
3385.50	5		0.25	3.91
3396.82	7	N		
3508.42	7	I	0.25	3.78
3567.84	8	I	0.00	3.47
3636.25	2		0.00	3.41
3647.77	5		0.51	3.91
3841.18	5		0.25	3.47
3968.46	3		0.00	3.12
4054.45	2		0.51	3.57
4124.73	5		0.00	2.99
4154.08	1		0.93	3.91
4518.57	20		0.00	2.74
5001.14	2		0.51	2.99
5402.57	4		0.00	2.29
6004.52	5		0.93	2.99
6055.03	5		0.25	2.29

[i]Energy level data taken from Klinkenberg (39).

Table 5. (Continued)

Wavelength[a] (Å)	Intensity	Origin[b]	Energy levels	
			Lower	Upper
		Scandium[j]		
2965.86*	1	I	0.00	4.16
2974.01	3		0.00	4.15
2980.75	4		0.02	4.16
3015.36	4		0.00	4.09
3019.35	5		0.02	4.11
3030.77	1		0.02	4.09
3255.68	5		0.00	3.70
3269.90	20		0.00	3.77
3273.62	25		0.02	3.79
3613.84	2	II	0.02	3.44
3630.74	1		0.01	3.41
3907.48	75	I	0.00	3.16
3911.81	75		0.02	3.18
3933.38	30		0.02	3.16
3996.61	35		0.00	3.09
4020.40	60		0.00	3.07
4023.69	60		0.02	3.09
4047.79	10		0.02	3.07
4054.55	35		0.00	3.04
4082.40	40		0.02	3.04
4133.01	2		1.93	4.92
4140.30	2		1.95	4.93
4152.35	2		1.96	4.93
4165.18	3		1.98	4.94
4729.23	3		1.43	4.04
4734.09	3		1.42	4.03
4737.64	4		1.43	4.03
4741.02	7		1.43	4.04
4743.81	10		1.44	4.04
4753.15	20		0.00	2.60
4779.35	15		0.02	2.60
4791.50	3		0.02	2.60
5070.25	1		1.43	3.86
5081.55	8		1.44	3.87
5083.71	5		1.43	3.86
5085.55	3		1.43	3.85

[j]Energy level data taken from Russell and Meggers (40).

Table 5. (Continued)

Wavelength[a] (Å)	Intensity	Origin[b]	Energy levels	
			Lower	Upper
		Scandium[j] (Continued)		
5086.95	3	I	1.42	3.85
5099.23	2		1.43	3.85
5301.94	2		0.00	2.33
5342.96	5		0.00	2.31
5349.70	15		0.02	2.33
5356.10	2		1.86	4.16
5481.99	2		1.86	4.11
5484.62	2		1.84	4.09
5514.21	2		1.84	4.08
5520.50	3		1.86	4.09
5671.80	20		1.44	3.62
5686.83	20		1.43	3.60
5700.23	20		1.43	3.59
6210.68	80		0.00	1.99
6239.41	20		0.00	1.98
6239.78	60		0.00	1.98
6258.96	50		0.02	1.99
6276.31	10		0.02	1.99
6305.67	100		0.02	1.98
6344.83	3		0.00	1.95
6378.82	15		0.00	1.93
6413.35	20		0.02	1.95
6448.10	2		0.02	1.93
		Yttrium[k]		
2948.40	1	I	0.00	4.20
2964.97	1		0.07	4.23
2974.59	1		0.00	4.15
2984.26	2		0.07	4.20
3021.72	1		0.07	4.15
3022.28	1		0.07	4.15
3045.37	1		0.07	4.12
3552.69	4		0.00	3.47

[k]Energy level data taken from Meggers and Russell (41).

Table 5. (Continued)

Wavelength[a] (Å)	Intensity	Origin[b]	Energy levels	
			Lower	Upper
		Yttrium[k] (Continued)		
3592.91	15	I	0.00	3.43
3600.73	1	II	0.18	3.61
3620.94	15	I	0.07	3.47
3710.29	2	II	0.18	3.51
3774.33	2		0.13	3.40
3788.70	1		0.10	3.36
3968.43	1	N	unclassified	
4039.83	7	I	0.00	3.05
4047.63	12		0.00	3.05
4077.37	35		0.00	3.03
4083.71	8		0.00	3.02
4102.38	35		0.07	3.07
4128.30	35		0.07	3.05
4142.84	30		0.00	2.98
4167.51	10		0.07	3.03
4174.13	10		0.07	3.02
4235.94	8		0.07	2.98
4487.47	1		1.35	4.10
4505.95	1		1.37	4.11
4527.24	2		1.42	4.15
4527.79	1		1.39	4.12
4643.70	30		0.00	2.66
4674.85	20		0.07	2.71
4760.97	5		0.07	2.66
5472.4 **	2	N		
5527.54	2	I	1.39	3.63
5581.87	1		1.37	3.58
5630.4 **	1	N		
6222.60	8	I	0.00	1.98
6402.00	2		0.07	1.99
6435.00	40		0.07	1.98
6557.39	2		0.00	1.88
6687.60	10		0.00	1.85
6793.70	5		0.07	1.85

Two important conclusions can immediately be drawn from the data presented in Table 5. First, the number of lines actually emitted is much greater than is apparent from the spectra recorded with the DK-2. Praseodymium and neodymium, for example, have fairly strong lines which are not obviously present in the recorded spectra of these elements shown in Figure 7. The second conclusion which can be drawn from the table is in regard to the nature of the line spectra of the rare earths emitted in this flame. Although incomplete, enough excitation potential data are available to conclude that the majority of these lines arise from transitions involving the lowest energy levels of the rare earth atom. This accounts for the differences in intensity between the arc and flame lines since the former arise from relatively high energy levels. In fact, many of the strong arc lines originate from the singly ionized rare earth. A few weak ion lines are also observed in the flame. Their appearance is not unexpected since the degree of ionization of rare earth atoms at the temperature of the flame is not insignificant (25, p. 302).

The classification of the first spectrum of the lanthanide series has presented formidable problems to the atomic spectroscopist. This is borne out by the incompleteness of the excitation potential data in Table 5. Since arc discharges contain such a high percentage of singly

ionized spectra which overlap with the neutral atom spectra, the resulting spectra are very rich in lines. Consequently the assignment of the individual lines to the correct state of ionization is a singularly difficult task. With only a few exceptions, all of the lines shown in Table 5 arise from energy states within 3.5 ev of the ground state of the atom. Thus, the spectra observed in this flame provide a simple means for identifying the lines originating from the low lying states in the neutral atom.

V. EXCITATION MECHANISM

Comparison of the oxygen-hydrogen spectra of the rare earths shown in Figure 1 with the oxygen-acetylene spectra whose features are given in detail in Figures 7-12 and in Table 5, reveals a great difference in the character of the spectra excited in these two flames. In this section these differences will be examined in light of the accepted theories of flame excitation. Although a detailed exposition of the exact process(es) taking place in the oxygen-acetylene flame which account for the appearance of the strong line spectra is far beyond the scope of this work, inferences may be drawn which give good insight into the type of mechanism(s) involved.

A. Flame Excitation Theories

When solutions containing compounds of metallic elements such as the rare earths are aspirated into a flame, a number of complex processes occur as the aerosol and its residue pass through the flame. The exact nature of these processes is not well understood. However, a qualitative discussion of their nature is given below. The sequence in which they occur probably corresponds closely to the given sequence (1, p. 31; 42).

1. The solvent is vaporized, leaving small particles of dry salt.
2. The dry salt is vaporized.
3. The salt either dissociates into atoms or forms a stable compound with some constituent of the flame gases. The exact path taken here is dependent on the ability of the element to form highly stable compounds and on the environmental conditions in the flame gases.
4. Excitation of the atoms or molecules (or both) takes place.
5. Ionization can occur, with the subsequent excitation of the ion exactly as in step 4.
6. The excited species returns to the ground state with the subsequent emission of light.

The mechanisms which provide the driving force for these processes may be conveniently divided into two broad classifications: thermal and chemiluminescent.

The thermal mechanism is undoubtedly the most important since it is always operative and can be invoked to explain the flame spectra of many elements quite satisfactorily. In this mechanism, the thermal energy liberated by the combustion process is used to perform each of the processes leading to eventual excitation of spectra. The degree to which any spectra will be excited is determined by the amount of energy available from the combustion process. The flame temperature is, of course, a measure of the amount of energy available when only purely thermal phenomena are operative.

The thermal energy in a flame is distributed among the

various translational, rotational, vibrational, electronic, and ionic states of the particles in the flame (42).

If the distribution of energies within any one of the states follows the Maxwell-Boltzmann distribution law, this state possesses a unique temperature. If the temperatures of all of the possible states are equal, the flame may be said to be in thermal equilibrium. If any form of energy distribution other than the Maxwell-Boltzmann is followed, the term "temperature" completely loses its meaning and the state cannot be defined in terms of this parameter. It is therefore possible to think of a system being completely thermal in character only when the distribution of energies is the same for all of the energy states.

There are many ways in which an absence of thermal equilibrium can manifest itself in the spectra of flames. When a line or band system having an excitation energy much higher than could be provided by the flame gases appears in a spectrum, the phenomenon is spoken of as chemiluminescence (42). This type of excitation is generally considered to be due to the formation of the emitting species directly in the excited state due to some chemical reaction, hence the name. The recent observation by Gilbert (43) of many metallic lines of high excitation potential in the "cool" air-hydrogen flame is an interesting example of this type of excitation. Abnormal excitation of CH, C_2, and OH molecules has also been

shown to be due to a chemiluminescent phenomenon (44).

It is a matter of some interest to determine the extent to which the spectra of the rare earth elements can be explained in terms of these excitation mechanisms. More specifically, it would be desirable to explain the great differences between the spectra excited in oxygen-hydrogen and oxygen-acetylene flames. Before the great enhancements in line intensity can be explained, however, it is necessary to have a quantitative measure of their magnitude. The exact degree of line enhancement for all of the rare earth elements is given in Table 6. Also included in this table are the dissociation energies of the rare earth monoxide molecules where these values are available.

The enhancement values were obtained by aspirating solutions of rare earth perchlorates dissolved in ethanol as previously described, into an oxygen-hydrogen flame for a period of one hour. The Wadsworth spectrograph was used to integrate the radiation for this period. Included on the same plate was a fifteen second exposure of the same rare earth solution in an oxygen-acetylene flame. The concentration of the rare earth solutions was 1.0 percent rare earth oxide. Optimal excitation conditions were used for both flames. Sample aspiration rates into both flames were nearly identical, minimizing any differences in rare earth line intensity which might be caused by variations in salt

Table 6. Enhancement of atomic spectra provided by the O_2-C_2H_2 flame compared to O_2-H_2

Element	Enhancement O_2-C_2H_2/O_2-H_2	D_0 (MO) ev
Lanthanum	>1500	8.4 (45)[a]
Cerium	----	8.3 (46)[a]
Praseodymium	>2400	7.7 (46)[a]
Neodymium	>6000	7.4 (45, 46)[a]
Samarium	570	6.1 (47)
Europium	3.44-I 25.2-II	---
Gadolinium	1000	5.9 (48)
Terbium	>3000	---
Dysprosium	550	---
Holmium	450	---
Erbium	850	---
Thulium	160	---
Ytterbium	4.78-I 12.0-II	---
Lutetium	700	5.3 (48)
Scandium	1100	7 (48)
Yttrium	950	7.0 (47)

[a]White, D., Columbus, Ohio. Revised values. Private communication. 1961.

concentration in the flame. Using one hour exposures, it was possible to detect a few lines of many of the rare earths in the oxygen-hydrogen flame. No lines of lanthanum, praseodymium, neodymium, or terbium could be observed in oxygen-hydrogen, however; and only one very weak line could be observed for gadolinium. The method of calculating the enhancements was that given on page 23. This value was then multiplied or divided by the time factor of 960 depending on which exposure provided the greatest line intensity. Up to six lines of each element were measured in order to obtain the values shown in Table 6. With the exception of europium and ytterbium, for which different enhancements were obtained for atom and ion lines, the enhancement values were similar for all lines of a given element. For those elements which exhibited no lines in oxygen-hydrogen, the value shown in the table is a minimum value depending on the intensity of the strongest line in oxygen-acetylene. The enhancement values for these elements are listed as being greater than the minimum value shown.

As was mentioned previously, the high stability of the rare earth monoxide molecules appears to be the limiting factor in preventing the formation of free rare earth atoms in the oxygen-hydrogen flame. This fact becomes obvious when the cases of europium and ytterbium are considered. It is well known that these two elements are more similar to the

alkaline earths than to the rare earths in many of their chemical and physical properties. In this instance their behavior is no exception. The weak band emission which they display in oxygen-hydrogen (see Figure 1) has never been characterized but Gilbert (49) has speculated that the emitters may be EuOH and YbOH rather than the monoxides of these elements. At the same time both ytterbium and europium exhibit strong resonance lines in oxygen-hydrogen which are only slightly intensified by the oxygen-acetylene flame. The resonance lines require from 2.2 to 2.7 ev for their excitation. The remaining members of the series require from 1.9 to 3.4 ev for their excitation; the minimum value of 1.9 ev being found in lanthanum, for which no lines can be observed in oxygen-hydrogen, even after an exposure of one hour! The difference is obviously related to the much greater stability of the LaO molecule. In this same context, it is interesting to note the correlation between the enhancement provided by oxygen-acetylene and the stability of the rare earth monoxides. Table 6 shows that the most stable monoxides exist for those elements which show the greatest enhancements. The lack of complete data on the dissociation energies and the possibility of other factors entering into the intensification make it unwise to attempt to conclude that the amount of enhancement is directly proportional to the stability of the monoxide but nevertheless a direct correlation does exist.

It should also be noted that those elements which show the greatest enhancements in Table 6 also show the weakest line spectra in oxygen-acetylene.

The maximum theoretical (adiabatic) temperature of the oxygen-hydrogen flame is 3050°K (50). As seen in Table 6 the D_0 values range from 5.3 ev for LuO to 8.1 ev for LaO. Assuming that these temperatures actually obtain in these flames and that complete thermal equilibrium is realized for both flames, it is possible to calculate, from the Maxwell-Boltzmann relationship, the ratios of the number of particles in the two flames with sufficient energy to dissociate the rare earth molecules. The equation for this calculation is:

$$\frac{N_1}{N_2} = (\exp)\ \frac{E}{k}\ \left(\frac{1}{T_2} - \frac{1}{T_1}\right)$$

The subscript 1 refers to the oxygen-acetylene flame, and the subscript 2 to the oxygen-hydrogen flame. For an energy of 5.3 ev, the ratio is 4.6, and for 8.4 ev it is 11.1. Obviously this temperature difference cannot account for the increased line emission in the oxygen-acetylene flame. It must be emphasized, however, that these values give only a very rough idea of the enhancement which could be expected from the temperature difference since important effects such as the difference in excitation caused by the difference in flame temperatures have been neglected.

Another important factor which seems to discount a thermal mechanism as being the lone source of rare earth line spectra is the fuel-rich character of the oxygen-acetylene flame which produces maximum rare earth line intensity. Although the maximum temperature of this flame should lie on the fuel-rich side (25, p. 299), this very rich flame should be operating at some temperature significantly below its maximum. Since the line intensity increases by approximately a factor of five in going from a near stoichiometric flame to a very fuel-rich flame, the increase in line intensity obviously does not correlate with the change in flame temperature.

A chemiluminescent mechanism is attractive at first glance as a cause of the appearance of the strong lines. The increase in the concentration of carbon containing species in the fuel-rich oxygen-acetylene flame permits speculation on whether these radicals react directly with the rare earth monoxides to reduce them to free rare earth atoms. This possibility will be considered in greater detail later in the discussion. The chemiluminescent mechanism is dealt a severe blow by the excitation potential data in Table 5. Although these data are incomplete, they do indicate that the great majority of the lines originate from the lowest lying levels of the atom. It will be recalled from the earlier discussion on the nature of

chemiluminescence that abnormally high excitation is encountered when this mechanism is operative. However, without some proof of the degree of thermal equilibrium which exists in the fuel-rich flame, it is not proper to discount this mechanism completely.

B. The Measurement of Flame Temperature

It is obvious from the preceding discussion that in order to gain any understanding of the process which accounts for the appearance of the rare earth line spectra, it is necessary to have some information as to the operating temperatures of the flames under discussion and the degree of thermal equilibrium present in these flames. No systematic study of such parameters has ever been conducted for the type of flame formed by the Beckman burner, making such a study necessary in its own right.

As has already been discussed, it is possible that the translational, vibrational, and ionic states may each possess its own temperature. It is necessary, therefore, to measure the temperature of each state separately. The methods of measuring flame temperatures have been reviewed extensively by Gaydon and Wolfhard (25, pp. 234-301), and more recently by Mavrodineanu (42). Of all the possible techniques, only those which would give direct information as to the state of

equilibrium were considered for use here. The one which was chosen made it possible to measure two of the temperatures: rotational and electronic. The experimental difficulties involved in measuring vibrational, translational, and ionic temperatures were so great as to make impossible their inclusion in this study.

In the method selected, the effective excitation temperature of a certain species which radiates in the flame is measured by accurately measuring the relative intensities of several emissions (lines or band components) of this species. Two types of temperatures were actually measured using this technique. They were effective rotational temperatures using OH rotational band components, and effective electronic temperatures using atomic iron lines.

1. OH rotational temperatures

The OH band system which is emitted in both flames under consideration has its strongest band head at 3063.6 Å corresponding to the O-O vibrational transition. Rotational components of this band system have been classified by Dieke and Crosswhite (51). Intensities of these rotational components are sensitive to changes in the temperature of the flame, while the wavelengths remain constant. The method (51) of calculating the flame temperature using relative intensities is outlined below: For any spectral line the

Intensity due to a transition n--m is given by the equation:

$$I_{nm} = N_n A_{nm} h\nu_{nm}$$

where A_{nm} is the transition probability for the transition n--m and N_n is the number of emitters (in this case OH molecules) in the initial state, h is Planck's constant, and ν_{nm} is the frequency of the transition. If a Boltzmann distribution of energies has been established, N_n will be given by:

$$N_n = N_0 \text{ (exp) } - E_n/kT$$

where N_0 is a constant, E_n is the energy of the state n (the excitation potential), T is the absolute temperature, and k is Boltzmann's constant. Combining these two equations and taking common logarithms:

$$\log I_k/A_k = C - (E_k \log e/kT)$$

C is a constant for a given wavelength. A plot of $\log I_k/A_k$ vs. E_k will be a straight line with a slope of $-(\log e)/kT$. The temperature can easily be calculated from this slope. If the band components used to construct the curve are chosen so that no self reversal mars the intensity measurements, then deviation from straight line behavior of the curve indicates a departure from rotational equilibrium in the source. In the derivation of the equation it was assumed

that the energies of the particles followed a Boltzmann distribution and were therefore in equilibrium. Consequently, any other distribution of energies will cause the curve to assume a non-linear form.

It is necessary to have knowledge of the transition probabilities and the excitation potentials of the individual band components in order to calculate temperature in this fashion. For band systems, the transition probabilities may be theoretically calculated. These values have been calculated for the OH molecule by Dieke and Crosswhite using the expression derived by Earls (52) from the general expressions of Hill and Van Vleck (53).

One must use a dispersing device of high resolving power and dispersion to resolve the closely spaced rotational components of OH. The Wadsworth spectrograph just fulfills this requirement in the first order. Unfortunately, the fuel-rich oxygen-acetylene flame does not emit the OH band system strongly enough to make possible intensity measurements of some of the weaker band components to the degree of accuracy needed for temperature calculations. The strong band components suffer from a high degree of self reversal and are useless for temperature measurements. It was found possible to use the OH band for temperature measurements in the oxygen-hydrogen flame, however. Six components of the R_2 branch were used for this measurement. Table 7 lists the

Table 7. Band components used for rotational temperature measurements

Component	Wavelength (Å)	$E_k x 10^{-3} (cm^{-1})$	A_k
R_2-6	3070.478	33.38	20.7
R_2-14	3071.145	36.39	53.2
R_2-15	3073.028	36.91	57.2
R_2-4	3074.369	32.95	12.8
R_2-3	3077.028	32.78	8.9
R_2-17	3078.071	38.00	65.3

components used, their excitation potentials, and transition probabilities. The designation of the band components follows that of Dieke and Crosswhite (51) and the atlas of Bass and Broida (54) which was used as an aid in identifying the individual components.

The results obtained when this method is used to measure the temperature of the oxygen-hydrogen flame are shown in Figure 13. Oxygen and hydrogen flow rates for this flame were 2.61 l/min and 5.71 l/min respectively, which were the flow rates which produced maximum emission of the rare earth monoxide band spectra. The sample aspiration rate was 0.71 ml/min. Absolute ethanol was aspirated through the burner while the exposure was being made. The slope of the line in Figure 13 is -2.097×10^{-4} cm, corresponding to a temperature

Figure 13. OH-rotational temperature plot for O_2-H_2 flame

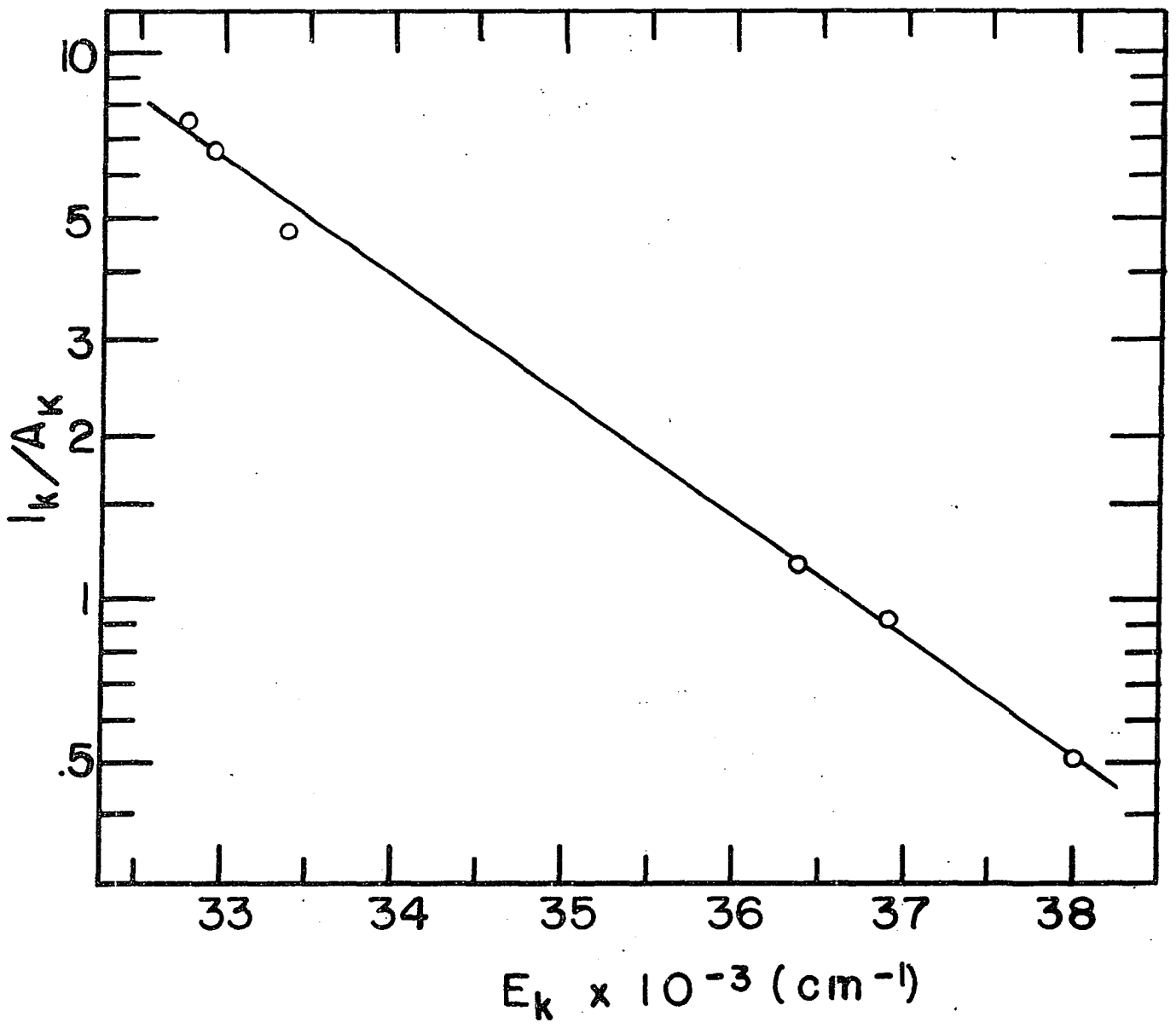
10
5
3
2
1
.5
I_k/A_k
33
34
35
36
37
38
$E_k \times 10^{-3}$ (cm^{-1})

of 2970°K, only 80° less than the maximum theoretical temperature of oxygen-hydrogen. Linearity in the temperature plot indicates the presence of rotational equilibrium in this flame.

2. Fe electronic temperatures

Since the rotational temperature measurements were not applicable to the fuel-rich oxygen-acetylene flame, it was necessary to use another means which would be applicable to both flames of interest. The technique selected was that of Broida and Shuler (50). These investigators assessed several atomic iron lines with regard to their applicability as an "electronic thermometer". They proposed a method which is analogous to the one already discussed for the measurement of rotational temperatures. However, since the equations used have a slightly different form, the derivation of the method is given here. The intensity of an electronic line is given by:

$$I_{nm} = CA_{nm}N_n h\nu_{nm}$$

where A_{nm} is the Einstein transition probability for spontaneous transition between the electronic levels n and m, C is a numerical constant, and N_n is the number of atoms in the state n. If a Maxwell-Boltzmann distribution holds for the electronic energy states, then

$$N_n = \frac{g_n\ (exp)\ -\ E_n/kT}{Q}$$

where g_n is the degeneracy of the level n (statistical weight), E_n, the energy of the level n, and Q, the electronic partition function. At a given temperature, Q will be a constant. If these two equations are combined:

$$I_{nm} = C\ g_n A_{nm} \nu_{nm}\ (exp)\ -\ E_n/kT$$

If $\ln g_n A_{nm} \nu_{nm}/I_{nm}$ is plotted vs. E_n, a straight line with a slope of $1/kT$ is obtained. As before, if the true intensity is measured, any deviation from linear behavior represents a departure from a Maxwell-Boltzmann distribution of energies. The temperature obtained from this slope is the effective electronic temperature of the atom.

Since Einstein transition probabilities for electronic transitions are not derivable in the same manner as those for rotational band components, it is necessary to determine these constants experimentally. The values used and recommended by Broida and Shuler were those measured by Dieke and Crosswhite (55). Other values which were needed, g_n and E_n, are well known for the iron atom (35). Broida and Shuler recommended the use of ten iron lines which they found to be free from self reversal in the flame. Table 8 lists these lines along with the data needed to use them for the measurement of temperature. Broida and Shuler measured the

Table 8. Iron lines used for temperature measurements

Wavelength (Å)	$E_n x10^{-3}(cm^{-1})$	$\ln g_n A_{nm} \nu_{nm}$
3824.44	26.14	3.401
3856.37	26.34	3.541
3679.91	27.17	2.984
3705.57	27.39	3.558
3497.84	29.47	3.187
3465.86	29.73	4.019
3687.46	34.04	5.124
3709.25	34.33	5.497
3815.84	38.18	6.882
3827.82	38.68	6.841

temperature of a stoichiometric premixed oxygen-acetylene flame and found it to be 3190°K. They also found a value of 2835°K for the stoichiometric premixed oxygen-hydrogen flame.

For temperature measurements of the flames of interest here, iron was aspirated into the flame from an $Fe(ClO_4)_3$ solution dissolved in absolute ethanol. Applicability of this method to this flame is illustrated by the temperature plot in Figure 14. The oxygen and acetylene flow rates were 2.88 and 3.51 l/min respectively, yielding a sample aspiration rate of 0.78 ml/min. The slope of the line is $4.64x10^{-4}$ cm, corresponding to a temperature of 3080°K. A straight line here indicates the presence of electronic equilibrium in the source.

In order to derive maximum precision and accuracy from this method of temperature measurement a least

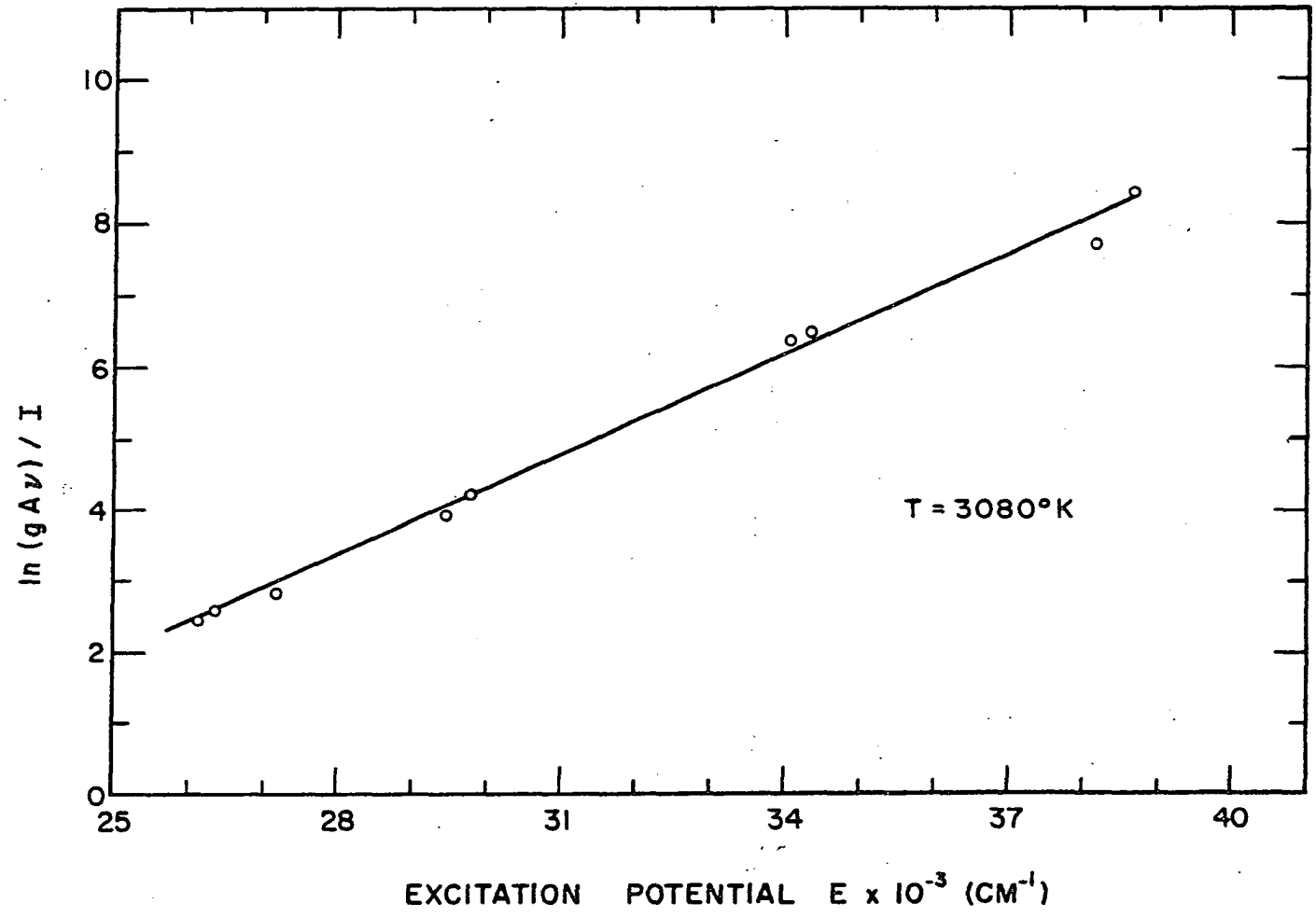

Figure 14. Fe-electronic temperature plot for fuel-rich O_2-C_2H_2 flame

Table 9. Precision of effective Fe-electronic temperature measurements

Determination No.	Temperature (°K)	Average	Standard deviation
1	3080		
2	3040		
3	2970		
4	3052		
5	3090		
		3046	15.5

squares[1] fit was made to the ten experimental points. Since this treatment yields the slope directly, it is not necessary to draw the line once the linear behavior of the temperature plot has been established. For the particular case encountered here, that of ten points each having a constant abscissa, the equation for the slope (m) reduces to:

$$m = \frac{10 \sum_{i=1}^{10} (\ln gA\nu/I)_i (E)_i - 311.47\times10^{-3} \sum_{i=1}^{10} (\ln gA\nu/I)_i}{2.076\times10^{9}}$$

To determine the precision of this procedure, five separate measurements of the temperature were performed over a period of two months. Flame parameters were identical with those specified previously. Table 9 lists the measured temperatures, their average, and the standard deviation.

[1] A derivation of this method can be found in many texts on statistics. cf., e.g., Beers (56) p. 35.

Using this method, the variation of temperature was studied as a function of several flame parameters.

In order to assess the effect of solvent and anion on the temperature, three separate iron solutions were used. These solutions each contained 1.0 per cent Fe as metal and were composed as follows: $Fe(ClO_4)_3$ in absolute ethanol, $Fe(ClO_4)_3$ in water, and $FeCl_3$ in water. The solutions were aspirated under flame conditions identical to those given above. Temperatures measured for these solutions were respectively: 3040°K, 2980°K, and 2970°K. These values indicate very little influence on the flame temperature from the solvent and none from the anion. The slightly lower temperature obtained on substituting water for absolute ethanol as the solvent is probably significant but is much less than that measured or estimated by other investigators (1, p. 62). From these observations it can be seen that it is difficult to explain the intensification of the rare earth lines provided by organic solvents on the basis of an increase in flame temperature.

The variation of Fe-electronic temperature with height along the flame axis was also studied. Using the adjustable mount described previously, the position of the burner was varied with respect to the optical axis of the spectrograph. The oxygen and acetylene flow rates were identical to those used previously and the $Fe(ClO_4)_3$-absolute ethanol solution

Table 10. Variation of Fe-electronic temperature with height along the flame axis

Distance above burner tip (mm)	Temperature (°K)
12-19	3060
19-26	3052
26-33	3106
33-40	3100
40-47	3092

was used for all exposures. Results of this study are presented in Table 10. This striking constance of temperature throughout the flame is not surprising in view of the homogenous physical appearance of the flame. Lewis and von Elbe (57) observed similar behavior for rich premixed flames of air-natural gas.

Variation of fuel and oxygen flow rates showed that a maximum Fe-electronic temperature of 3185 °K could be attained with the oxygen-acetylene flame of the Beckman burner. To achieve this temperature, the $Fe(ClO_4)_3$-absolute ethanol solution was aspirated into the flame at 1.25 ml/min at oxygen and acetylene flow rates of 3.60 l/min and 3.51 l/min respectively. Agreement with the value of 3200 °K reported by Broida and Shuler (50) for a stoichiometric premixed oxygen-acetylene flame is quite good.

The rare earth line emission was of much lower intensity in this flame than in the more fuel-rich flames. The exact

reduction in intensity varied for each element, being smallest for europium and ytterbium and greatest for lanthanum. Dysprosium showed a fivefold decrease in intensity, with the other elements showing decreases which were in approximately the same ratio as the enhancement values in Table 6. The flame producing this temperature had an oxygen/acetylene ratio of 1.03, which is still significantly fuel-rich but was more nearly stoichiometric than the oxygen/acetylene ratio of 0.84 which yielded maximum rare earth line intensity.

The Fe-electronic temperature was also measured in an oxygen-hydrogen flame operated under the same conditions used for the OH rotational measurements. A value of 2900°K was obtained. This value is 70° lower than the OH rotational temperature reported earlier and 55° higher than Broida and Shuler's measurement on a stoichiometric premixed oxygen-hydrogen flame.

The excellent results obtained with the Fe-electronic technique appear to vindicate its use as a means of assessing flame temperature and electronic equilibrium. It should be pointed out, however, that the temperatures reflect only that portion of the flame which is favorable to the existence and excitation of iron atoms. Conditions under which large temperature gradients can exist within flames have been discussed by Tourin (58). The homogeneity of the fuel-rich flame would seem to minimize the possibility that such gradients could

be a significant source of error in the temperatures reported here.

During the course of the temperature measurements it was noted that the absolute intensities of the iron lines increased in consort with the flame temperature. This behavior is in direct contrast to that of the rare earth lines. FeO, having a dissociation energy of 4.3 ev (59), is the most stable compound formed by iron at elevated temperatures. Evidently this compound is sufficiently unstable for thermal dissociation to be an important process leading to the excitation of iron line spectra. In spite of this behavior, there seems to be little doubt that the use of iron as a "thermometer" is valid. The excellent agreement with theory and with other investigators makes such a conclusion inescapable.

An obvious extension of this technique would be the use of the rare earth lines for similar studies. The only one for which sufficient data are available is scandium. An analysis of its spectrum, providing excitation potential and statistical weight values, was completed long ago (40). More recently, the oscillator strengths (from which Einstein transition probabilities may be calculated) of many scandium lines have been measured (60). A study of the feasibility of using this element as an electronic "thermometer" would be both interesting and valuable.

C. Conclusions

It was not possible to include a complete study of the behavior of individual rare earth lines as a function of flame temperature and the many other variables inherent in flame spectroscopy. However, the experimental data which were obtained make it possible to draw two conclusions as to what processes are <u>not</u> involved in the excitation of rare earth line spectra. They are:

1. The process(es) involved in the appearance of the rare earth lines is not controlled by the flame temperature, i.e. a purely thermal mechanism cannot be invoked to explain the character of the fuel-rich oxygen-acetylene spectra.
2. The process(es) involved do not require non-equilibrium conditions for their fulfillment, i.e. the mechanism apparently involves no chemiluminescence.

These are essentially identical to the conclusions drawn earlier from a consideration of possible excitation mechanisms and the appearance of the spectra. They are repeated here in a more concise form because of the unequivocal support which the flame temperature measurements give them.

Having thus stated what the flame excitation mechanisms for rare earths are not, it is pertinent to inquire what they may be. The overall process seems to require at least two separate steps. Conditions in the fuel-rich oxygen-acetylene flame appear to provide a more favorable environment for the

production of unexcited rare earth atoms, which may be subsequently excited by the thermal energy of the flame. Hence, the process seems to involve the rare earth monoxide molecule directly, either by dissociating it or by preventing its original formation.

Beyond a few scattered observations, there is no data concerning the composition of the flame gases in a fuel-rich flame of this type. Therefore any mechanisms which may be formulated to account for the formation of rare earth atoms must lie in the realm of speculation. It is also quite likely that the effect cannot be adequately described by a simple mechanism but represents the sum total of many processes. The brief discussion which follows will attempt to describe a few of the types of processes which could account for the production of free rare earth atoms in the flame.

It is well known that fuel-rich flames of hydrocarbons burning in oxygen contain appreciable concentrations of atomic carbon, solid carbon, CH, C_2, C_3 radicals, and other carbon-containing species (50). Because of the highly exothermic nature of the reaction between atomic oxygen and these species, the atomic oxygen concentration in these flames is markedly less than in stoichiometric or oxygen-rich flames (61). This is borne out by the spectrum of the flame background shown in Figure 6. One explanation of the low OH band intensity in the flame used here is the lowered

oxygen concentration in the flame gases. The possibility that the low oxygen concentration leads to lower rare earth monoxide concentrations than in stoichiometric flames is an attractive one. The dissociation equilibrium for the monoxide molecules will certainly be driven in the direction of free rare earth atoms when the partial pressure of oxygen atoms in the flame gases is lowered. Similarly, there will be fewer oxygen atoms with which the rare earth atoms can react to form the monoxides if, indeed, this type of reaction is necessary to form the monoxide molecule. The extent to which this type of process may be responsible for the presence of free rare earth atoms cannot be easily determined since the exact sequence of events leading to the formation of the radiating species is unknown. Since an enhancement of the monoxide band spectra (approximately ten fold) is observed along with the much greater enhancement in line spectra, conditions favorable to the existence of atoms may be confined to restricted portions of the flame. One observation which can be interpreted as supporting the hypothesis that the free atoms are formed without passing through the monoxide stage is the behavior of the line intensity as a function of the vertical portion of the flame sampled. Bulewicz and Sugden (62) have studied this phenomenon and concluded that line spectra of those elements which do not form stable compounds in the flame are less sensitive to variations in flame height

than the line spectra of elements which form stable monoxides, hydroxides, or hydrides in the flame. It was reported earlier that the rare earth line spectra diminish by only about a factor of two over a fifteen millimeter change in the flame position when absolute ethanol is used as the solvent, compared to complete quenching over the same distance when aqueous solutions are used. This suggests that the organic solvent may allow the rare earth salt to be transformed directly to the atom, while the water with greater oxygen content and higher heat of vaporization may promote the formation of the monoxide.

Another interesting type of mechanism which may lead to the formation of rare earth atoms involves the reaction of atomic carbon particles (or other species containing carbon) with the rare earth monoxide molecules according to the equation:

$$C + MO \rightleftarrows CO + M^{O}$$

The high stability of the CO molecule makes this reaction attractive, especially in view of the increased carbon formation which seems to go hand in hand with increased rare earth line emission. Reactions of this type may liberate energies up to 256 kcal (50). Taking the stability of the rare earth monoxides into account the actual energy liberated will probably still be appreciable though significantly lower than

this value. It is this exothermicity, however, which causes this mechanism not to fit in with the experimentally observed spectra. If such a large amount of energy is liberated, it is difficult to see why at least some of it should not go directly into excitation of the metallic atom resulting in a chemiluminescent phenomenon. Since chemiluminescence has been ruled out as an important mechanism, this reaction must be viewed with suspicion. It is included as a possibility since the exact amount of energy liberated by this reaction and its subsequent disposition are not known. A study of the energy distributions among the various states of the CO molecule might help clarify this matter.

There are scattered observations recorded in the literature which provide confirmation that free-atom populations of other elements are increased in fuel-rich hydrocarbon flames. The enhancement of the line spectra of magnesium in highly reducing oxygen-acetylene flames observed by Knutson (63) appears to be a manifestation of the same phenomenon observed here. The dissociation energy of MgO reported by Veits and Gurvich (64) is 4.3 ev. An enhancement of the atomic absorption spectra should also be a discernible consequence of an increase in the free atom population in these flames. David (65) has reported that the ground state atom population in air-acetylene flames is critically dependent on the air/acetylene ratio. For air-rich flames, negligible atomic

absorption occurred for molybdenum concentrations at the 50 ppm level, whereas 35 percent absorption occurred in a fuel-rich "reducing flame". Brewer[1] has estimated the dissociation energy of MoO as 5 ± 0.6 ev. Eshelman et al. (66) found that the resonance lines of aluminum could be excited in an oxygen-acetylene flame similar to that used in this study while these lines were not excited in the oxygen-hydrogen flame. They also found that the maximum intensity of these lines occurred in fuel-rich flames, but made no attempt to interpret these observations. There do not seem to be any recorded observations where more than one or two lines of an element are enhanced by this technique. In degree at least, the great intensification of the vast number of rare earth lines reported here is unique in flame spectroscopy.

---

[1]Brewer, L., Berkeley, California. Private Communication. 1961.

VI. ANALYTICAL APPLICATIONS

The striking chemical similarity of the rare earth elements has rendered classical analytical techniques all but useless in determining the individual elements in rare earth mixtures. The few methods for these determinations and the methods for separating and/or determining the rare earths as a group have recently been reviewed by Banks and Klingman (67). Because of these chemical similarities, the analyst has turned to measurements of their physical properties to solve this difficult problem. Of the physical properties, the various types of spectra characteristic of the rare earths have found the greatest application. A recent review by Fassel (68) obviates the necessity of describing these methods in detail here.

Except in the case of lanthanum, the rare earth monoxide band spectra excited in flames have not proven to be sufficiently free from spectral interference to be of more than limited utility. The rare earth line spectra which are reported here possess many advantages over the band spectra. Because of the inherently narrow width of the atomic lines, direct spectral interference (such as that suffered by the broad band spectra) is vastly decreased, while the relative simplicity of the line spectra (as compared to spectra excited in arcs and sparks) makes it possible to use small

table model monochromators and direct reading electronic systems for recording of the spectra. This leads to reductions in cost of equipment and analysis time. Furthermore, the high sensitivity of the lines is enhanced by the fact that they lie in a wavelength region where the photocathodes of the most sensitive photomultiplier tubes have their maximum response. Their position in the spectrum also relieves them of interference caused by the monoxide bands.

Studies to be reported in this section were undertaken in order to show the general analytical utility of these lines. The equipment used for all analytical work was the grating flame photometer described earlier.

A. Recording of Line Spectra

In order that the extent of interference could be determined, it was necessary to obtain complete recordings of the rare earth spectra. Spectra were scanned over the wavelength region from 3000 to 5000 Å, since all of the lines having potential analytical utility lie in this region. The experimental conditions used for recording the spectra are given in Table 11. The spectra obtained in this fashion are shown in Figures 15-20. In order to show maximum detail in the recordings, the conditions were chosen so that the strongest lines would exceed full scale deflection. However, no lines

Table 11. Experimental conditions for recording of rare earth line spectra

Gas flow rates	oxygen: 2.65 l/min acetylene: 3.19 l/min
Sample aspiration rate	0.98 ml/min
Concentration and constitution of solutions	Rare earth perchlorates dissolved in absolute ethanol. Concentrations are given on spectra.
Slit width	0.025 mm
Amplifier input sensitivities	2800-3500 Å: 2×10^{-7} amp full scale 3500-4500 Å: 1×10^{-6} amp full scale 4500-5000 Å: 2×10^{-6} amp full scale
Photomultiplier voltage	1500
Scan speed	50 Å/min
Chart speed	1 in/min
Zero suppression	-0.10 mv
Recorder sensitivity	10 mv full scale

were allowed to exceed full scale deflection by more than a factor of two. The lines which significantly exceed full scale deflection are marked with an asterisk. The appearance of the lines in these figures corresponds much more closely to the wavelengths in Table 5 than do the spectra recorded on the Beckman DK-2. Line spectra are apparent for all of the rare earths except cerium.

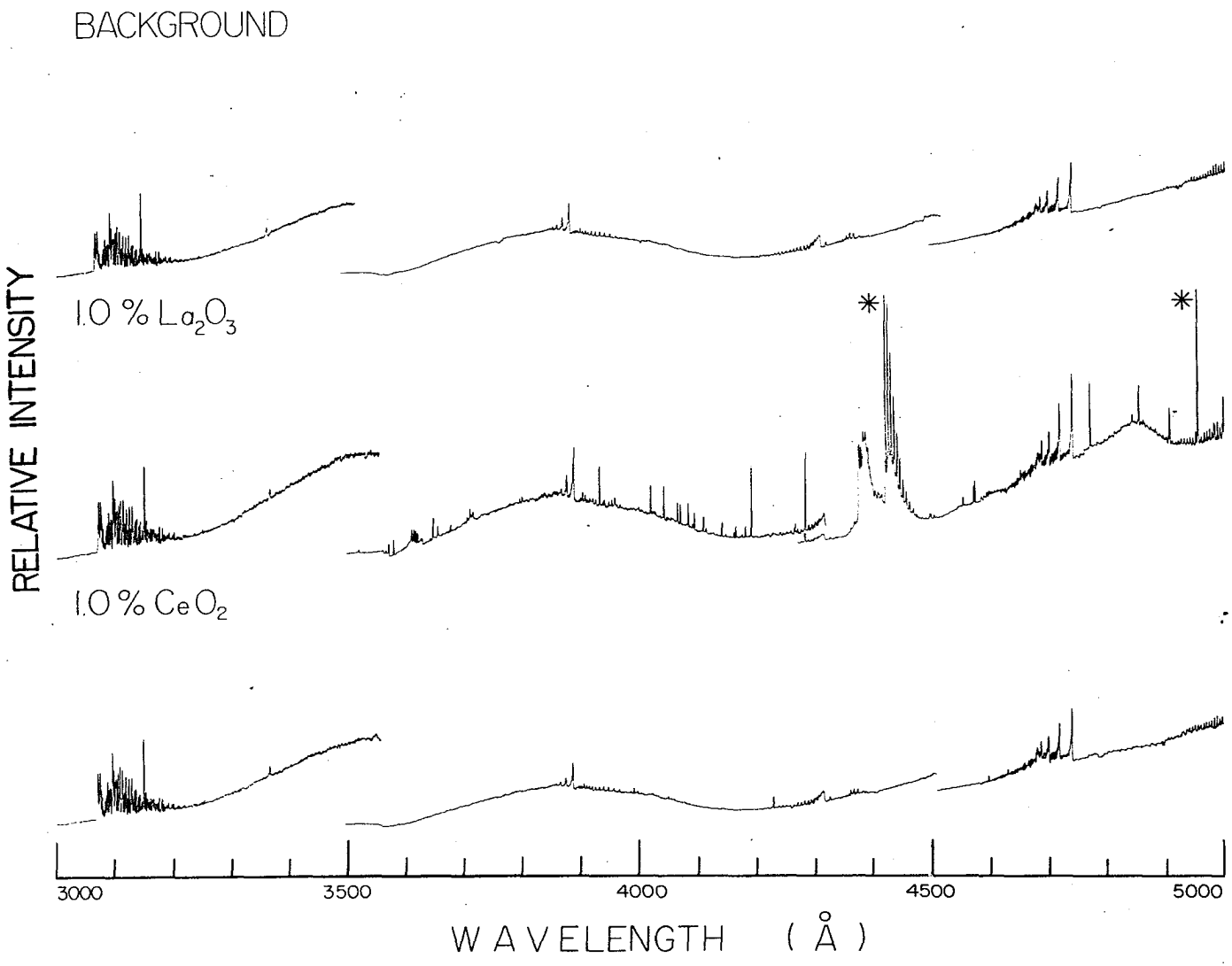

Figure 15. Fuel-rich O_2-C_2H_2 spectra of flame background, lanthanum and cerium (3000-5000 Å)

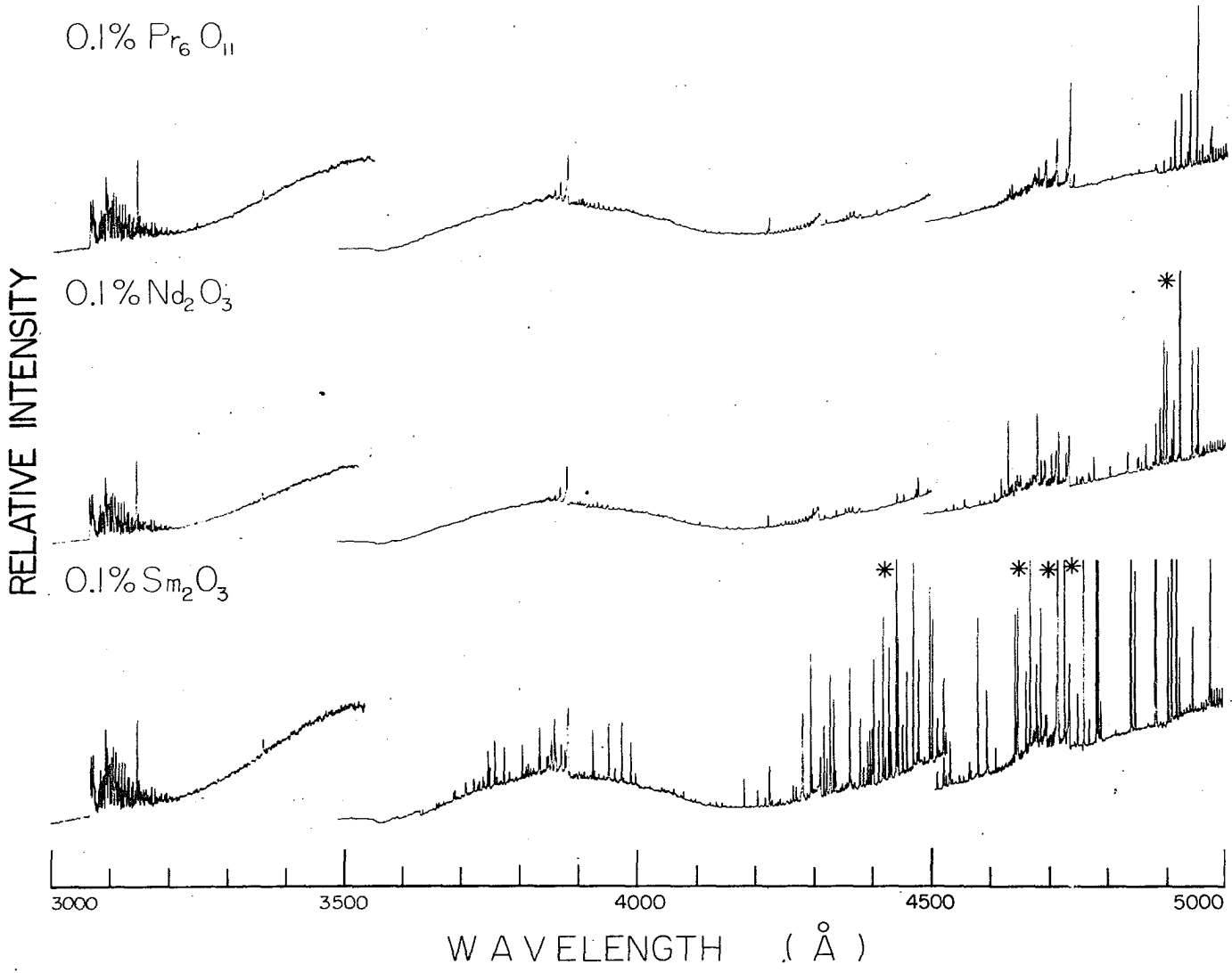

Figure 16. Fuel-rich O_2-C_2H_2 flame spectra of praseodymium, neodymium, and samarium (3000-5000 Å)

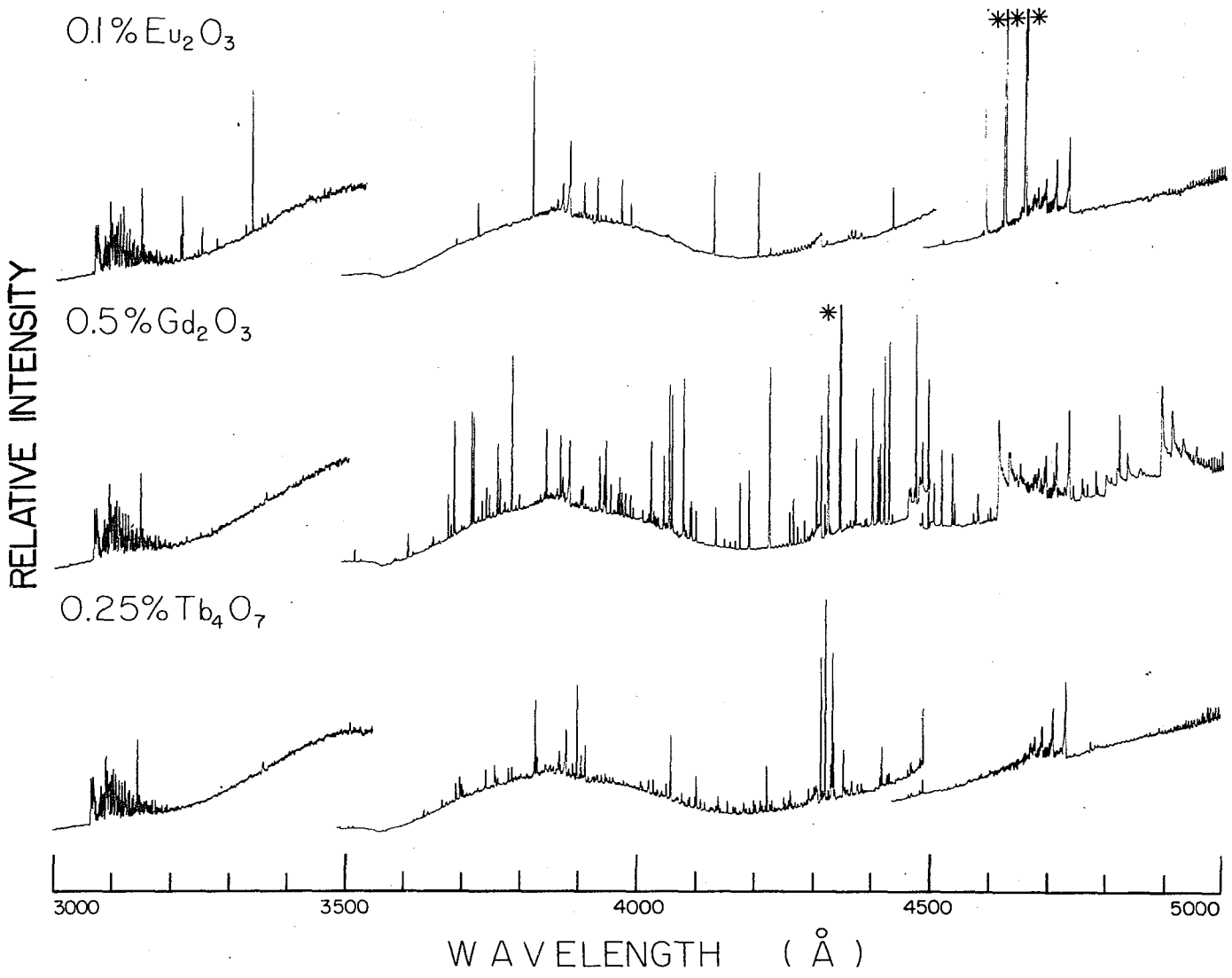

Figure 17. Fuel-rich O_2-C_2H_2 flame spectra of europium, gadolinium, and terbium (3000-5000 Å)

Figure 18. Fuel-rich O_2-C_2H_2 flame spectra of dysprosium, holmium, and erbium (3000-5000 Å)

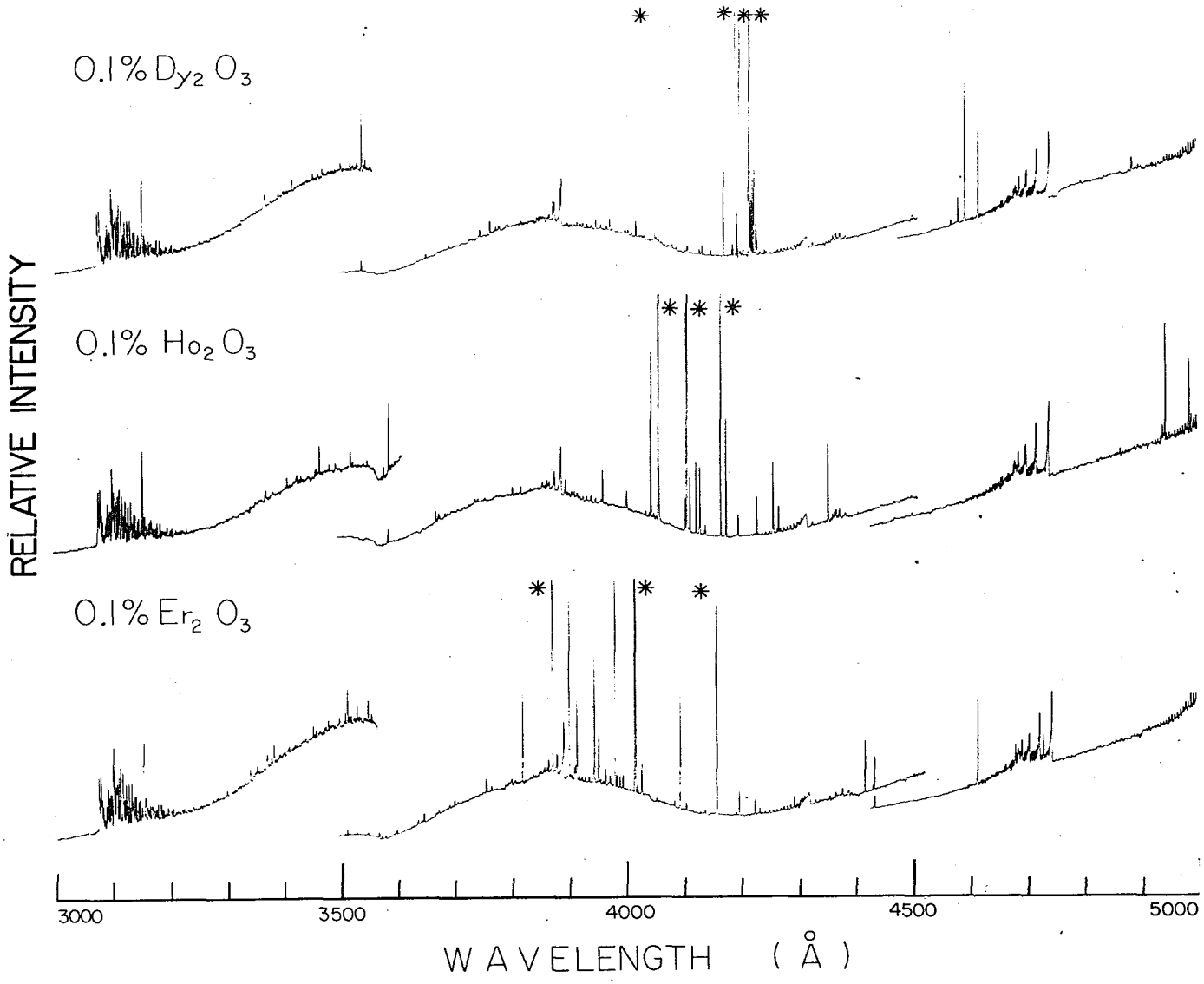
0.1% Dy_2O_3
0.1% Ho_2O_3
0.1% Er_2O_3
RELATIVE INTENSITY
3000
3500
4000
4500
5000
WAVELENGTH (Å)

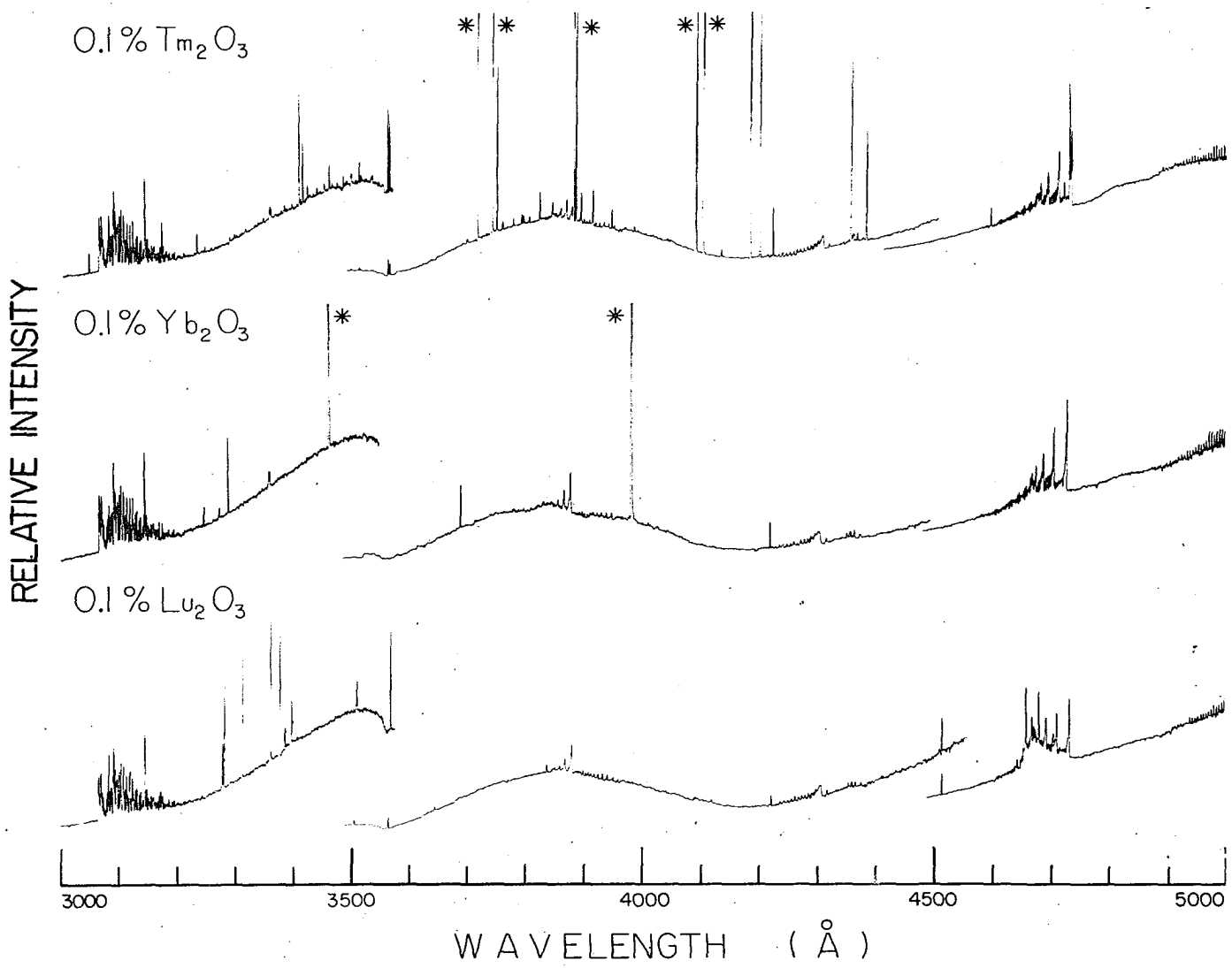

Figure 19. Fuel-rich O_2-C_2H_2 flame spectra of thulium, ytterbium, and lutetium (3000-5000 Å)

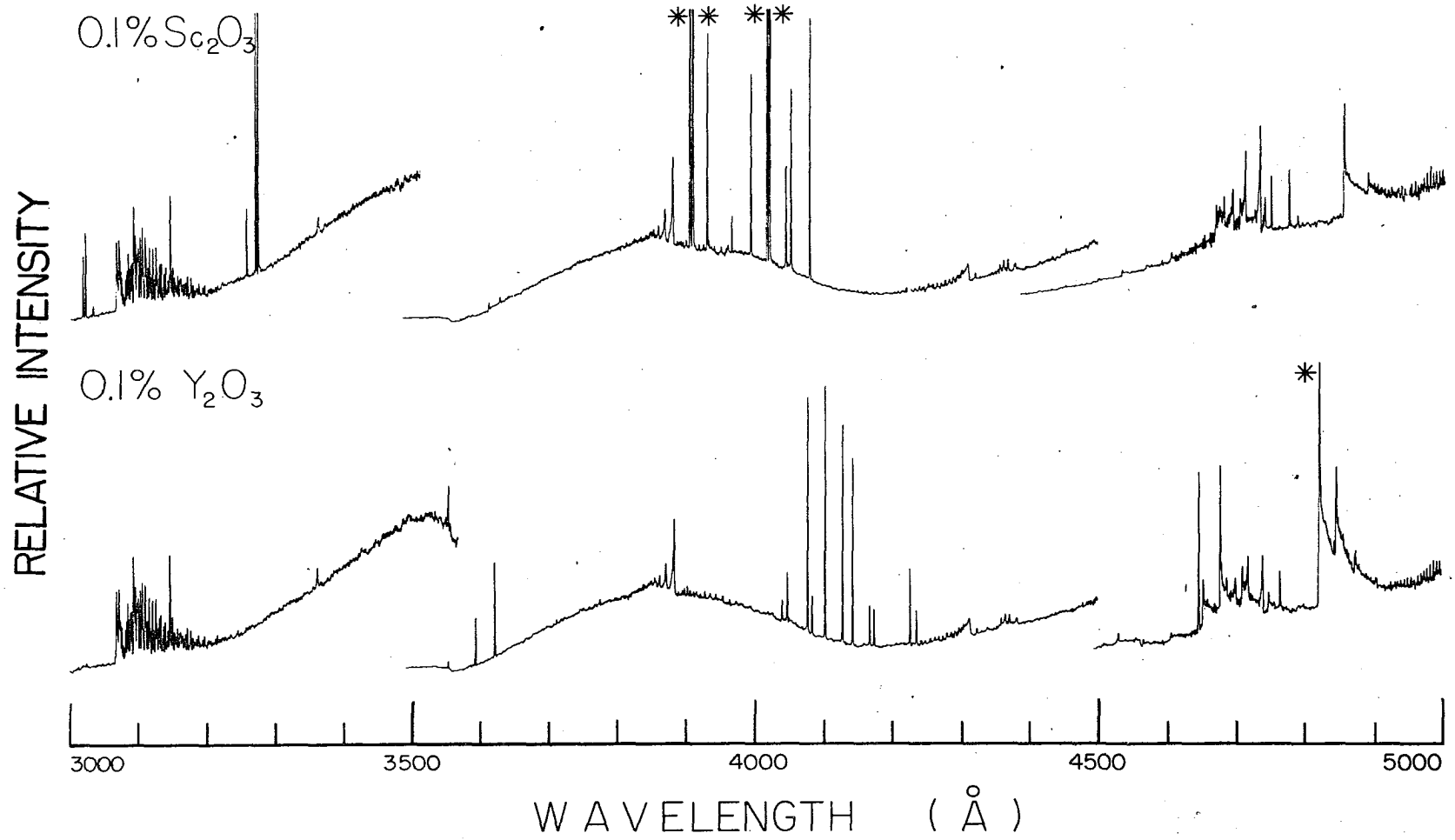

Figure 20. Fuel-rich O_2-C_2H_2 flame spectra of scandium and yttrium (3000-5000 Å)

B. Interference Assessment and Detection Limits

Using the wavelengths in Table 5 and the recordings in Figures 15-20, the strongest lines of each element were selected. The feasibility of using these lines for analytical purposes was determined by assessing their possible rare earth interferences and their analytical sensitivity (detection limit). All lines in Table 5 within ± 2 Å of the line being studied were listed as possible interferences. This value was used because it would allow complete resolution of two lines, even under unfavorable relative intensity conditions. The criterion chosen for defining the detection limit of the strongest lines was dictated by the fact that the sensitivity of the line is determined by the background fluctuation. The detection limit is defined in this study as that concentration of the element (or oxide) which yields a line intensity equal to twice the standard deviation of the background fluctuation (noise) when entrance and exit slits having a width of 0.025 mm are used. This definition is similar to those suggested by Alkemade (69) and by Hagenah et al. (70). In practice this value was determined for each line by scanning dilute solutions of the element under instrumental conditions which yielded a background fluctuation of about four to ten percent of full scale signal. Each line was measured at three or four concentrations under identical

experimental conditions. A baseline was then constructed so that the average deviation of the background fluctuation would be very nearly zero. The deviations from the baseline were measured every 0.5 Å on both sides of the line for 5 Å, giving 20 values from which the standard deviation of the noise could be determined. The net line intensities were measured by subtracting the intensity of the baseline at the point directly under the line from the peak intensity of the line. The net intensities were plotted against concentration. A straight line was obtained which could be extrapolated to the concentration corresponding to twice the standard deviation of the background fluctuation. This value was taken to be the detection limit.

Table 12 lists the wavelengths of the lines which were found to have the most potential analytical utility. The detection limits and possible rare earth interferences as defined above are also listed, along with the spectrographically measured relative intensities of the interfering lines.

Two important factors must be kept in mind when the data in Table 12 are used to assess the feasibility of a given analysis. The spectrographic intensities are intended to be only a qualitative guide to the relative intensities of the lines. The relative intensity scale appears to be compressed, probably because of inadequate correction for the continuous background on the plates.

Table 12. Evaluation of lines for analysis of rare earth mixtures

Element	Wavelength (Å)	Detection limit (ppm as oxide)	Interferences
La	4187.32	600	Dy 4186.81-60 Er 4185.72-3 Tm 4187.62-50
	4280.26	750	Sm 4282.20-15
Pr	4951.36	55	La 4949.77-3 Nd 4950.28-1 4950.72-1 4952.51-3
Nd	4924.53	30	Pr 4924.59-5 Sm 4924.06-7
Sm	4783.10	25	none
	4841.70	30	none
	4883.78	25	Nd 4883.01-8 4885.01-2
Eu	4594.02	0.02	Nd 4594.67-1
	4627.12	0.04	Nd 4626.50-2 4627.99-3
	4661.85	0.15	Pr 4660.91-1 4663.55-18
Gd	4401.85	190	Sm 4401.17-20 4403.05-40 Ho 4403.27-2
Tb	4318.85	30	Sm 4319.53-15
	4326.48	30	Sm 4325.15-2 4326.13-2 Gd 4325.57-5 4327.10-4
	4338.45	65	Sm 4339.35-2 4339.93-2

Table 12. (Continued)

Element	Wavelength (Å)	Detection limit (ppm as oxide)	Interferences
Dy	4211.72	1.3	none
Ho	4053.92	1.6	Sm 4054.51-1 Gd 4053.65-6 4054.73-3 Lu 4054.45-2 Sc 4054.55-35
	4103.84	1.0	La 4104.88-2 Tb 4105.38-1 Dy 4103.88-6 Tm 4105.84-65 Y 4102.38-35
Er	3973.04	10	Sm 3974.66-10 Eu 3971.99-5 Dy 3973.88-1
	4007.97	3.8	La 4007.66-2
	4087.64	12	La 4089.61-1 Ho 4087.35-1
	4151.11	5.5	Sm 4151.21-2 Gd 4150.61-1 Sc 4152.35-2
Tm	4094.18	1.3	Er 4092.90-1
	4105.84	1.4	La 4104.88-2 Tb 4105.38-1 Dy 4103.88-6 Ho 4103.84-75
Yb	3987.99	0.18	Er 3987.66-5
Lu	3278.97	25	none
	3281.74	15	none
	3312.11	10	none
	3359.56	6.0	none
	3376.50	13	none

Table 12. (Continued)

Element	Wavelength (Å)	Detection limit (ppm as oxide)	Interferences
Sc	3269.90	25	none
	3273.62	12	none
	3907.48	1.9	Eu 3907.11-5 Tb 3907.91-1 Er 3906.32-1
	3911.81	2.5	Ho 3911.80-2
	4020.40	4.0	Er 4020.52-8
	4023.69	3.5	Gd 4023.35-5 Dy 4023.72-2 Er 4021.96-3
Y	4077.37	15	La 4079.18-2 Gd 4078.71-6 Dy 4077.97-3 Er 4077.97-3
	4102.38	11	Dy 4103.88-6 Ho 4101.09-15 4103.84-75
	4128.30	15	Eu 4129.62-15 4129.74-15 Dy 4129.13-2 Ho 4127.16-35
	4142.84	13	Tb 4143.53-2 Dy 4141.52-2

Consequently, dividing the spectrographic intensity of the proposed analysis line by that of the interfering line in order to gain some idea of the amount of the interfering element which may be tolerated is not recommended. Since the intensity scale is compressed, the interferences will

be less serious than this method would indicate. An interesting example will be given later for the case of the scandium interference with the holmium line at 4053.92 Å. It is also important to take into account the likelihood of encountering the interfering element. Thus, the samarium interference with the gadolinium line at 4401.85 Å is serious since these two elements are likely to be found together. However, the scandium interference with the holmium line at 4053.92 Å will seldom be encountered since scandium is very rare and is not likely to be found with holmium in sufficient amounts to cause an appreciable error.

It is convenient to divide the rare earths into three classes in terms of the applicability of this method to their determination. The first class consists of those elements which possess very strong lines with little or no serious interference. Nine of the sixteen rare earths may be placed in this class. These are: samarium, europium, dysprosium, holmium, erbium, thulium, ytterbium, lutetium, and scandium. The second class comprises those elements which have moderately strong lines but which suffer possible serious interferences from rare earths likely to occur with them in mixtures. The four elements which appear to meet this criterion are praseodymium, neodymium, terbium, and yttrium. Lanthanum, cerium, and gadolinium are the elements making up the third class. These elements have no lines strong enough,

or free enough of interference, or both, to be determined by this method.

C. Calibration Experiments

1. Preparation of standards

The standard solutions used to obtain the data for the analytical curves were prepared synthetically from pure rare earth oxides. They were prepared by weighing together the proper amounts of the previously dried and ignited oxides, dissolving them in perchloric acid, evaporating, and redissolving in absolute ethanol as previously described. When cerium was used as a component of a standard, it was added by volume from a previously prepared solution immediately before the final dilution. In every standard solution the total weight of the oxides was such as to give a solution containing 1.0 percent rare earth oxide after dilution to the proper volume. The composition of the standards was similar to that of rare earth mixtures likely to occur in practice. For this reason, yttrium was considered as lying between gadolinium and terbium and scandium was placed after lutetium. In order to maintain the number of solutions at a reasonable value, each rare earth appears in only six or seven different concentrations in the range from 1 or 2 percent up to 100 percent. Table 13 gives the composition of the standard solutions which contained more than one rare earth.

Table 13. Composition of standard rare earth solutions

	1	2	3	4	5	6	7	8	9	10	11	12	13	14
% La_2O_3	50	20		10		5						1		2
% CeO_2									2			6		10
% Pr_6O_{11}		50	20		5		10							2
% Nd_2O_3		25	50	10	2	5								1
% Sm_2O_3		5	25	50	10						2			1
% Eu_2O_3			5	25	50	10						2		1
% Gd_2O_3				5	25	50	10					2		1
% Y_2O_3					5	25	50	10				2		1
% Tb_4O_7					1	5	25	50	10	2				
% Dy_2O_3					2		5	25	50	10				1
% Ho_2O_3								5	25	50	10	2		1
% Er_2O_3									5	25	50	10		2
% Tm_2O_3								10		5	25	50		2
% Yb_2O_3									5	1	2	10	50	25
% Lu_2O_3									1	2	10	5	50	25
% Sc_2O_3	50								2	5	1	10		25

2. Analytical curves

The six elements which were selected to illustrate the analytical utility of the line spectra were dysprosium, holmium, erbium, thulium, lutetium, and scandium. Preliminary experiments indicated that the concentration range from 1 to 100 percent could best be covered in two overlapping segments: 1 to 25 percent and 5 to 100 percent. It was found that all of these elements could be determined quantitatively under similar experimental conditions. All but lutetium were run at a total rare earth concentration of 0.10 percent. The lower intensity of the lines of lutetium made it necessary to use a total rare earth concentration of 1.0 percent in order to maintain the other conditions at nearly the same values as for the other five elements. One-tenth percent solutions were prepared by diluting the stock solutions by a factor of ten with absolute ethanol. It is always desirable to use the lowest total salt concentration possible in quantitative flame photometry since intensity fluctuations due to encrustation of dry salt on the burner tip and capillary are less likely at low concentrations (71).

Many of the experimental conditions were identical for all of the concentration ranges for all of the elements. Table 14 lists these.

Table 14. Constant experimental conditions for analytical calibrations

Gas flow rates	oxygen: 2.68 l/min acetylene 3.16 l/min
Sample aspiration rate	0.68 ml/min
Amplifier input sensitivities	1- 25%: 1×10^{-6} amp full scale 5-100%: 2×10^{-6} amp full scale
Slit width	0.025 mm
Recorder sensitivity	10 mv full scale
Scan speed	20 Å/min
Chart speed	1 in/min

Intensity values for construction of the analytical curves were obtained by measuring the net intensity (line plus background minus background) for the rare earth line at each concentration. For each line, a baseline was drawn connecting the average readings on both sides of the line. Background was measured on this baseline directly under the midpoint of the line. A zero setting was employed such that the average value of the background intensity would be five percent of full scale signal. Variation of the photomulti-

plier voltage allowed the total line intensity to be set at any desired value. In order that reproducible instrumental conditions could be maintained, the net intensity of the most concentrated standard in either range was set at 90 percent. To minimize errors due to recorder overshoot and local intensity fluctuations, two successive scans of each concentration were made. An average of these two values was taken in order to obtain one value for the intensity. The experimental conditions used to set the span for each element and concentration range, along with the wavelengths of the analysis lines, are given in Table 15.

Three runs (each consisting of two scans) were used to establish the analytical curves shown in Figures 21-26. Both high and low concentration ranges are included in each graph. The shape of most of the analytical curves is typical of lines which undergo a small degree of self reversal. In the more concentrated solutions, a greater percentage of unexcited atoms are present which can reabsorb some of the emitted light and cause a diminution in line intensity and a consequent loss of linearity in the upper portion of the analytical curve.

Only one serious interference was encountered in preparing these curves. Table 12 shows that the 4053.92 Å holmium line has an interference due to a strong scandium line at 4054.55 Å. The one per cent Ho_2O_3 standard contained

Table 15. Variable experimental conditions for analytical calibrations

Element	Wavelength (Å)	Total rare earth conc. (%)	Conc. range (%)	Photo-multiplier voltage	Zero suppress. (mv)
Dy	4211.72	0.10	1-25	1460	-0.31
			5-100	1400	+0.50
Ho	4053.92	0.10	2-25	1450	-1.15
			5-100	1400	+0.20
Er	4007.97	0.10	2-25	1450	-0.80
			5-100	1460	-0.25
Tm	4094.18	0.10	2-25	1500	-1.00
			5-100	1450	-0.01
Lu	3359.56	1.00	1-25	1560	-0.20
			5-100	1500	+0.50
Sc	3911.81	0.10	1-25	1460	-0.30
			5-100	1440	+0.10

25 percent Sc_2O_3 making a relative intensity measurement of the holmium line impossible. However, the two percent holmium standard contained ten percent Sc_2O_3 causing both lines to be approximately equal in intensity and well enough resolved to make it possible to measure the intensity of the holmium line quite accurately.

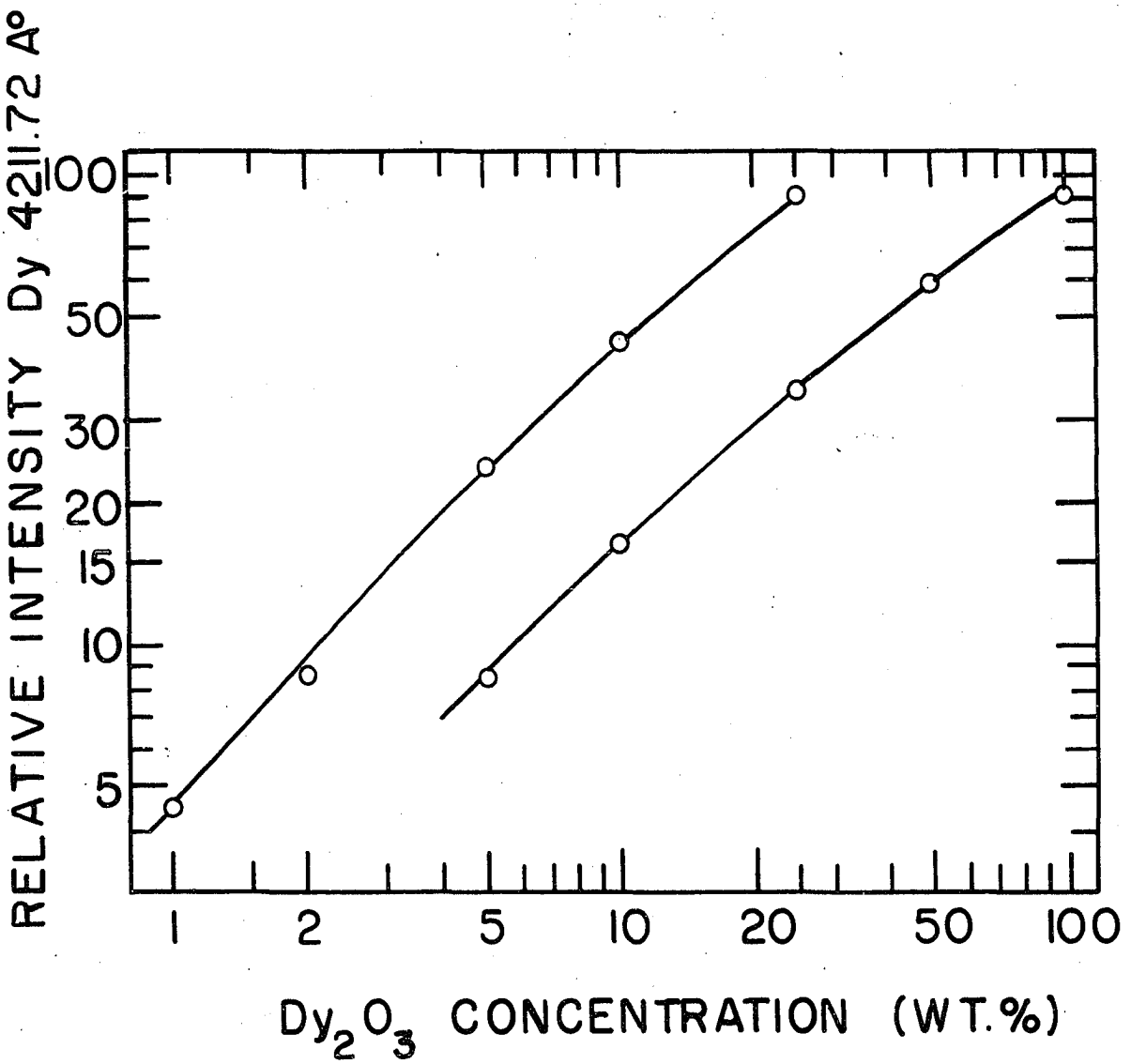

Figure 21. Analytical curves for the determination of Dy_2O_3 in rare earth mixtures

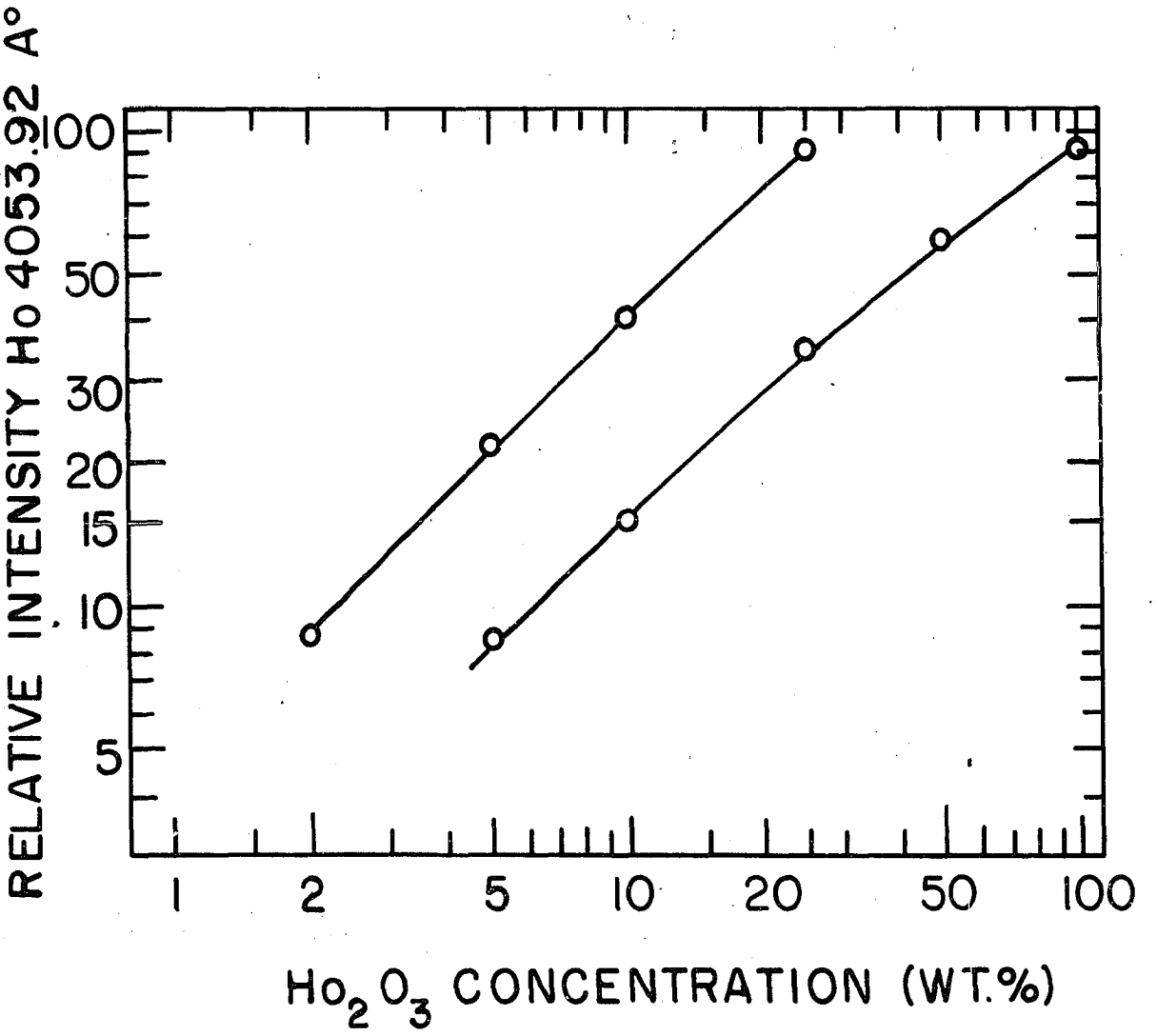

Figure 22. Analytical curves for the determination of Ho_2O_3 in rare earth mixtures

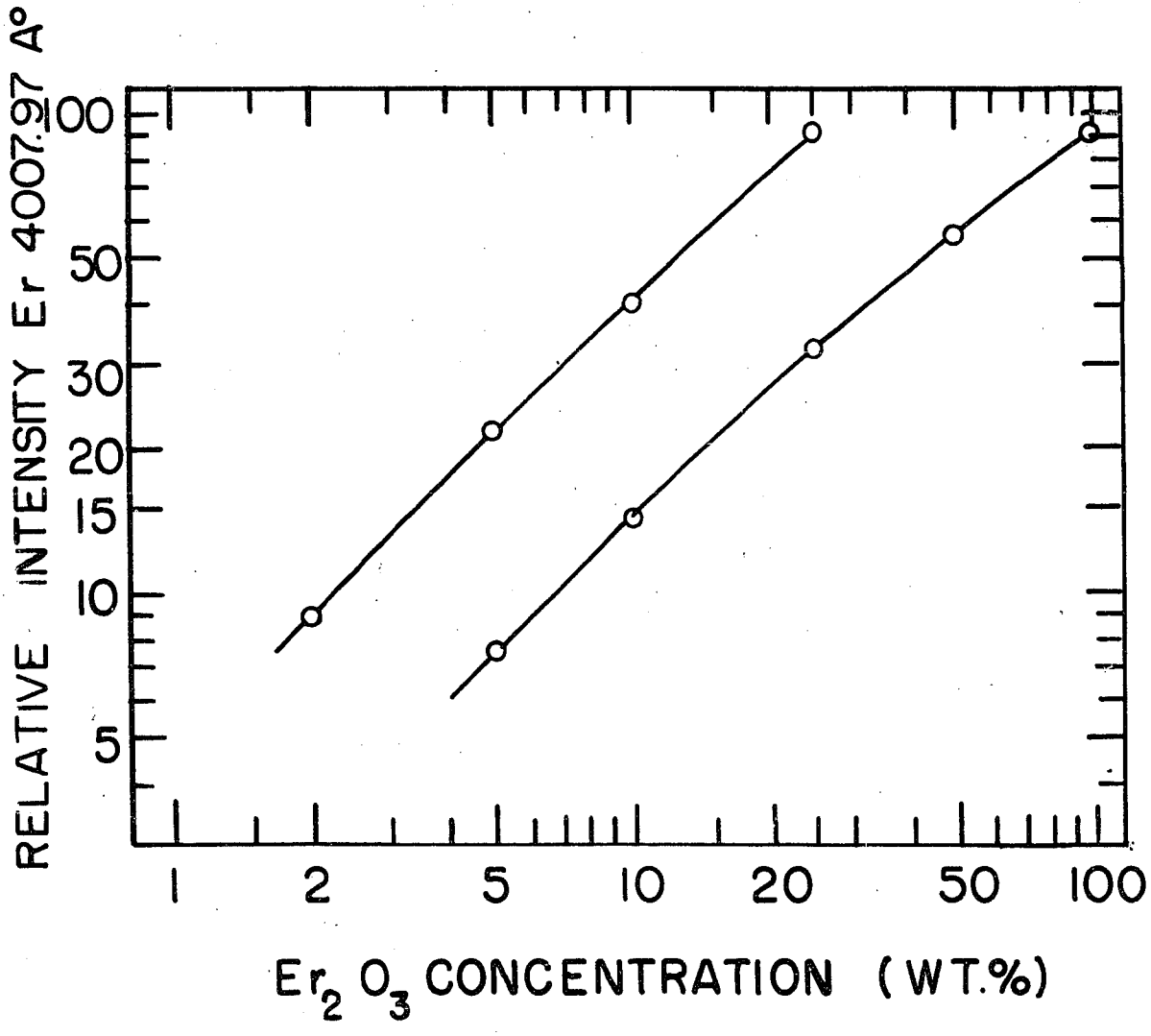

Figure 23. Analytical curves for the determination of Er_2O_3 in rare earth mixtures

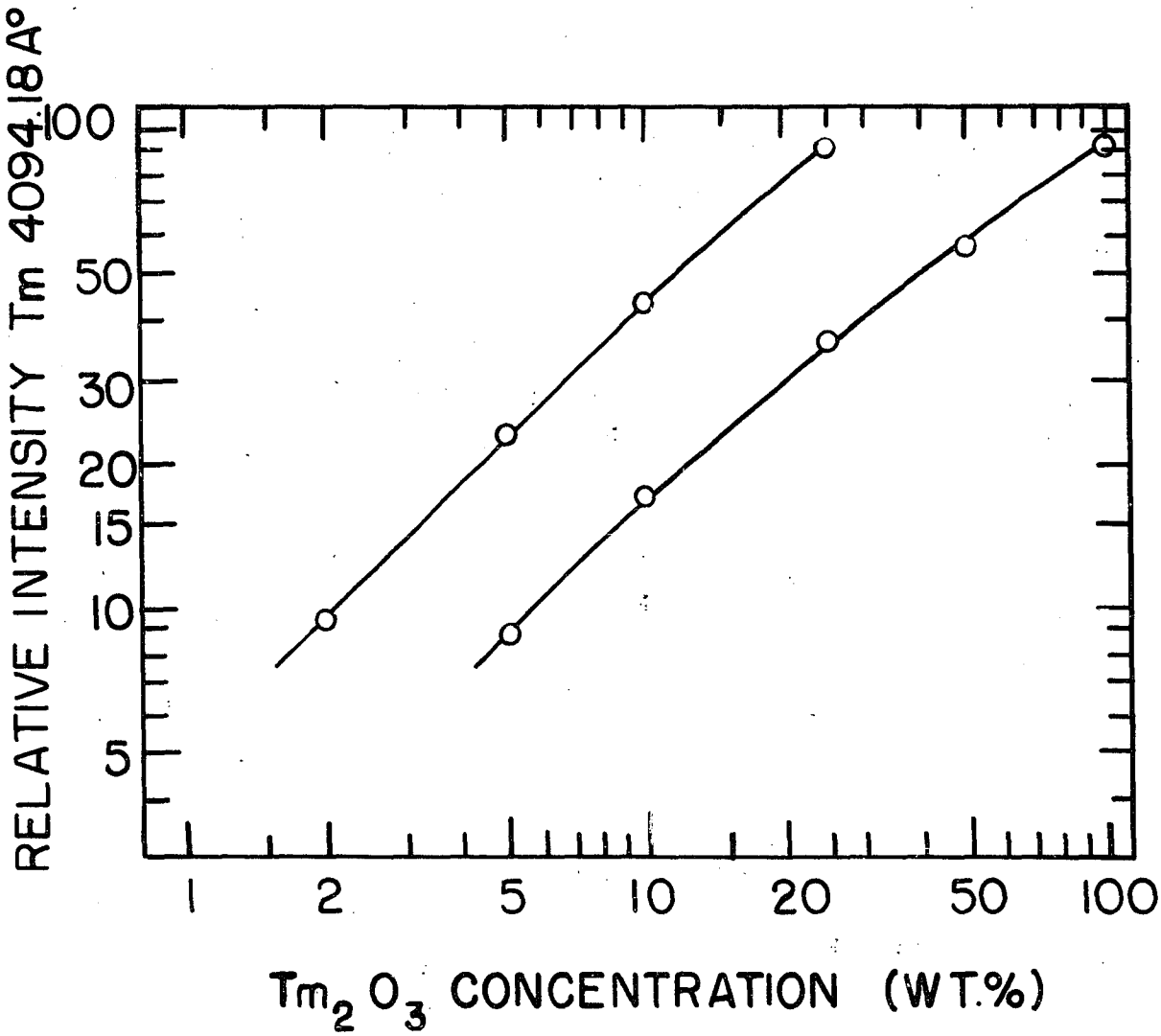

Figure 24. Analytical curves for the determination of Tm_2O_3 in rare earth mixtures

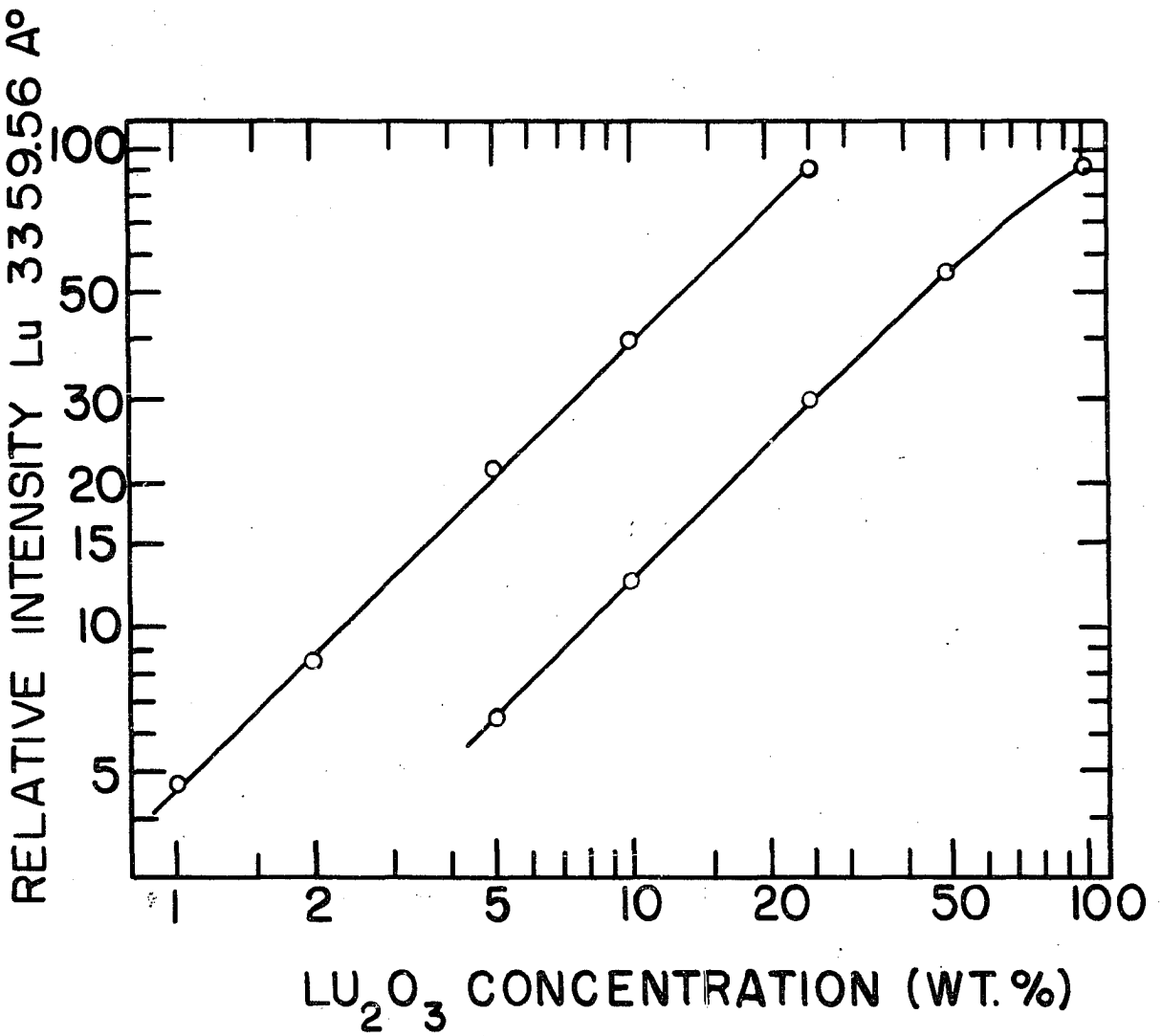

Figure 25. Analytical curves for the determination of Lu_2O_3 in rare earth mixtures

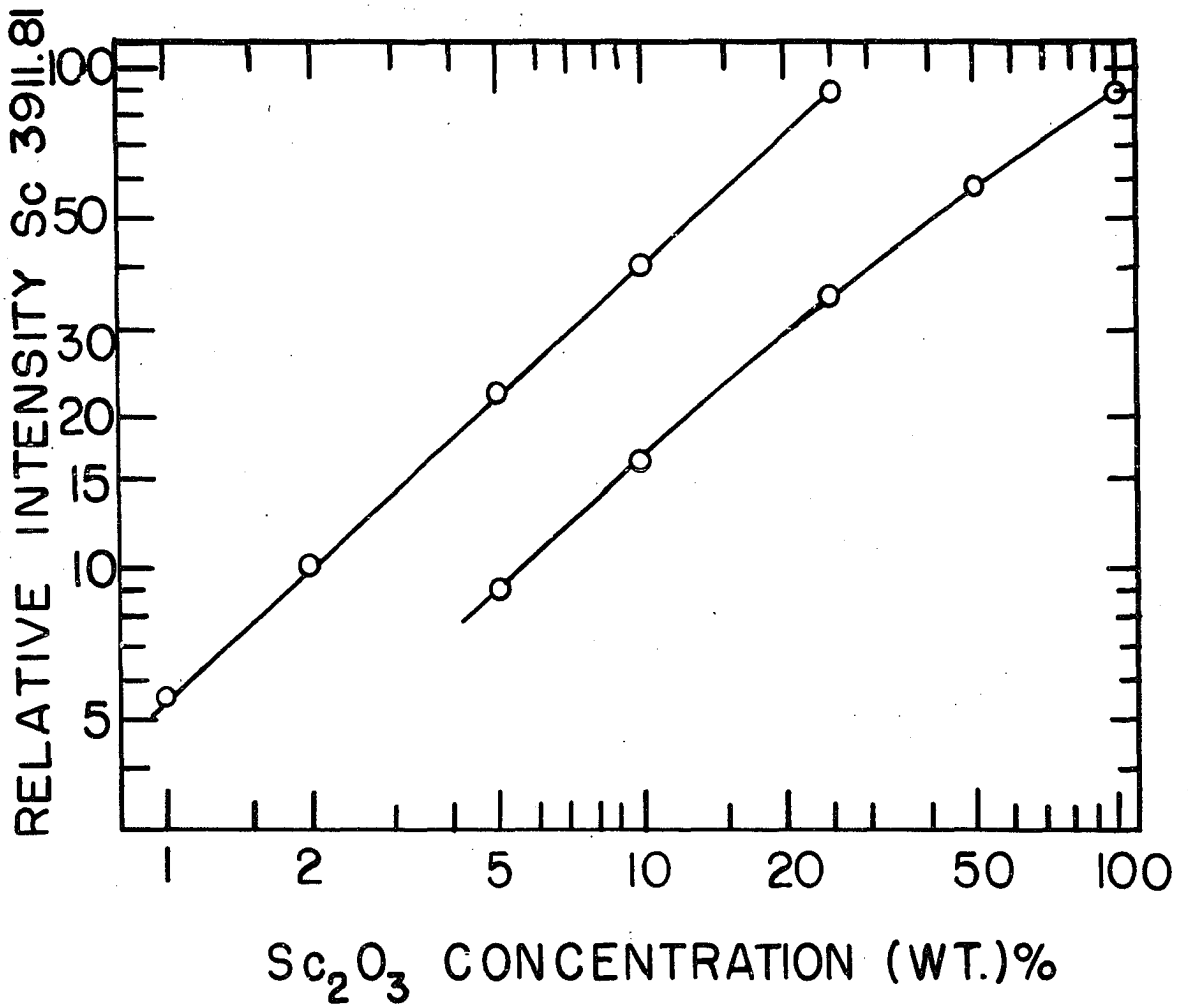

Figure 26. Analytical curves for the determination of Sc_2O_3 in rare earth mixtures

Since the purpose of these calibrations was to show the applicability of this method to rare earth complex mixture determinations, no detailed study of precision and accuracy was carried out. However it may be stated qualitatively that the precision of the method seems to be very good. Since the excellent stability of the recording electronics places most of the burden on the aspirator-burner, this method should be at least equally as precise as other methods reported in the literature in which this burner was employed.

VII. SUGGESTIONS FOR FUTURE WORK

There are many opportunities for future work on both the physical and analytical aspects of the phenomenon observed here. Because of the great number of elements and experimental variables involved, it was necessary to restrict this study to general observations in many cases. More specific studies which would treat the rare earths as individual elements rather than as a class are certainly necessary if the analytical potential of the method is to be exploited fully.

Atomic absorption, which is enjoying a rapid gain in popularity at the present time, should benefit from this technique since its success depends on a large free atom population in the flame.

The physical processes underlying the formation of the free rare earth atoms will require much study to be understood completely. Detailed correlations of line and band intensities with flame temperature should prove valuable. A study of the intensity changes in the lines and bands horizontally across the flame would give information concerning the portion of the flame in which the various emitting species exist. The problems, both experimental and interpretive, would be formidable in this type of study but the results would probably make the effort worthwhile. For

instance, if the enhancement of both the band and line spectra is due to their emission from different portions of the flame, such a study would reveal this. The atomic absorption technique should prove quite valuable for experiments of this type since it measures the relative free atom population directly, permitting studies of atomic population independently of excitation.

Investigations should not be restricted to the oxygen-acetylene flame. Other hydrocarbon fuels such as methane, ethane, and ethylene burning in oxygen produce flames of slightly lower temperature than oxygen-acetylene and have different compositions. The ability of these flames to produce line spectra might well shed some light on the excitation process.

The present lack of knowledge concerning the composition of fuel-rich diffusion flames is the most serious stumbling block to the elucidation of this phenomenon. Without this knowledge, studies of the type suggested above cannot be correlated properly. It is strongly suggested here that any future studies be undertaken only after serious consideration has been given to all of the possible methods by which these compositions may be calculated or experimentally determined.

VIII. SUMMARY

Of all the rare earth elements, only europium and ytterbium emit intense atomic lines in oxygen-hydrogen flames. In oxygen-acetylene, however, almost all of them emit line spectra ranging in intensity from moderate to very strong. The wavelengths of over 1200 lines have been measured and their relative intensities estimated.

The fuel-rich character of the flame which produced maximum line emission prompted an inquiry into the nature of the processes responsible for the appearance of the lines. Effective electronic temperature measurements and other observations indicated that neither a purely thermal nor a chemiluminescent mechanism could be invoked to explain the character of the spectra. Speculations have been made concerning the mechanisms which could account for these spectra.

The analytical potentialities of the line spectra have been evaluated in terms of their sensitivity and freedom from interference. Of the sixteen rare earth elements, all but lanthanum, cerium, and gadolinium possess lines which are both strong enough and free enough from interference to make their determination in rare earth mixtures possible. Analytical curves covering the range from one or two to 100 percent rare earth oxide were developed for six of these elements: dysprosium, holmium, erbium, thulium, lutetium, and scandium.

IX. LITERATURE CITED

1. Dean, John A. "Flame Photometry" New York, N.Y. McGraw-Hill Book Co., Inc. 1960.

2. Nachtrieb, N.H. "Principles and Practice of Spectrochemical Analysis" New York, N.Y. McGraw-Hill Book Co., Inc. 1950.

3. Lundegårdh, H. "Die Quantitative Spektralanalyse der Elemente" Vol. 1, Jena, Germany. G. Fischer Verlagsbuchhandlung. 1929; Vol. 2, Jena, Germany. G. Fischer Verlagsbuchhandlung. 1934.

4. Piccardi, G. Nature 124, 129 (1929).

5. Piccardi, G. Nature 124, 618 (1929).

6. Piccardi, G. Atti accad. Lincei 14, 578 (1931).

7. Piccardi, G. and A. Sberna. Atti accad. Lincei 15, 83 (1932).

8. Piccardi, G. and A. Sberna. Atti accad. Lincei 15, 309 (1932).

9. Piccardi, G. and A. Sberna. Atti accad. Lincei 15, 577 (1932).

10. Piccardi, G. Gazz. Chim. Ital. 63, 127 (1933).

11. Piccardi, G. Atti accad. Lincei 21, 584 (1935).

12. Piccardi, G. Atti accad. Lincei 21, 589 (1935).

13. Piccardi, G. Atti accad. Lincei 25, 44 (1937).

14. Piccardi, G. Atti accad. Lincei 25, 87 (1937).

15. Piccardi, G. Atti accad. Lincei 25, 730 (1937).

16. Piccardi, G. Spectrochim. Acta 1, 249 (1939).

17. Piccardi, G. Spectrochim. Acta 1, 533 (1941).

18. Pinta, M.J. J. recherches centre natl. recherche sci. Labs. Bellevue (Paris) 21, 260 (1952).

19. Tremmel, C.G. "Flame Spectrometric Determination of Lanthanum in Rare Earth Mixtures" Unpublished Masters

Thesis. Ames, Iowa. Library, Iowa State University of Science and Technology. 1958.

20. Rains, T.C., H.P. House, and O. Menis. Anal. Chim. Acta 22, 315 (1960).

21. Albiniti, J.F.P.de. Anales asoc. Quim. Argentina 43, 106 (1955).

22. Ishida, R. J. Chem. Soc. Japan, Pure Chem. Sect. 76, 56 (1955).

23. Menis, O., T.C. Rains, and J.A. Dean. Anal. Chem. 31, 187 (1959).

24. Poluektov, N.S. and M.P. Nikonova. Ukrain. Khim. Zhur. 25, 217 (1959).

25. Gaydon, A.G. and H.G. Wolfhard. "Flames: Their Structure, Radiation and Temperature" 2nd ed. New York, N.Y. Macmillan Co. 1960.

26. Feldman, C. and J.Y. Ellenburg. Spectrochim. Acta 7, 349 (1956).

27. Churchill, J.R. Ind. Eng. Chem., Anal. Ed. 16, 653 (1944).

28. Fastie, W.G. J. Opt. Soc. Am. 42, 641 (1952).

29. Smith, G.F. Anal. Chim. Acta 8, 397 (1953).

30. Gatterer, A. "Grating Spectra of Iron" Specola Vaticana. Citta del Vaticano. 1951.

31. Harrison, G.R., ed. "M.I.T. Wavelength Tables" New York, N.Y. J. Wiley and Sons, Inc. 1939.

32. Gatterer, A. and J. Junkes. "Spektren der Seltenen Erden" Specola Vaticana. Citta del Vaticano. 1945.

33. Gatterer, A., J. Junkes, and E.W. Salpeter. "Molecular Spectra of Metallic Oxides" Specola Vaticana. Citta del Vaticano. 1957.

34. Russell, H.N. and W.F. Meggers. Bur. Standards J. Res. 9, 625 (1932).

35. Moore, C.E. Natl. Bur. Standards Technical Note 36, 1 (1959).

36. Albertson, W. Phys. Rev. 47, 370 (1935).

37. Albertson, W. Phys. Rev. 52, 644 (1937).

38. King, A.S. Astrophys. J. 97, 323 (1943).

39. Klinkenberg, P.F.A. Physica 21, 53 (1955).

40. Russell, N.H. and W.F. Meggers. Sci. Papers Bur. Standards 22, 320 (1927).

41. Meggers, W.F. and N.H. Russell. Bur. Standards J. Res. 2, 733 (1929).

42. Mavrodineanu, R. Spectrochim. Acta 17, 1016 (1961).

43. Gilbert, P.T. Chemiluminescent flame spectrophotometry. (Abstract) Pittsburgh Conference on Analytical Chemistry and Applied Spectroscopy Program 1961, 65 (1961).

44. Broida, H.P. and D.F. Heath. J. Chem. Phys. 26, 223 (1957).

45. Goldstein, H.W., P.N. Walsh, and D. White. J. Phys. Chem. 65, 1400 (1961).

46. Walsh, P.N., D.F. Dever, and D. White. J. Phys. Chem. 65, 1410 (1961).

47. Walsh, P.N., H.W. Goldstein, and D. White. J. Am. Cer. Soc. 43, 229 (1960).

48. Herzberg, G.H. "Spectra of Diatomic Molecules" 2nd ed. Princeton, N.J. D. Van Nostrand Co., Inc. 1950.

49. Gilbert, P.T. Analytical flame photometry: new developments. Am. Soc. Test. Mat. Special Technical Publication 269 (1960).

50. Broida, H.A. and K.E. Shuler. J. Chem. Phys. 27, 933 (1957).

51. Dieke, G.H. and H.M. Crosswhite. (Photostated) The Johns Hopkins University, Applied Physics Laboratory Bumblebee Report No. 87 (1948).

52. Earls, L.T. Phys. Rev. 48, 423 (1935).

53. Hill, L. and J.N. Van Vleck. Phys. Rev. 32, 250 (1928).

54. Bass, A.M. and H.P. Broida. Natl. Bur. Standards Circular 541 (1953).

55. Dieke, G.H. and H.M. Crosswhite. The Johns Hopkins University, Applied Physics Laboratory Quarterly Report, October 1 through December 31, 1950 on JHB-3, Problem A (1951).

56. Beers, Y. "Introduction to the Theory of Error" Reading, Mass. Addison-Wesley Publishing Co., Inc. 1953.

57. Lewis, B. and G. von Elbe. "Combustion, Flames and Explosions of Gases" New York, N.Y. Academic Press. 1951.

58. Tourin, R.H. Combustion and Flame 2, 353 (1958).

59. Menis, O. and T.C. Rains. Anal. Chem. 32, 1837 (1960).

60. Ostrovski, J.I. and N.P. Penkin. Optika i Spektroskopia 3, 391 (1957).

61. Fenimore, C.P. and G.W. Jones. J. Phys. Chem. 62, 178 (1958).

62. Bulewicz, E.M. and T.M. Sugden. Trans. Faraday Soc. 54, 830 (1958).

63. Knutson, K.E. Analyst 82, 241 (1957).

64. Veits, I.V. and L.V. Gurvich. Optika i Spektroskopia 1, 22 (1956).

65. David, D.J. Nature 187, 1109 (1960).

66. Eshelman, H.C., J.A. Dean, O. Menis, and T.C. Rains. Anal. Chem. 31, 183 (1959).

67. Banks, C.V. and D.W. Klingman. "Analytical Chemistry of the Rare Earths" In Spedding, F.H. and A.H. Daane, eds. "The Rare Earths" pp. 570-593. New York, N.Y. J. Wiley and Sons, Inc. 1961.

68. Fassel, V.A. Anal. Chem. 32, No. 11, 19A (1960).

69. Alkemade, C.T.J. Unpublished Ph.D. Thesis, Utrecht, Netherlands. 1954; Original not available; cited in

Dean, J.A. "Flame Photometry" p. 149. New York, N.Y. McGraw-Hill Book Co., Inc. 1960.

70. Hagenah, W.D., H. Kaiser, and H. Massmann. "Berechnung der Nachweis-und Bestimmungsgrenzen bei photoelektrischen Analysenverfahren" [To be published in Proceedings of the ninth Colloquim Spectroscopium Internationale 1961, ca. 1963].

71. Foster, W.H. and D.N. Hume. Anal. Chem. 31, 2028 (1959).

X. ACKNOWLEDGMENTS

The author wishes to express his gratitude to Dr. Velmer A. Fassel for his assistance and encouragement throughout the course of this work.

Thanks are also extended to Mr. Richard N. Kniseley for many helpful discussions during the early part of the investigation and to Mr. Henry J. Hettel for his help in editing the manuscript.

The assistance of Messrs. Robert B. Myers and Royce K. Winge in running some of the spectra is gratefully acknowledged.

Appreciation is also extended to Dr. Frank H. Spedding and Dr. Jack Powell who supplied the pure rare earth oxides necessary for these studies.